EXPLORATION OF THE ROLE OF CIB1 IN CELL SURVIVAL AND TUMOR GROWTH

Justin Layne Black

A dissertation submitted to the faculty at the University of North Carolina at Chapel Hill in partial fulfillment of the requirements for the degree of Doctor of Philosophy in the Department of Biochemistry and Biophysics in the School of Medicine.

Chapel Hill
2015

Approved by:

Leslie V Parise

Wolfgang Bergmeier

Sharon Campbell

Keith Burridge

Klaus Hahn

© 2015
Justin Layne Black
ALL RIGHTS RESERVED

ABSTRACT

Justin Layne Black: Exploration of the role of CIB1 in cell survival and tumor growth
(Under the direction of Leslie V. Parise)

CIB1 is an intracellular protein with diverse functions in cancer cell biology. Here I explore two important functions of CIB1: 1) The role of CIB1 in cell survival and tumor growth in triple negative breast cancer; and 2) The interaction between CIB1 and α-integrin cytoplasmic tails and the role of this interaction in cell biology.

Triple negative breast cancer (TNBC) is an aggressive breast cancer subtype with an unmet need for novel targeted therapeutics. We previously demonstrated that CIB1 is necessary for cancer cell survival and proliferation via regulation of two oncogenic signaling pathways, RAS-RAF-MEK-ERK and PI3K-AKT. Because these pathways are often upregulated in TNBC, we hypothesized that CIB1 may play a broader role in TNBC cell survival and tumor growth. Here we find that CIB1 is necessary for cell survival in multiple TNBC cell lines *in vitro*, and TNBC xenograft tumor growth *in vivo*. Furthermore, elevated AKT activation status and low PTEN expression were key predictors of sensitivity to CIB1 depletion in TNBC cells. Importantly, CIB1 knockdown caused dramatic shrinkage of MDA-MB-468 xenograft tumors *in vivo*. RNA sequence analysis showed that CIB1 depletion activates gene programs associated with decreased proliferation and increased cell death. Taken together, our data are consistent with the emerging theory of non-oncogene addiction, where a large subset of TNBCs depend on CIB1 for cell survival and tumor growth, independent of CIB1 expression levels.

Integrins are heterodimeric transmembrane receptors important for cell adhesion to the extracellular matrix and transmission of signals through the cell membrane. Integrins are regulated via binding of cytoplasmic proteins to the integrin cytoplasmic tail. CIB1 was discovered as a binding partner of one integrin, αIIb, but the role of CIB1 in binding and regulating additional integrins was previously unknown. Here I also present evidence that CIB1 interacts with integrin αV via residues in the transmembrane portion of the integrin, can access these residues in the presence of a cell membrane, and that CIB1-integrin binding may contribute to cell signaling and proliferation. In summary, CIB1 is a diverse protein with important functions in TNBC cell survival and proliferation, as well as integrin biology.

ACKNOWLEDGMENTS

The work presented in this dissertation represents only a portion of countless hours of effort I have spent studying and researching the protein CIB1 through the lenses of biochemistry, cell biology, genetics, and cancer biology. While this exercise has often pushed me to my intellectual limits, I would be remiss to provide any impression that this work is the product of my personal exertion alone. Consequently, I gratefully take this small space to acknowledge and publicly express my gratitude to several of the individuals who have contributed in a variety of ways to this dissertation. Each of these people have exemplified not only intellectual expertise, but also personal kindness. I have been changed for the better through my associations with these distinguished people.

I have been fortunate to work in a fantastic lab under the mentorship of Leslie Parise. I will always be grateful that Leslie gave me the freedom to pursue an unconventional project and non-traditional path. I owe a debt of gratitude to Tina Leisner and Thomas Freeman, who taught me everything I know about cell biology and biochemistry, as well as the other members of the Parise Lab. It has been a privilege to work with a team of kind and thoughtful people.

I also thank my excellent thesis committee, who have annually provided helpful criticism of my work and have always been optimistic and encouraging. In addition, I thank each member of my committee for taking time to provide occasional one-on-one mentoring.

Many others within and outside of the University community have helped me at various stages of my project. Several collaborators have provided significant contributions to my project. Thanks to Chuck Harrell for going above and beyond in gene expression analysis. Also thank you

to Corbin Jones and Dominik Reinhold for assistance with design and analysis of RNAseq experiments. A special thanks goes to Howard Fried who taught me molecular biology and served as a sounding board through much of the early months of my thesis project. Thank you to Tom Stewart for patient instruction of basic principles of statistics. I also want to thank the following people for their assistance in experimental design and data collection: Bob Bagnell and Vicky Madden of the UNC Microscopy Services Laboratory; Ash Tripathy of the Macromolecular Interactions Facility; and Charlene Santos and Mark Ross from the Animal Studies Core Facility.

I would also like to thank the team at Carolina Kickstart: Don Rose, Andy Kant, John Sheridan, and Jason Doherty. It is safe to say that without Carolina Kickstart my thesis project would have turned out very differently, and my experience at UNC would have been far less rewarding.

Finally, three special thanks to the people who made the effort worthwhile. First I thank my wife, Melissa, for everything. She is my best friend and has been my greatest advocate every step of the way. She inspires me to work harder and reach higher than I could on my own. Second, I thank my three kids: Andrew, Isaac, and Lydia. All three were born during graduate school (Andrew and Isaac – Sep 2010; Lydia – June 2013). Their smiles make going home every night even more enjoyable. Third, I thank my mom and dad, who have always supported and encouraged me to pursue my dreams, regardless of the path, and my brothers (Logan, Brandon, Keaton, Nathan, and Dallin). I have been blessed with an amazing family.

As stated above, this brief acknowledgment insufficiently recognizes the contributions of many people. Thank you to everyone, including those not listed here, who have helped, influenced, and supported me on my journey through graduate school.

TABLE OF CONTENTS

LIST OF FIGURES

LIST OF TABLES

LIST OF ABBREVIATIONS

7-AAD	7-Aminoactinomycin D
AKT	Protein Kinase B
ASK1	Apoptosis signal-regulating kinase 1
BRAF	V-Raf murine sarcoma viral oncogene homolog B1
CHO	Chinese hamster ovary cells
CIB1	Calcium and integrin binding protein 1
CnB	Calcineurin B
CTRL	Control
DMD	Discrete molecular dynamics
DNA-PKcs	DNA-Protein Kinase catalytic subunit
Dox	Doxycycline
EGFR	Epidermal growth factor receptor
EMT	Epithelial to mesenchymal transition
ERK	Mitogen-activated protein kinase 1
FAK	Focal adhesion kinase
FDA	Food and drug administration
H&E	Hematoxylin and eosin
HER2	Human epidermal growth factor receptor 2
HPLC	High pressure liquid chromatography
HUVEC	Human umbilical vein endothelial cells
ITC	Isothermal titration calorimetry
K_d	Equilibrium dissociation constant
KRAS	V-KI-Ras2 Kirsten rat sarcoma viral oncogene homolog
MBP	Maltose binding protein

MEF	Mouse embryonic fibroblast
MEK	Mitogen-activated protein kinase kinase kinase 1
MSP1	Membrane scaffold protein
MW	Molecular weight
NMR	Nuclear magnetic resonance
NRAS	Neuroblastoma ras viral oncogene homolog
pERK	phosphorylated ERK
PAK1	p21 activated kinase 1
pAKT	phosphorylated AKT
PARP1	Poly-ADP ribose polymerase
PBS	Phosphate-buffered saline
PDB	Protein databank
PDK1	3-phophoinositide-dependent protein kinase 1
PI3K	Phosphatidylinositol-3-kinase
PIK3CA	Phosphatidylinositol-3-kinase catalytic subunit
PIP2	Phosphatidylinositol-4,5-bisphosphate
PIP3	Phosphatidylinositol-3,4,5-triphosphate
PS	Phosphatidylserine
PTEN	Phosphatase and Tensin homolog deleted on chromosome Ten
PVDF	Polyvinylidene diflouride
RNAi	RNA interference
RNAseq	RNA sequencing
ROS	Reactive oxygen species
RTK	Receptor tyrosine kinase
SCR	Scrambled
SDS-PAGE	SDS polyacrylamide gel electrophoresis

SEM	Standard error of the mean
shRNA	small hairpin RNA
SK1	Sphingosine Kinase 1
TBS	Tris-buffered saline
TEV	Tobacco etch virus protease
Thr	Threonine
TNBC	Triple Negative Breast Cancer
TUNEL	Terminal deoxynucleotidyl transferase dUTP nick end labeling
WT	Wild-type

CHAPTER 1: AN INTRODUCTION

1.1 Cancer Introduction

Cancer is the second leading cause of death worldwide, with over 12 million new diagnoses and more than 7 million deaths attributed to cancer in 2008 (1). Cancer is a heterogeneous group of diseases in which normal cells become transformed and exhibit uncontrolled growth (2). At the molecular level, cancer is driven by genetic mutations resulting in activation of oncogenes or inactivation of tumor suppressor genes (the concept of oncogenes and tumor suppressor genes has been reviewed extensively – a few helpful and relevant references may be found here (2-7)). These events lead to unchecked cell proliferation and survival resulting in tumor formation and, eventually, metastasis to foreign tissue sites and patient death (Figure 1-1) (8,9). Cancer therapy presents significant challenges for physicians, and there is an unmet need for targeted treatments with improved efficacy and safety profiles.

Here I will review one particular cancer subtype, triple negative breast cancer (TNBC), then describe cancer at the cellular and molecular level with a focus on oncogenic signaling pathways and their contribution to TNBC.

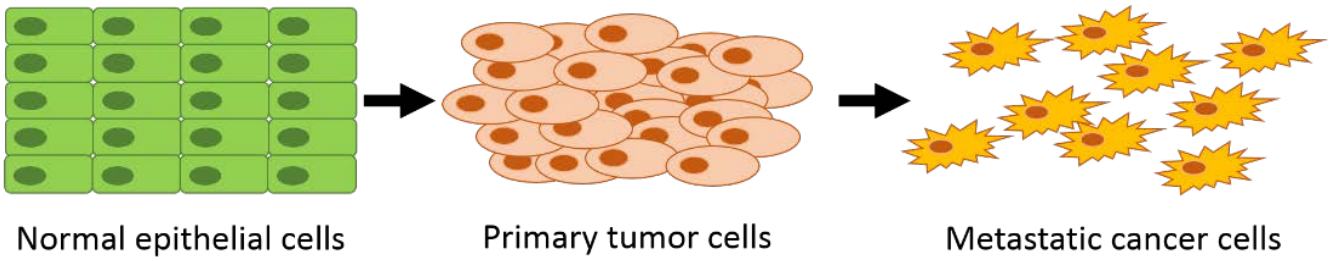

Figure 1-1. Cancer genesis. Normal cells experience a genetic mutation resulting in increased proliferation forming a primary tumor. Eventually tumor cells detach from the primary tumor site and metastasize to foreign tissues.

1.1.1 Triple negative breast cancer

Breast cancer is diagnosed in more than 230,000 women each year in the United States (10), and is the leading cause of cancer-related deaths among women worldwide (1). Approximately 15 percent of breast cancers are a subtype called triple negative breast cancer (TNBC), defined by lack of expression of three receptors: estrogen receptor (ER); progesterone receptor, and human epidermal growth factor receptor 2 (HER2) (11). TNBC is an aggressive cancer subtype with generally poor prognosis. Targeted treatments are used for ER-positive (e.g. Tamoxifen) and HER2-positive (e.g. Herceptin) breast cancers. These targeted treatments improve overall survival for patients with these sub-types (12). However, no targeted therapies are currently approved for TNBC (13). Although TNBC is sensitive to chemotherapy, the overall prognosis in TNBC is worse than non-TNBC sub-types due to high rates of relapse. TNBC patients also have a shorter overall survival rate relative to other breast cancer subtypes (14). Ongoing research has explored novel targets for TNBC therapy, and several targeted agents have progressed into clinical trials. However, there remains an unmet need for new targeted therapeutics with improved safety and efficacy to improve TNBC patient outcomes.

1.1.2 PI3K-AKT and RAS-RAF-MEK-ERK cancer signaling pathways

Cancer is caused by genetic alterations that lead to uncontrolled cell survival and proliferation. Genetic mutations typically lead to a nonfunctional gene product, which, if deleterious, is recognized by the cell and can lead to programmed cell death, an evolutionary mechanism through which a single cell self-destructs for the good of the greater organism (15). However, occasionally a genetic mutation may lead a cell to undergo transformation such that it begins proliferating uncontrollably, resulting in tumor formation (15). Gain of function mutations or amplification of oncogenes, and loss of function mutations or deletion of tumor suppressor

genes, often result in unrestrained activation of oncogenic signaling pathways. Several commonly mutated genes resulting in aberrant oncogenic signaling include PIK3CA, BRAF, KRAS, PTEN, and NRAS (see Table 1-1) (16). These particular mutations result in aberrant activation of PI3K-AKT and RAS-RAF-MEK-ERK, two commonly activated oncogenic signaling pathways in TNBC that are pertinent to the data presented herein (17). Cross-talk between these pathways enables cancer cells to compensate for inhibition of one pathway by activating the other pathway (17,18).

Gene name	Protein name	Oncogene/ Tumor Suppressor
PIK3CA	Phosphatidylinositol 4,5-bisphosphate 3-kinase catalytic subunit alpha	Oncogene
BRAF	V-Raf murine sarcoma viral oncogene homolog B1	Oncogene
KRAS	V-KI-Ras2 Kirsten rat sarcoma viral oncogene homolog	Oncogene
PTEN	Phosphatase and tensin homolog	Tumor Suppressor
NRAS	Neuroblastoma ras viral oncogene homolog	Oncogene

Table 1-1. Commonly mutated cancer genes. Selected genes from a list of the most commonly mutated cancer genes. See Lawrence et al. for complete list (16).

Aberrant activation of the RAS-RAF-MEK-ERK signaling pathway leads to unrestrained cell survival and proliferation. The RAS oncogene is one of the most commonly mutated genes in cancer (reportedly mutated in ~30% of all cancers) and the RAS signaling pathways have frequently been cited as targets for cancer therapy (19-21). Despite significant effort, scientists and drug developers have been unsuccessful at developing small molecule inhibitors of RAS, although recent advances in siRNA delivery technology may offer an effective alternative approach (22). However, RAS mutations are rare in TNBC (23). Several studies, including the

Cancer Genome Atlas study, reported RAS mutations in less than two percent of all breast cancers (24-26). In addition to RAS mutations, RAF is commonly mutated in cancer and also contributes to activation of MEK-ERK signaling and cell proliferation (27).

Although RAS mutations are rare in breast cancer, mutations activating PI3K-AKT signaling are more common in breast cancer, including activating PI3K mutations and inactivating mutations to PTEN. One cause of aberrant PI3K-AKT activation involves the catalytic subunit of PI3K, PIK3CA, which is mutated in up to 30% of epithelial cancers, including breast, colon, prostate, and endometrial cancers (28). Another common mutation leading to PI3K-AKT activation is mutation, deletion, or downregulation of the tumor suppressor PTEN (phosphatase and tensin homolog deleted on chromosome 10), a lipid/protein phosphatase that inactivates PI3K signaling via dephosphorylation of the lipid PIP3 (phosphatidylinositol-3,4,5-triphosphate) (29). PIP3 has an important role in PI3K-AKT pathway activation by binding PDK1 and promoting PDK1-dependent phosphorylation of AKT. PTEN inhibits the PI3K-PIP3-PDK1-AKT pathway by dephosphorylating PIP3 to PIP2 (Figure 1-2) (30-33). Therefore, PTEN functions as a clinically-relevant tumor suppressor by putting the molecular brakes on PI3K-AKT activation. In a recent study of breast cancer patients, PTEN expression negatively correlated with tumor size, suggesting that loss of PTEN may be an important driver of tumor growth (34). PTEN mutations/deletions also lead to a higher incidence of tumor formation in mice and humans (35,36).

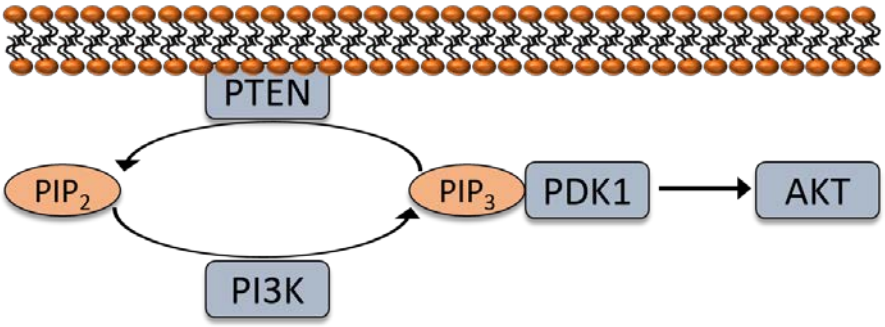

Figure 1-2. PTEN inhibits PI3K activation of PDK1 by dephosphorylating PIP_3. PI3K catalyzes the phosphorylation of PIP_2 to PIP_3. PIP_3 binding to PDK1 is necessary for PDK1 phosphorylation and activation of AKT. PTEN inhibits PI3K-PDK1-AKT activation by dephosphorylating PIP_3.

Due to the clinical relevance and the high rate of mutation in the PI3K-AKT and RAS-RAF-MEK-ERK signaling pathways, extensive work has been done to characterize these genes/pathways. Here I briefly summarize some of the relevant elements of these two important signaling cascades. Both RAS and PI3K signaling are stimulated by receptor tyrosine kinase (RTK) activation (28,37). For example, epidermal growth factor receptors (EGFR) are bound by extracellular epidermal growth factor (EGF), stimulating a conformational change and activation of EGFR. Active EGFR phosphorylates and activates its substrates, such as PI3K. PI3K stimulates activation of PDK1 via PIP_3, leading to AKT activation as well as downstream activities including cell survival, cell proliferation, and gene expression (see Figure 1-5). PI3K activity is inhibited by the phosphatase PTEN. Cells harboring PTEN mutations or PTEN deficiency exhibit activated PI3K signaling, leading to uncontrolled cell survival and growth.

1.1.3 Challenges of inhibiting PI3K and RAS pathways clinically

Inhibitors targeting PI3K, AKT, RAF, and MEK have been tested in clinical studies, with unexceptional efficacy and safety profiles. Here I will briefly review these pathway inhibitors and some of the challenges inhibiting their development. RAF inhibitors have proven to be effective only in BRAF-mutant cancers (e.g. BRAFV600E-mutant melanoma) but not in cancers with active RAS-RAF-MEK-ERK driven by other mutations (38). Similarly, MEK inhibitors have had limited efficacy in clinical trials when used as single-agent therapies (39). At least thirteen individual MEK inhibitors have been tested clinically, but only one (Trametinib, GlaxoSmithKline) has shown clinical efficacy and received FDA approval. Like RAF inhibitors, Trametinib is indicated only for patients with BRAF-mutated melanoma (40,41).

PI3K inhibitors have acceptable safety when used as monotherapy, but only modest antitumor effects (42), and of the 21 PI3K inhibitors in clinical trials, just one (Idelalisib, Gilead

Sciences) has received FDA approval for several indications in leukemia and lymphoma (43,44). PI3K inhibitors are likely to be most effective when used in combination with other inhibitors (i.e. chemotherapy, RTK inhibitors, and MEK inhibitors) (45,46). AKT inhibitors are also being developed and have demonstrated promising efficacy, but also have some safety concerns including skin rashes and hyperglycemia, and combination approaches are being explored (45-48). Due to the limitations of PI3K and AKT inhibitors in clinical studies, novel isoform-specific inhibitors, as well as inhibitor combinations, are being explored for clinical efficacy and safety.

Some of the lack of efficacy of PI3K-AKT and MEK-ERK pathway inhibitors that has been observed in clinical trials can be attributed to compensation. For example, MEK inhibitors block MEK-ERK signaling, but also promote PI3K-AKT pathway activation through RTK activation (49,50). This compensation in pro-survival signaling enables cancer cells and tumors to develop resistance to kinase inhibitors. Due to the disappointing efficacy of PI3K and MEK inhibitors as monotherapies, combination therapies with PI3K and MEK inhibitors have been explored in several clinical trials (51). In fact, approximately two-thirds of PI3K/AKT/mTOR inhibitor trials are testing combination approaches, including combinations with chemotherapy, as well as with additional kinase inhibitors (i.e. MEK inhibitors) (45). Although combined inhibition of both PI3K-AKT and MEK-ERK pathways improves efficacy and addresses pathway compensation challenges, several dual inhibitor treatments have failed due to significantly higher toxicities than monotherapies. (45,52). For example, drug-related toxicities were observed in 53.9% of patients when treated with combination of a MEK and a PI3K inhibitor (including transaminase elevations, skin rash, and mucositis), compared to only 18.1% in patients receiving monotherapy (45,51). Therefore, despite high expectations, combined inhibition of PI3K-AKT and RAS-RAF-MEK-ERK has not yet proven to be a viable therapeutic option. Nonetheless, simultaneous inhibition of both pathways remains an intriguing strategy to treat cancer. Researchers in this field continue to

explore alternative inhibitors, inhibitor combinations, and novel targets to safely and effectively inhibit these pathways for therapeutic benefit.

1.1.4 Oncogene and non-oncogene addiction

Many cancers in which PI3K-AKT and RAS-RAF-MEK-ERK pathways are activated may become entirely dependent on these pathways for cell survival and proliferation. The terms “oncogene addiction” and “tumor suppressor gene hypersensitivity” describe this dependency of cancer cells on particular genetic mutations or activation of oncogenic pathways to maintain the malignant phenotype (4,53). This addiction to a particular gene/protein provides a promising strategy for cancer treatment, as it suggests that targeted inhibition of a specific oncogene may be sufficient to impair cancer cell proliferation and induce cell death. Oncogene addiction results in a critical weakness that can be exploited to improve cancer therapy (53). For example, HER2-positive breast cancer is a breast cancer subtype driven by amplification of the RTK HER2, making it attractive for oncogene-targeted therapy. In 1998, the FDA approved trastuzumab (trade name Herceptin, Genentech), a monoclonal antibody targeted to the HER2 receptor, for the treatment of HER2+ breast cancer. Trastuzumab in combination with chemotherapy significantly reduces tumor size and improves overall patient survival compared to chemotherapy alone (54-56). Thus, targeting a specific oncogene is an effective and clinically-relevant method to treat cancer. Additional oncogenes and targeted oncogene inhibitors are being researched and developed as targeted cancer therapeutics.

In addition to identifying cancer targets via oncogene addiction, an emerging source of potential cancer therapy targets may be found via the study of non-oncogene addiction. The reliance of cancer cells on oncogenes is well-studied and continues to guide the discovery of therapeutic targets (57). Non-oncogene addiction, the dependence of a cancer cell on a gene that

is not mutated and unable to induce transformation, has begun to yield additional targeted treatment options (58,59). A key characteristic of non-oncogene addiction is the differential response in cancer versus normal cells. Cancer cells may become particularly reliant on, or addicted to, a non-oncogene to support proliferation and survival, whereas normal cells may tolerate loss of the same gene. For example, BRCA2-mutant cancers have a defect in double-strand DNA break repair and consequently are particularly sensitive to DNA damage inducing agents (e.g. cisplatin) (60,61). Interestingly, BRCA2 mutant cancer cells are also heavily reliant on single-strand DNA repair mechanisms. Inhibition of Poly-ADP-ribose polymerase (PARP1), a DNA single strand repair enzyme, has emerged as a viable treatment option in BRCA2-mutant cancers (62). PARP1 is not an oncogene, PARP1-/- mice are viable (63), and in the absence of genotoxic stress, PARP1 is not required for normal cell survival (64,65). Therefore, the dependence of BRCA2 mutant tumors on PARP1-mediated DNA repair is an example of non-oncogene addiction. PARP1 inhibitors are lethal in BRCA2 mutant cancer cells (62), and have been developed and successfully utilized in the clinic (66,67). Olaparib (Lynparza) received FDA approval in 2014 for patients with advanced ovarian cancer bearing BRCA mutations, and ongoing clinical trials are exploring the benefit of olaparib in BRCA-mutant breast cancer. These results confirm the clinical relevance of targeting non-oncogene addiction for therapeutic benefit.

New genes and proteins that function via oncogene and non-oncogene addiction to promote cancer cell survival and proliferation are being characterized. Identification of new targets leads to development of improved therapeutics against these novel targets, resulting in better outcomes for patients. There is a significant unmet need to identify novel therapeutic targets in TNBC and other cancers driven by PI3K-AKT and RAS-RAF-MEK-ERK signaling. This dissertation presents compelling evidence for CIB1 as a novel therapeutic target in TNBC.

1.2 CIB1 Introduction

CIB1 was discovered in 1997 as a binding partner of the integrin αIIb cytoplasmic tail (68). Over the past 18 years, CIB1 structure and function have been explored in cardiovascular disease, cancer, and other diseases. Here I will introduce CIB1 by reviewing CIB1 structure, binding partners, cell biology, and relevant diseases.

1.2.1 CIB1 structure

CIB1 is a 191 amino acid (22kDa) calcium-binding protein with an N-terminal myristoylation site (68-70). The structure of CIB1 was determined by multiple studies, utilizing techniques including NMR (71-74), circular dichroism (69), and X-ray crystallography (75,76). The current consensus CIB1 structure is primarily influenced by the crystal structure solved by Gentry et al (75), and NMR studies performed by Hans Vogel and colleagues (71). CIB1 is composed of 10 α-helices including 4 EF-hands, helix-loop-helix structures capable of divalent cation binding, which form the core structure of CIB1 (75). Two of these EF-hand domains bind divalent cation. Calcium binds tightly to EF-III (1.9 μM) and EF-IV (0.5 μM) (71,75). Mg^{2+} binds EF-III as well, but with lower affinity than Ca^{2+}. Two additional auxiliary Ca^{2+}-binding sites exist on the surface of the N-terminal domain and contribute to CIB1 folding. The N-terminal and C-terminal α-helices do not participate in the EF-hand structure. The C-terminal α-helix (H10) of CIB1 lays in a hydrophobic binding pocket and is proposed to undergo displacement to enable CIB1 interaction with integrin αIIb and other binding partners (71,72).

The structure of CIB1 changes when bound by different divalent cations. For example, Mg^{2+}-bound CIB1 is more flexible in the C-terminus than Ca^{2+}-bound CIB1 (71). These structural differences may suggest that CIB1 undergoes conformational changes in response to cellular divalent cation availability, as has been shown for several CIB1 homologs (71,77). For example, CIB1 has been proposed to function as a Ca^{2+}/myristoyl switch protein (78-80). Further studies are required to explore whether cation-dependent conformational changes are relevant to CIB1

function. In summary, CIB1 is a small, divalent cation binding protein with a hydrophobic binding pocket capable of interacting with multiple binding partners.

1.2.2 CIB1 Binding partners

CIB1 was discovered as a binding partner of the integrin αIIb cytoplasmic tail, and has since been shown to bind many other proteins. CIB1 reportedly binds to at least 41 partners, making it a promiscuous and functionally diverse protein (see Table 1-2). Binding partners include nuclear, cytoplasmic, and transmembrane proteins (see Figure 1-3). It has been proposed that CIB1 is diffusely expressed throughout the cytoplasm and nucleus in normal resting cells, but that CIB1 can localize to a particular subcellular area or binding partner upon cellular activation or stimulation, such as fluctuations in intracellular Ca2+ concentration (70,78,79,81-85). Further work is necessary to fully characterize CIB1 interactions, including cell type specificity, and responses to signals and stimuli.

The interaction of CIB1 with several serine/threonine kinases, PAK1 and PDK1, as well as the aforementioned interaction between CIB1 and integrin cytoplasmic tails, are of particular interest to this discussion. CIB1-integrin binding will be introduced below, and discussed in detail in Chapter 3.

CIB1-dependent activation of PAK1 (p21 protein(Cdc42/Rac)-activated kinase 1) has important implications in cell migration and in pro-survival and pro-proliferation signaling (86). CIB1 binds to two sites within the N-terminus of PAK1 and induces PAK1 autophosphorylation, and this stimulation of PAK1 activity occurs independent of known PAK1 activators, the small GTPases Cdc42 and Rac (86). CIB1-dependent activation of PAK1 may have several consequences, including regulation of cell migration (see Section 1.2.4), and MEK-ERK and AKT signaling. PAK1 binds and phosphorylates both RAF and MEK, thereby promoting RAS-RAF-

MEK-ERK signaling (87-91). Interestingly, PAK1 may also facilitate MEK-ERK pathway activation independent of its kinase activity by serving as a scaffold to facilitate RAF-MEK binding and activation (92). This scaffolding function was previously observed in PI3K-PDK1-AKT signaling, where PAK1 functions as a scaffold between PDK1 and AKT to facilitate AKT Threonine (Thr) 308 phosphorylation (93-95). It is probable that CIB1 regulates AKT and ERK signaling via its interaction with PAK1 (96).

CIB1 also binds and activates PDK1 (3-phophoinositide-dependent protein kinase 1), the enzyme that links PI3K and AKT signaling (97). PI3K generates PIP3, and PIP3 binding to PDK1 is necessary for PDK1 activity. Therefore, localization of PDK1 to the cell membrane is a prerequisite for PDK1 activation of its substrates, including phosphorylation of AKT at Thr 308 (98-100). Zhao et al discovered CIB1 as a PDK1 binding partner, and proposed that CIB1 shuttles PDK1 to the cell membrane, thereby facilitating PDK1-AKT interaction and AKT phosphorylation (97). Importantly, CIB1-PDK1 binding was demonstrated to be important for cancer cell survival and inhibition of stress-induced apoptosis (97).

Taken together, these studies suggest that CIB1 binding to PAK1 and PDK1 is essential to promote the MEK-ERK and PI3K-AKT signaling pathways, as well as cell survival and proliferation.

CIB1 binding partner	Method to Determine Interaction	Location of Interaction	CIB1 effect (↑) Activates (↓) Inhibits (−) Interacts/ Unknown
AID	Y2H (101), In Vitro Pulldown (101), Co-IP (101)	Nucleus	−
DNA-PKcs	Y2H (102), In Vitro Pulldown (102,103), Co-IP (104)	Nucleus	↑
EDD	Y2H (105), In Vitro Pulldown (105), Co-IP (105)	Nucleus	−
hTERT	Y2H (104), Co-IP (104)	Nucleus	↑
PAX3	Y2H (106), In Vitro Pulldown (106)	Nucleus	↓
TRF2	Y2H (103), In Vitro Pulldown (103)	Nucleus	↑
InsP(3)R	In Vitro Pullodwn (107), Co-IP (85)	ER Membrane	↓
Presenilin-2	Y2H (108), Affinity Chromatography (108), Co-IP (108), In vitro Pulldown (80)	ER Membrane	↑
G1P3	Y2H (109), In Vitro Pulldown (109), Co-IP (109)	Mitochondria	−
ASK1	Y2H (84), In Vitro Pulldown (84), Co-IP (84,85)	Cytoplasm	↓
Calcineurin B	Y2H (110), In Vitro Pulldown (110), Co-IP (110)	Cytoplasm	↑
Caspase-2S	Y2H (111), In Vitro Pulldown (111), Co-IP (111)	Cytoplasm	−
FAK	Co-IP (112)	Cytoplasm	↑
FNK (PLK3)	Y2H (113), ELISA (113,114), Co-IP (114,115)	Cytoplasm	↓
LMO3	Y2H (116), Co-IP (116)	Cytoplasm	−
Myo1c	Co-IP (117), In Vitro Pulldown (117)	Cytoplasm	−
NBR1	Y2H (118)	Cytoplasm	−
PAK1	Co-IP (86), ELISA (86), SPOT peptide assay (86)	Cytoplasm	↑
PDK1	Co-IP (97)	Cytoplasm	↑
Rac3	Y2H (119), Co-IP (119)	Cytoplasm	−
SCG10 (Stathmin 2)	Y2H (120), In Vitro Pulldown (120)	Cytoplasm	↓
SNK (PLK2)	Y2H (113), ELISA (113), Co-IP (121)	Cytoplasm	↓
Sphingosine Kinase 1	Y2H (78), In Vitro Pulldown (78), Co-IP (78)	Cytoplasm	↑
Src	Co-IP (122)	Cytoplasm	−
WASP	Y2H (123), SPR (123), Co-IP (123)	Cytoplasm	−
Bcl-2	Co-IP (109)	Plasma Membrane	−
EphrinA2	Co-IP (82)	Plasma Membrane	↑
Integrin αIIb	Y2H (68), Co-IP (81,83), In Vitro Pulldown (68), ELISA (124), ITC (70,124), Intrinsic Tryptophan Fluorescence (69), NMR (74)	Plasma Membrane	↑(83) ↓(81)
Integrin αV/α5	Co-IP (124), ELISA (124), ITC (124)	Plasma Membrane	−
Integrin α2/α3/α4/αM/αL	ELISA (124), ITC (124)	Plasma Membrane	−
Integrin α11	Y2H (125), Co-IP (125)	Plasma Membrane	−
L-type Calcium Channel	Co-IP (126)	Plasma Membrane	−
NCX1	Co-IP (126)	Plasma Membrane	−
Tas1r2	Y2H (79), Co-IP (79)	Plasma Membrane	↓
Factor VIII	Y2H (127), Co-IP (127)	Extracellular	−

Table 1-2. Table of CIB1 binding partners. A comprehensive list of CIB1 binding partners reported in the literature, including techniques used to detect the interaction, the cellular location of the interacting protein, and the role of CIB1 binding (e.g. activation).

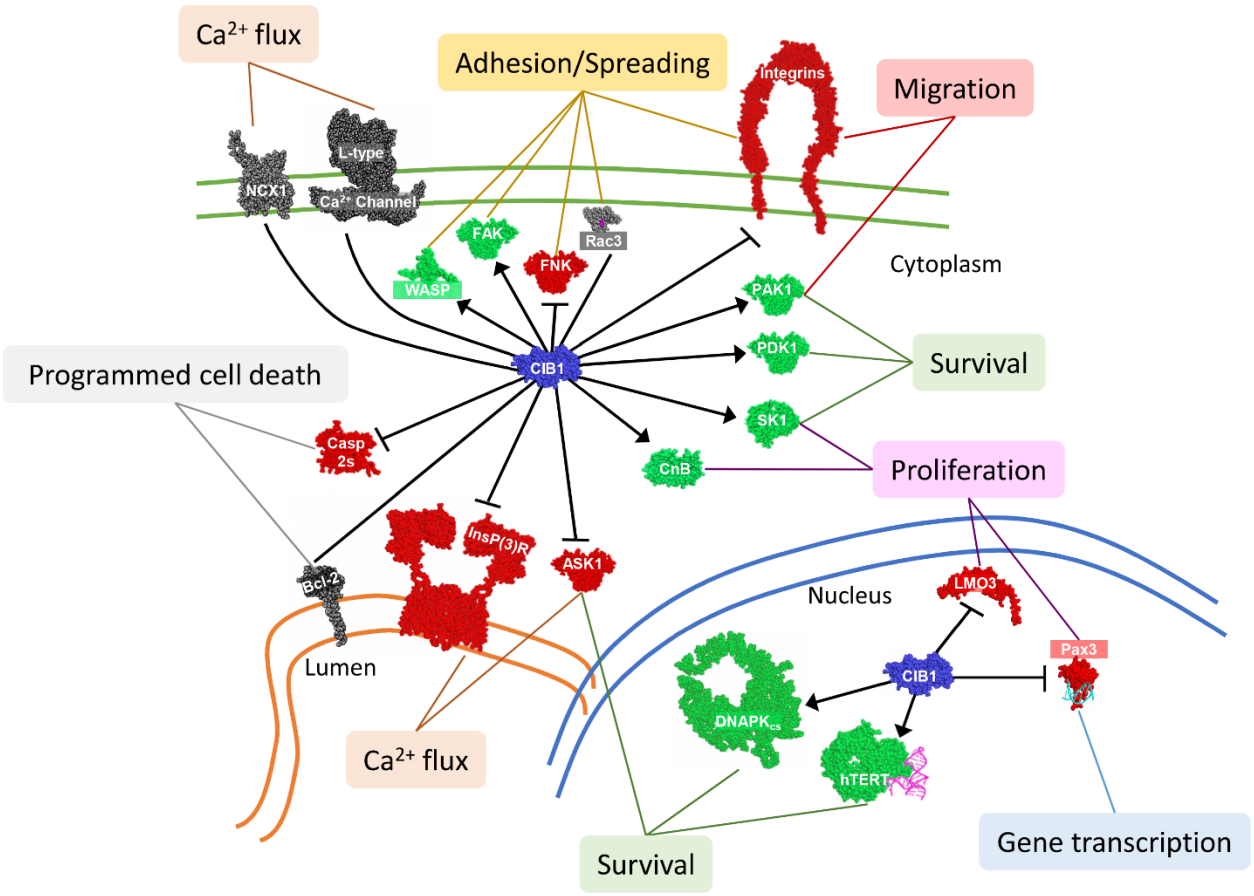

Figure 1-3. Network of CIB1 binding partners. CIB1 (blue) interacts with numerous binding partners in the cytoplasm and nucleus. CIB1 often inhibits (red) or enhances (green) a protein's activity, but in some cases the effect of CIB1 binding is unresolved (gray).

1.2.3 CIB1 in integrin αIIbβ3 signaling and function

Following identification of CIB1 as a binding partner for the platelet-specific integrin αIIb cytoplasmic tail, early studies from our lab and others focused on understanding the molecular and cellular consequences of this interaction. Platelets are anucleate circulating blood cells that become “activated” and contribute to thrombus/clot formation in response to vascular injury. As the major adhesion receptor on platelets and megakaryocytes (platelet precursor cells), integrin αIIbβ3 plays a critical role in the process of platelet-platelet adhesion (aggregation) and spreading. It was hypothesized that CIB1 may play an important role in platelet function by either regulating αIIbβ3 activation (inside-out signaling) or αIIbβ3 ligand binding and downstream signaling (outside-in signaling) (see Figure 1-4). Because platelets are not amenable to direct genetic manipulation, many of the early studies exploring CIB1 function utilized primary megakaryocytes and megakaryocyte-like cell lines to understand how CIB1 may regulate αIIbβ3 outside-in and/or inside-out signaling events.

Yuan, et al explored the role of CIB1 in αIIbβ3 inside-out signaling, and reported that overexpression of CIB1 in megakaryocytes completely inhibits agonist-induced fibrinogen binding, while overexpression of a CIB1 mutant that does not bind to the αIIb tail fails to suppress αIIbβ3 activation (81). In addition, RNAi depletion of CIB1 enhances agonist-induced αIIbβ3 activation, indicating that CIB1 is a negative regulator of αIIbβ3 activation (81). Taken together, the data from this study suggest that CIB1 is an inhibitor of integrin αIIbβ3 inside-out signaling.

Alternatively, some evidence supports a role for CIB1 in integrin αIIbβ3-dependent outside-in signaling. Several studies show that CIB1 promotes platelet and megakaryocyte adhesion to fibrinogen, potentially by stimulating FAK activity (123,128). Furthermore, multiple pieces of evidence suggest that CIB1 preferentially binds to activated integrin αIIbβ3 compared to resting αIIbβ3 (81,129). In addition to the studies exploring the role of CIB1 in platelets and megakaryocytes, CIB1-dependent regulation of integrin αIIb has been investigated in

complementary studies in Chinese Hamster Ovary (CHO) cells overexpressing integrin αIIbβ3. CIB1 overexpression in these cells resulted in increased cell spreading and cell migration on fibrinogen, reportedly through the interaction between CIB1 with Rac3 (119,122). Cumulatively, these studies suggest that CIB1 may promote integrin αIIbβ3 dependent outside-in signaling.

We and others used CIB1 knockout (CIB1-/-) mice to study the role of CIB1 in platelet function, with somewhat differing results from different groups. Naik, et al reported that CIB1-/- mice have impaired hemostasis (extended tail bleeding time). Because they found that CIB1-/- platelets are also defective in spreading on fibrinogen (the ligand for αIIbβ3) compared to WT platelets (130), and that blocking CIB1 with anti-CIB1 antibody decreased platelet spreading (83), they concluded that CIB1 is required for outside-in signaling. However, Denofrio, et al found no defects in CIB1-/- mouse hemostasis or platelet spreading (131). While much is known about the molecular interaction between CIB1 and integrin αIIb, further studies are required to elucidate the specific role of CIB1 in inside-out versus outside-in signaling, and to definitively determine whether CIB1 is necessary for hemostasis regulation.

Although CIB1 was originally discovered as a binding partner of the αIIb cytoplasmic domain, recent evidence published by Freeman, et al indicates that CIB1 may bind to and regulate all integrins via interaction with multiple α-integrin tails. (124) Because CIB1 binds many integrins, and is expressed in many tissue types, it is plausible that CIB1 may be a broad regulator of integrin function, including integrin-dependent adhesion and migration in many cell types (108,111,118,124,132).

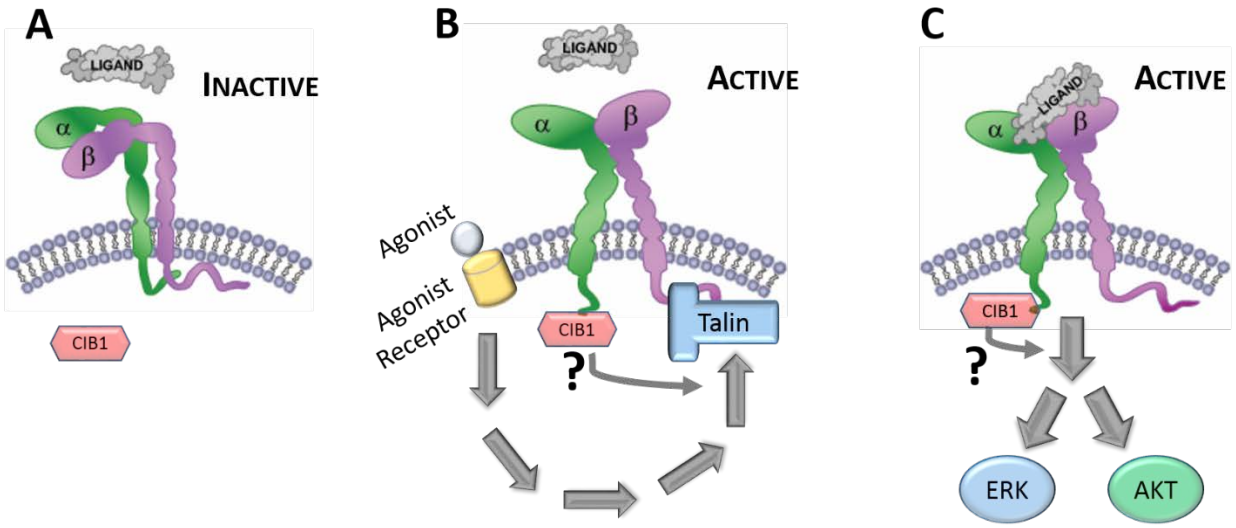

Figure 1-4. Integrin inside-out and outside-in signaling and potential roles of CIB1 A) Integrin αβ heterodimer in resting (bent) conformation, or inactive low affinity state. B) Agonist induced inside-out integrin activation. An agonist binds to a receptor on the cell surface. A cascade of intracellular signaling events is triggered, culminating in binding of talin and other activating factors to the β-integrin cytoplasmic tail, inducing a conformational shift and integrin activation that allow high-affinity ligand binding. It is unclear whether CIB1-integrin binding affects inside-out integrin signaling. C) Integrin outside-in signaling. Ligand binding to integrin αβ heterodimer induces transmission of signals into the cell, including activation of pathways known to be regulated by CIB1. The role of CIB1-integrin binding on outside-in signaling is also unknown.

1.2.4 CIB1 in cell migration

The role of CIB1 in cell migration has been explored in multiple contexts, and an interesting dichotomy has emerged with some studies concluding that CIB1 inhibits cell migration, and contradictory reports suggesting that CIB1 promotes cell migration. Several studies concluded that CIB1 expression resulted in increased cell migration on fibronectin in CHO, T47D, HUVEC, primary mouse endothelial cells, and megakaryocytes (122,128,133,134). One proposed mechanism through which CIB1 could promote cell migration is through activation of kinases ERK and PI3K (122). In contrast to these reports, Leisner, *et al* published that CIB1 inhibits cell migration on fibronectin in fibroblast cells via interaction with PAK1. CIB1 binds to PAK1 via the NH_2-terminal autoinhibitory domain, thereby activating PAK1 and stimulating PAK1-dependent LIMK/cofilin signaling resulting in decreased actin polymerization, and consequently decreased migration (135). Although multiple studies have observed CIB1-dependent effects on cell migration, different studies have reported different outcomes on cell migration. It is possible that these discrepancies are due to varying cell types and/or fibronectin concentrations used. Nonetheless, these studies indicate that CIB1 plays an important role in regulating cell migration via activation of cellular signaling pathways.

1.2.5 CIB1 in calcium signaling

Calcium has long been shown to be relevant to CIB1 function. Numerous publications indicate that intracellular Ca2+ and Mg2+ concentrations may affect the interactions between CIB1 and many of its binding partners (68,70,78,79,84,107,120,124). As discussed above (see Section 1.2.1) divalent cation binding alters the CIB1 structure and facilitates its molecular binding to the integrin αIIb cytoplasmic tail and presumably other binding partners (70,74,136). The binding affinity between CIB1 and integrin αIIb CT is significantly enhanced in the presence of

either Ca2+ or Mg2+. Although cation-dependent structural differences in CIB1 allude to functional consequences such as altered ligand binding, no significant difference in CIB1 binding to αIIb CT has been observed between Ca2+-CIB1 and Mg2+-CIB1 (70,74).

Several studies have explored how CIB1 regulates Ca2+ signaling, as well as how intracellular Ca2+ concentrations affect CIB1 function. Interaction of CIB1 with the inositol 1,4,5 triphosphate receptor (InsP3R) Ca2+ release channel was found to inhibit Ca2+ release from the endoplasmic reticulum (79). In separate studies, ASK1 was shown to bind competitively to CIB1 and decrease CIB1-InsP3R binding, resulting in increased Ca2+ release, and ROS-induced cell death (85). Interestingly, increased Ca2+ decreases CIB1-ASK1 binding, suggesting a potential feedback mechanism by which CIB1 may regulate, and be regulated by, intracellular Ca2+ release (84). This interplay between CIB1 and intracellular Ca2+ has potentially significant functional consequences. CIB1 binding to ASK1 inhibits ASK1 kinase activity, interferes with ASK1 binding to additional binding partners (e.g. TRAF2), and mitigates ROS-induced cell death in SH-SY5Y neuroblastoma cells (84). These results indicate an important role for CIB1 in the relationship between ASK1 and InsP3R in Ca2+-dependent signaling and maintenance of cell viability. Further studies are necessary to better understand the cellular consequences of Ca2+ concentration on CIB1 interactions and function. Although many details remain unknown, these results suggest that changes in intracellular divalent cation concentrations and binding to CIB1 are likely to influence CIB1 function.

1.2.6 CIB1 myristoylation

CIB1 is N-terminally myristoylated, a modification that may have important implications in CIB1 cellular localization and signaling (78-80,110). Myristoylation, the post-translational addition of a 14-carbon saturated fatty acid myristoyl moiety to the N-terminal glycine of a target protein,

is an essential cellular process with implications in cancer and infectious diseases (137). Interfering with CIB1 myristoylation via mutations or protein fusions at the CIB1 N-terminus interferes with the cellular functions of CIB1 (78,79,97,108,110). Several publications concluded that CIB1 myristoylation is important to direct CIB1 to the membrane (79) and to facilitate shuttling of CIB1 binding partners, such as sphingosine kinase 1 (SK1) (78) and calcineurin B (CnB) (110), to the membrane. Some myristoylated proteins such as recoverin and visinin-like protein 1 (VILIP-1) behave as Ca2+/myristoyl switches, where the protein undergoes a conformational shift upon binding to Ca2+, leading to the exposure of the buried N-terminal myristoyl moiety to the intracellular environment (138,139). While no structural evidence exists that CIB1 behaves in such a manner, Jarman, et al reported that CIB1 functions as a Ca2+/myristoyl switch and shuttles SK1 to the cell membrane in an agonist- and Ca2+-dependent manner. CIB1 interacts with the calmodulin binding site of SK1 and is required for SK1-dependent generation of the anti-apoptotic signaling molecule sphingosine-1-phosphate to promote SK1-dependent cell survival (78). The authors proposed an interesting model, whereby cytoplasmic CIB1 binds to Mg2+ under basal conditions which prevents the interaction of CIB1 and SK1. Upon increased intracellular Ca2+, the myristoyl group is released, enabling CIB1 to shuttle various binding partners to the membrane. Despite some controversy over whether CIB1 functions as a Ca2+/myristoyl switch per se (79,80), these findings suggest a mechanism by which CIB1 can regulate binding partner function at the cell membrane. Further studies are necessary to determine whether CIB1 in fact functions as a Ca2+/myristoyl switch and to further define how CIB1 myristoylation affects cell biology and disease.

1.2.7 CIB1 in cell survival and proliferation

A growing body of evidence supports an important role for CIB1 in promoting cancer cell survival and proliferation. Cells vigilantly regulate their survival and proliferation via several signaling pathways. Uncontrolled cell survival and proliferation can result in tumor development

and cancer, as well as other diseases. The first reported observation of a CIB1-dependent effect on cell proliferation came in 2006, when Yuan, et al reported that MEFs derived from CIB1-/- embryos proliferated at a slower rate than WT MEFs (140). In subsequent studies, endothelial cells derived from CIB1-/- mice also showed reduced proliferation rates compared to WT controls, providing additional evidence for a compelling link between CIB1 and proliferation (133). Recently, several independent reports have suggested that CIB1 promotes cancer cell proliferation and survival by regulating oncogenic signaling pathways (78,84,85,96,141,142). Leisner et al. explored one potential mechanism through which CIB1 promotes proliferation and survival and found that CIB1 promotes the activation of ERK and AKT, essential components of two pro-proliferation and pro-survival signaling pathways frequently activated in breast cancer (96,143). The Ras-Raf-MEK-ERK and PI3K-AKT pathways are frequently activated in cancer cells (144). RNAi knockdown of CIB1 in MDA-MB-468 breast cancer cells and SK-N-SH neuroblastoma cells led to decreased ERK and AKT phosphorylation and induced translocation of GAPDH to the nucleus. Nuclear GAPDH either induces or correlates with several additional events, including the activation of histone variant γH2AX and checkpoint protein CHK1. These events are markers of, or directly lead to, DNA damage, dysregulation of cell cycle checkpoints, and induction of non-apoptotic cell death (96). It is likely that CIB1 promotes ERK and AKT activation via its interactions with PAK1 and PDK1 (see Figure 1-5). Additional studies provide evidence that CIB1 promotes ERK and AKT activation and signaling, supporting the mechanism proposed by Leisner, et al (82,122,135).

A growing body of evidence indicates that CIB1 depletion may lead to decreased cancer cell proliferation and survival. Further work is necessary to better understand the primary and secondary pathways involved in this important cellular phenotype, and to understand how CIB1 may regulate cell survival and proliferation in various diseases, including cancer.

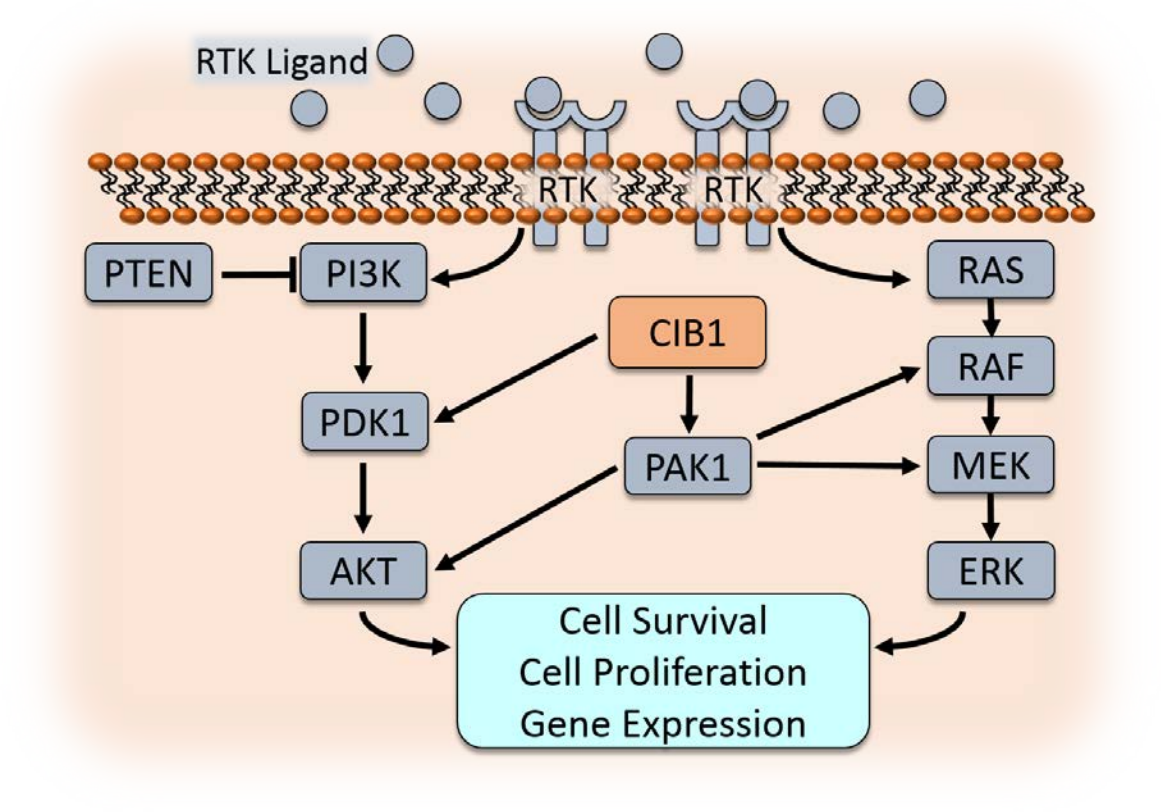

Figure 1-5. Role of CIB1 in activation of AKT and ERK signaling pathways Extracellular RTK ligands (e.g. EGF) bind to RTK (receptor tyrosine kinase, e.g. EGFR) leading to RTK activation. Activated RTK, either directly or indirectly, activates PI3K and RAS, initiating a cascade of events that promote cell survival, cell proliferation, and gene expression. CIB1 binds to and activates PAK1, which activates MEK-ERK signaling and facilitates activation AKT. CIB1 also binds and activates PDK1, a direct upstream activator of AKT. Through its interaction with PAK1 and PDK1, CIB1 promotes activation of MEK-ERK and PI3K-AKT signaling, resulting in cell survival, cell proliferation, and gene expression.

1.2.8 CIB1 in Cancer

Cancer is a heterogeneous disease caused by oncogene activation and/or tumor suppressor inactivation. Cancer cells become reliant on cell signaling pathways to promote cell survival and proliferation (53). For example, many basal-like breast tumors exhibit activated ERK and AKT signaling pathways (28,145,146). In addition, cancer cells may become reliant on non-oncogenes via non-oncogene addiction, a description of non-mutated non-overexpressed genes/proteins that are essential for cancer cell survival but dispensable for normal cells (58).

In addition to internal factors driving tumor cell survival and proliferation, growing tumors depend on a steady blood supply to provide nutrients and oxygen (147). As tumors grow, they stimulate new blood vessel growth, a process termed tumor-induced angiogenesis. Angiogenesis inhibitors have been researched and used clinically to prevent tumor growth and induce tumor regression (e.g. bevacizumab) (148,149). The role of CIB1 in tumor-induced angiogenesis has been explored using molecular, cellular, and in vivo models.

CIB1 is important in two critical aspects of tumor growth: cell survival and tumor-induced angiogenesis. As described above (Section 1.2.7), numerous publications have reported that CIB1 depletion from cancer cell lines results in a decrease in proliferation and/or an increase in cell death (78,84,85,96,141,142). Furthermore, high CIB1 expression has been implicated in cancer progression and incidence. CIB1 expression was found to be higher in breast tumor tissues relative to patient-matched control tissues (114). In an examination of hepatocellular carcinoma tissues, CIB1 expression was found to be elevated in the tumor margin and tumor center compared to non-tumor tissue, and high CIB1 expression was more prevalent in late stage compared to early stage tumors (141). In addition to its role in cancer cells, CIB1 expression is also essential for endothelial cell function and tumor-induced angiogenesis. Zayed et al demonstrated that CIB1 depletion impaired endothelial cell migration (133). Furthermore, CIB1-/- mice did not support tumor growth; murine tumors grafted into CIB1-/- mice were necrotic due to

a reduced blood supply (150). These data suggest that CIB1 is critical for both tumor cell survival, as well as tumor-induced angiogenesis. CIB1 should be further interrogated in specific cancer subtypes to determine whether it might be a novel therapeutic target.

The significant unmet need for improved therapeutic options for TNBC, and the research demonstrating a role for CIB1 in cancer cell survival and proliferation, served as the stimulus for the research questions explored in Chapter 2 of this dissertation. Here I present compelling evidence that CIB1 is essential for cell survival and tumor growth in one cancer sub-type, TNBC. The growing body of literature, in combination with the data presented herein, supports a potential role for CIB1 in additional cancers as well. Taken together, these data validate CIB1 as a novel therapeutic target for the treatment of cancer, and warrant further investigation in TNBC and other cancer subtypes.

CHAPTER 2: CIB1 DEPLETION IMPAIRS CELL SURVIVAL AND TUMOR GROWTH IN TRIPLE NEGATIVE BREAST CANCER

2.1 Introduction

Breast cancer is diagnosed in over 230,000 people each year in the United States (10). Approximately 16% of all new breast cancer diagnoses are triple negative breast cancer (TNBC), a subtype of breast cancer that lacks expression of estrogen receptor, progesterone receptor, and human epidermal growth factor receptor 2 (11). Many breast cancer therapies target one of these three receptors and are therefore ineffective for the treatment of TNBC.

In breast cancer, and other cancers, cell survival and cell proliferation are driven by oncogenic signaling pathways. A majority of TNBC cases are basal-like, and typically exhibit constitutively activated RAF-MEK-ERK and PI3K-AKT signaling pathways (11,151). Dual inhibition of both ERK and AKT signaling pathways has been identified as a promising approach to treat TNBC (151,152). However, preclinical and clinical studies have suggested that combined inhibition of both PI3K and MEK may improve efficacy at the expense of increased toxicity (17,45,51). New targeted therapies with enhanced efficacy and safety are necessary to improve patient outcomes (14,153).

CIB1 is a small intracellular protein that regulates kinase activity and integrin biology (78,81,84,86,96,113,124), and has an emerging role in cancer cell survival and proliferation via regulation of oncogenic signaling pathways (78,84,85,96,141). For example, CIB1 promotes AKT and ERK activation (82,96), and may regulate these pathways via interaction with the

serine/threonine kinase PAK1 (86,122). We recently showed that CIB1 depletion in two cancer cell lines (SK-N-SH neuroblastoma and MDA-MB-468 TNBC) disrupted both AKT and ERK signaling, resulting in the induction of a DNA damage response and a unique mechanism of non-apoptotic cell death (96).

Because of our initial observation that CIB1 is essential for MDA-MB-468 TNBC growth and survival in vitro, we hypothesized that CIB1 may have a broader role in TNBC and in tumor growth in vivo. Here we present evidence that CIB1 is necessary for proliferation and survival in TNBC cell lines with elevated AKT activation and/or low PTEN expression. We further demonstrate that CIB1 depletion results in dramatic TNBC tumor shrinkage in vivo. To gain further insight into the effects of CIB1 depletion, we present RNA sequence (RNAseq) analysis revealing that CIB1 depletion induces genetic programs that correlate with decreased proliferation and survival, and cell differentiation. We show that high CIB1 expression is not associated with susceptibility to CIB1 depletion or with TNBC patient prognosis. Taken together, these findings are consistent with the emerging theory of non-oncogene addiction, where a subset of TNBCs appear to be reliant on a non-oncogenic protein, CIB1, for cell survival and tumor growth. Our results further suggest that CIB1 may be a novel target for TNBC therapy.

2.2 Results

2.2.1 CIB1 depletion induces cell death in a TNBC cell line panel

Recent reports have indicated that CIB1 promotes survival and proliferation in several cancer cell lines, including one TNBC cell line (84,85,96,141). We therefore screened a panel of eleven TNBC cell lines for their susceptibility to shRNA-mediated CIB1 depletion. We found that CIB1 depletion significantly increased cell death in eight of eleven (73%) cell lines tested (Figure 2-1A). One cell line that showed only a moderate increase in cell death that was not statistically

significant, HCC1143 (Figure 2-1A, P=0.08), did exhibit a significant decrease in proliferation rate (Figure 2-2A, P<0.003). Ultimately, we observed some response in either cell viability, cell proliferation, or both, in nine out of eleven TNBC cell lines.

Pharmacological inhibition of both the ERK and AKT signaling pathways, but not either pathway alone, induces TNBC cell death (96,154). We previously showed that CIB1 depletion impaired both ERK and AKT activation, leading to significant cell death in MDA-MB-468 cells (96).

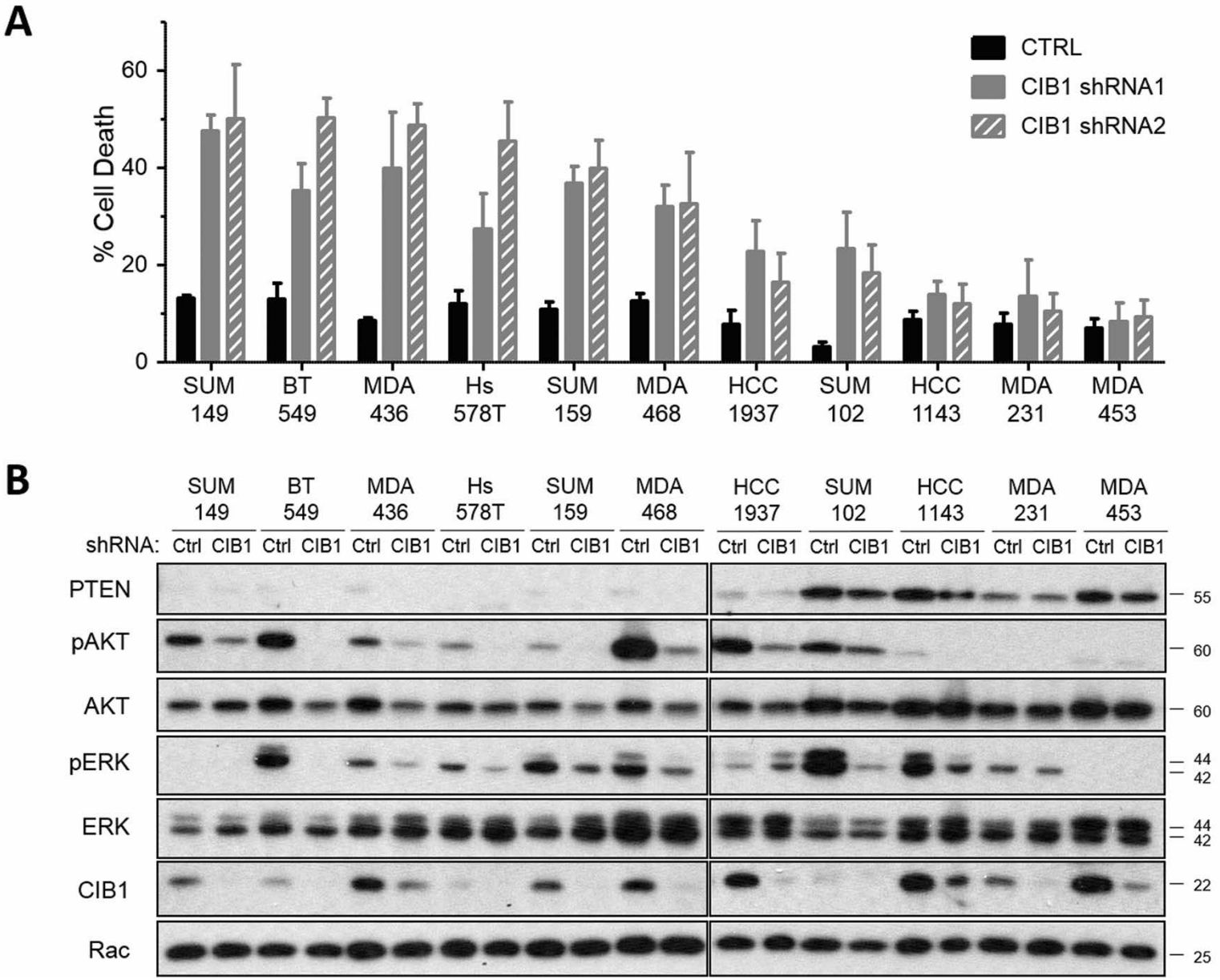
A
% Cell Death
0
20
40
60
CTRL
CIB1 shRNA1
CIB1 shRNA2
SUM 149
BT 549
MDA 436
Hs 578T
SUM 159
MDA 468
HCC 1937
SUM 102
HCC 1143
MDA 231
MDA 453
B
shRNA: Ctrl CIB1
PTEN
pAKT
AKT
pERK
ERK
CIB1
Rac
55
60
60
44
42
44
42
22
25

Figure 2-1. CIB1 depletion induces cell death in a panel of TNBC cell lines. A) A panel of 11 TNBC cell lines were transduced with either control (CTRL) or two separate CIB1 shRNA targeting sequences. Results are expressed as the mean percentage of dead cells (i.e. trypan blue positive cells) from both adherent and floating cell populations, data represent mean ± SEM from n ≥ 3 experiments. P-values were calculated using Student's T-test. **P<0.01; *P<0.05. B) Relative protein levels of PTEN, pAKT, AKT, pERK, ERK, CIB1, and Rac (additional loading control) in TNBC cell lines treated with CTRL or CIB1 shRNA as in (A). All membranes were processed under the same conditions. Blots are representative of three independent experiments. Figure used with permission from (155).

Therefore, we compared activated (phosphorylated) ERK (pERK) and AKT (pAKT) levels in CIB1-depleted versus control cells in the TNBC cell line panel (Figure 2-1B). We first noted that CIB1 depletion resulted in decreased pERK and pAKT in most cell lines. Interestingly, we observed that CIB1 depletion increased cell death in all eight cell lines that have relatively high basal levels of pAKT, and noted that seven out of these eight cell lines also had elevated pERK. However, pERK is also elevated in two out three cell lines that did not respond to CIB1 depletion and, therefore, ERK phosphorylation status does not appear to be a good predictor of sensitivity to CIB1 depletion.

Because the tumor suppressor PTEN is an upstream inhibitor of AKT activation and several of the cell lines from our TNBC panel have PTEN mutations (Table 2-1), we also interrogated the PTEN status in each TNBC cell line. Interestingly, PTEN protein expression was absent or reduced in seven of eight cell lines that responded to CIB1 depletion, but was normal in all three cell lines that were not sensitive to CIB1 depletion (Figure 2-1B). These results suggest that PTEN status may be an additional predictor of responsiveness to CIB1 inhibition. To further explore differences between sensitive and insensitive cell lines, we examined gene expression microarray data (156) for each cell line in the panel. Using Significance Analysis of Microarrays, we identified two genes that were significantly (false discovery rate equal to zero) upregulated in cells that are insensitive to CIB1 depletion, NBEA (fold change +5.6) and FUT8 (fold change +4.9). As both of these genes are involved in cell differentiation, we compared the average Differentiation Score (156,157) of the sensitive and insensitive cell lines and found that cell lines that were not sensitive to CIB1 depletion trended toward a more differentiated state compared to the cell lines that were sensitive to CIB1 depletion (Figure 2-2). Finally, we observed that CIB1 expression was variable in the TNBC cell line panel, and that there was no association between high CIB1 expression and sensitivity to CIB1 depletion. These results indicate that CIB1 inhibition

may be a therapeutic approach to induce TNBC cell death regardless of CIB1 expression levels, particularly in cells with high basal levels of pAKT and/or low levels of PTEN.

To determine whether CIB1 depletion induces cell death in other breast cancer subtypes, we measured the effect of CIB1 depletion in three non-TNBC mammary cell lines: ZR-75-1 (Luminal A subtype); SKBR3 (HER2 overexpressing); and ME16C (non-cancerous mammary epithelial cell line). We observed a significant increase in cell death in CIB1-depleted ZR-75-1 cells (Figure 2-3). Consistent with our observations from the TNBC cell line panel, the ZR-75-1 cells are PTEN-null, whereas SKBR3 and ME16C are PTEN WT and do not have increased cell death upon CIB1 depletion. These data suggest that, in addition to TNBC, CIB1 inhibition may be effective in additional PTEN-null breast cancers and other cancers.

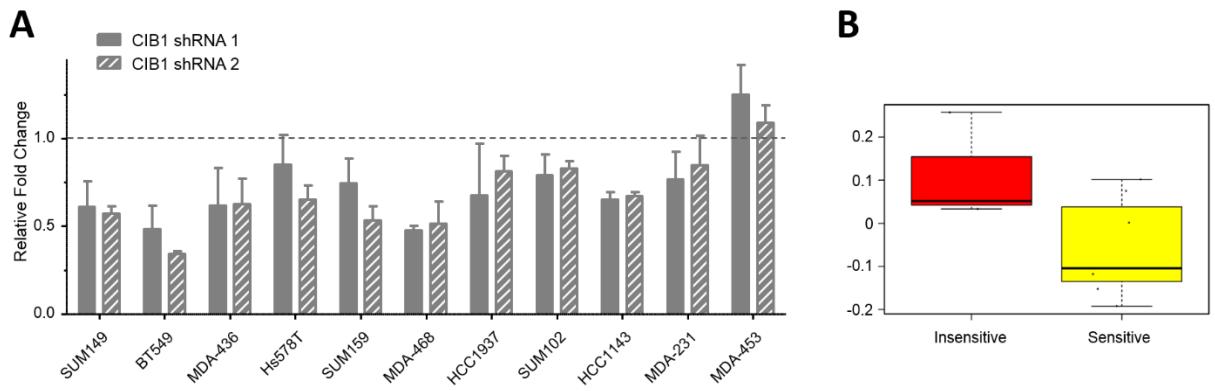

Figure 2-2. CIB1 depletion reduces cell proliferation in a panel of TNBC cell lines. A) A panel of 11 TNBC cells lines were transduced with either control (SCR) or two separate CIB1 shRNA targeting sequences (CIB1 shRNA1 or shRNA2). SCR was normalized to 1.0 (dotted line) and graph represents relative mean fold change in total cell count ± SEM for each CIB1 shRNA treated sample ($n \geq 3$). B) Average differentiation score of sensitive and insensitive cell lines from TNBC cell line panel. Cell lines sensitive to CIB1 depletion trend toward a lower differentiation score than insensitive cell lines ($p = .0695$). Figure used with permission from (155).

Cell Line	PTEN mutation	PTEN Protein	Source
SUM149	GPM (micro-CNI)	Null	(35,158)
BT549	822delG (L295X)	Null	(35,159)
MDA-436	GPM (micro-CNI)	Null	(35)
Hs578T	WT	Positive	(35)
SUM159	WT	Positive	(35,158)
MDA-468	IVS4+1G4T (A72fsX5)	Null	(35,159)
HCC1937	GPM (HD)	Null	(35,159)
SUM102	WT	Unknown	(158,160)
HCC1143	WT	Positive	(161,162)
MDA-231	WT	Positive	(35)
MDA-453	919G4A (E307K)	Positive	(35,159)

Table 2-1. PTEN status in TNBC cell line panel. Known PTEN mutations and the PTEN expression status according to published sources. Table used with permission from (155).

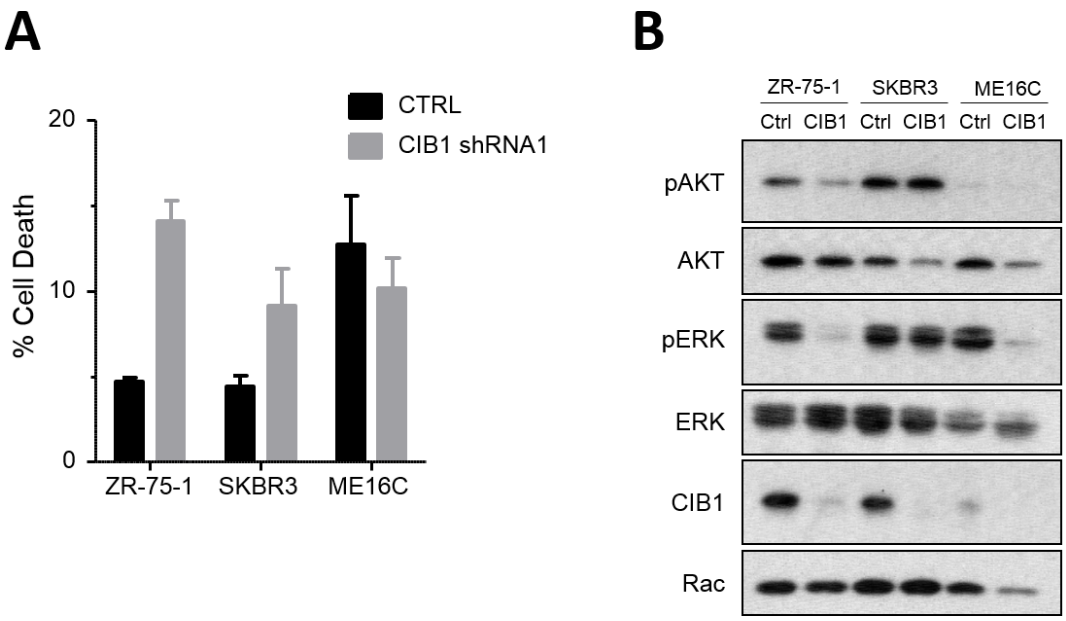

Figure 2-3. Effect of CIB1 depletion on cell death in non-TNBC cell lines. A) A panel of three non-TNBC cell lines were transduced with either control or CIB1 shRNA. Graph represents average percent cell death ± SEM for each sample (n = 3). ZR-75-1 had significantly higher cell death upon CIB1 depletion. B) Relative levels of pAKT, AKT, pERK, ERK, CIB1, and Rac (loading control) in CIB1-depleted and control samples. CIB1 depletion results in reduction in pAKT and pERK in ZR-75-1 cells, corresponding to increased cell death. Figure used with permission from (155).

2.2.2 CIB1 depletion from MDA-MB-468 TNBC cells decreases proliferation and increases cell death

Data presented here and elsewhere demonstrate that CIB1 depletion increased cell death of MDA-MB-468 (MDA-468) cells (Figure 2-1) (96), but not in non-cancerous cells (133,163). While these data suggest that CIB1 may be a promising target for TNBC therapy, we sought in vivo validation. We utilized a doxycycline-inducible shRNA system to regulate CIB1 expression in MDA-468 tumor xenografts. MDA-468 cells were engineered to express either CIB1 shRNA (MDA-468-CIB1shRNA) or control (scrambled) shRNA (MDA-468-SCRshRNA) in response to the antibiotic doxycycline (Dox). MDA-468-CIB1shRNA cells treated with doxycycline showed significant depletion of CIB1 by Western blot (Figure 2-4C). Consistent with previous findings (96), CIB1 depletion decreased phosphorylation of ERK and AKT and increased phosphorylation of the DNA damage marker, γH2AX (Figure 2-4C).

Because treatment response in the 2D clonogenic survival assay in vitro typically agrees with tumor treatment response in vivo (164), we performed a 2D clonogenic assay to measure MDA-468-CIB1shRNA and MDA-468-SCRshRNA colony formation in 2D cell culture. CIB1 depletion in MDA-468 cells (MDA-468-CIB1shRNA+Dox) resulted in a complete loss in the ability to form colonies (Figure 2-5A). Importantly, doxycycline treatment of control cells (MDA-468-SCRshRNA+Dox) had no effect on colony formation ability. We next measured the effect of CIB1 depletion on MDA-468 cell proliferation and survival in culture. CIB1 depletion resulted in arrested proliferation and a ~12-fold increase in cell death (Figure 2-4A). To better quantify the cell death induced by CIB1 depletion, we performed flow cytometry to measure phosphatidylserine (PS) cell surface expression via Annexin V staining, and cell permeability to 7-AAD. The majority of CIB1 depleted cells were in either early (Annexin V positive – 22.6%) or late (Annexin V positive and 7-AAD positive – 37.3%) stages of cell death (Figure 2-4B). Thus, in cell culture, conditional

shRNA knockdown of CIB1 recapitulates the effects of CIB1 depletion using conventional shRNA knockdown.

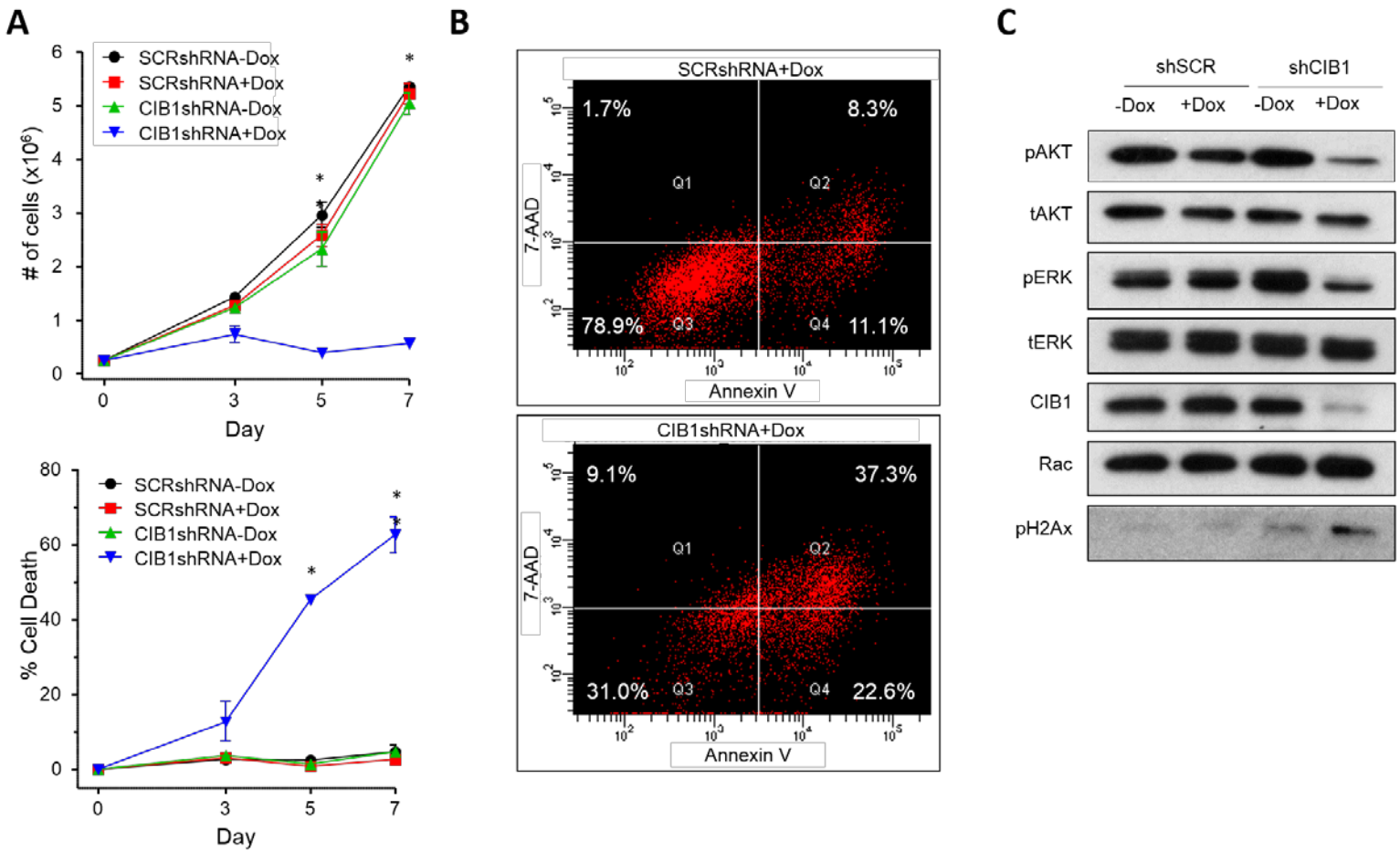
A
SCRshRNA-Dox
SCRshRNA+Dox
CIB1shRNA-Dox
CIB1shRNA+Dox
# of cells (x10^6)
Day
% Cell Death
B
SCRshRNA+Dox
1.7%
8.3%
78.9%
11.1%
Q1
Q2
Q3
Q4
7-AAD
Annexin V
CIB1shRNA+Dox
9.1%
37.3%
31.0%
22.6%
C
shSCR
shCIB1
-Dox
+Dox
-Dox
+Dox
pAKT
tAKT
pERK
tERK
CIB1
Rac
pH2Ax

Figure 2-4. CIB1 depletion decreases TNBC cell proliferation and increases cell death *in vitro* and *in vivo*. A) CIB1 depletion decreases MDA-468 proliferation and viability. Graphs represent mean total cell number ± SEM (Upper panel) and mean percentage of dead cells ± SEM (Lower panel) at each time point (n=3). *P<.001; ** P<.01. B) Measurement of cell surface phosphatidylserine (Annexin V binding) and cell permeability to 7-AAD. A higher percentage of MDA-468-CIB1shRNA+Dox cells were positive for both Annexin V and 7-AAD, indicating a higher percentage of dead cells. C) Relative levels of pAKT, AKT, pERK, ERK, CIB1, γH2AX, and Rac (loading control) in CIB1-depleted and control samples *in vitro* from proliferation and survival assays (A). MDA-468-CIB1shRNA+Dox exhibit complete depletion of CIB1, decreased pERK and pAKT, and increased γH2Ax (C). Figure used with permission from (155).

2.2.3 CIB1 is required for MDA-MB-468 xenograft tumor growth

To test whether CIB1 was necessary for TNBC tumor growth and survival in vivo we used a xenograft model and injected MDA-468-CIB1shRNA and MDA-468-SCRshRNA cells subcutaneously into the flanks of immunocompromised mice. Once tumors reached a volume of approximately 100 mm^3, mice were randomized into groups receiving sucrose, or sucrose plus doxycycline, and tumor volume was monitored for 5 weeks. We observed a rapid arrest of tumor growth followed by a drastic decrease in tumor volume in CIB1-depleted tumors (Figure 2-4B). In contrast, control tumors continued to grow steadily throughout the treatment period. After 5 weeks, CIB1-depleted tumors were not visible compared to control tumors, which were visibly bulging from the flanks of the mice. Upon completion of the study, tumors were resected and weighed. The average mass of CIB1-depleted tumors was significantly smaller than control tumors (Figure 2-5C).

To better understand how CIB1 depletion affects TNBC tumors, resected xenograft tumors were fixed, stained, and analyzed by microscopy. Histological analysis revealed that CIB1-depleted tumors had relatively few remaining cells and were composed mostly of non-cellular tissue (pink), whereas control tumors were composed of densely packed cells (blue) (Figure 2-5D). Because CIB1 is essential for maintaining double strand break repair in TNBC cells (96,103), we asked whether CIB1-depleted TNBC tumors exhibited increased TUNEL staining, which detects dead or dying cells by labeling DNA double-strand breaks. Images of TUNEL-stained sections revealed that more of the remaining CIB1-depleted cells were TUNEL-positive compared to control tumors (Figure 2-6B). Finally, a portion of each tumor was lysed for analysis by Western blotting. Consistent with CIB1 depletion *in vitro*, CIB1-depleted tumors had lower CIB1 expression, and decreased pERK and pAKT levels compared to control tumors (Figure 2-6A). This initial examination of the role of CIB1 in tumor growth *in vivo* suggests that CIB1 inhibition may be an effective therapeutic strategy for the treatment of TNBC tumors.

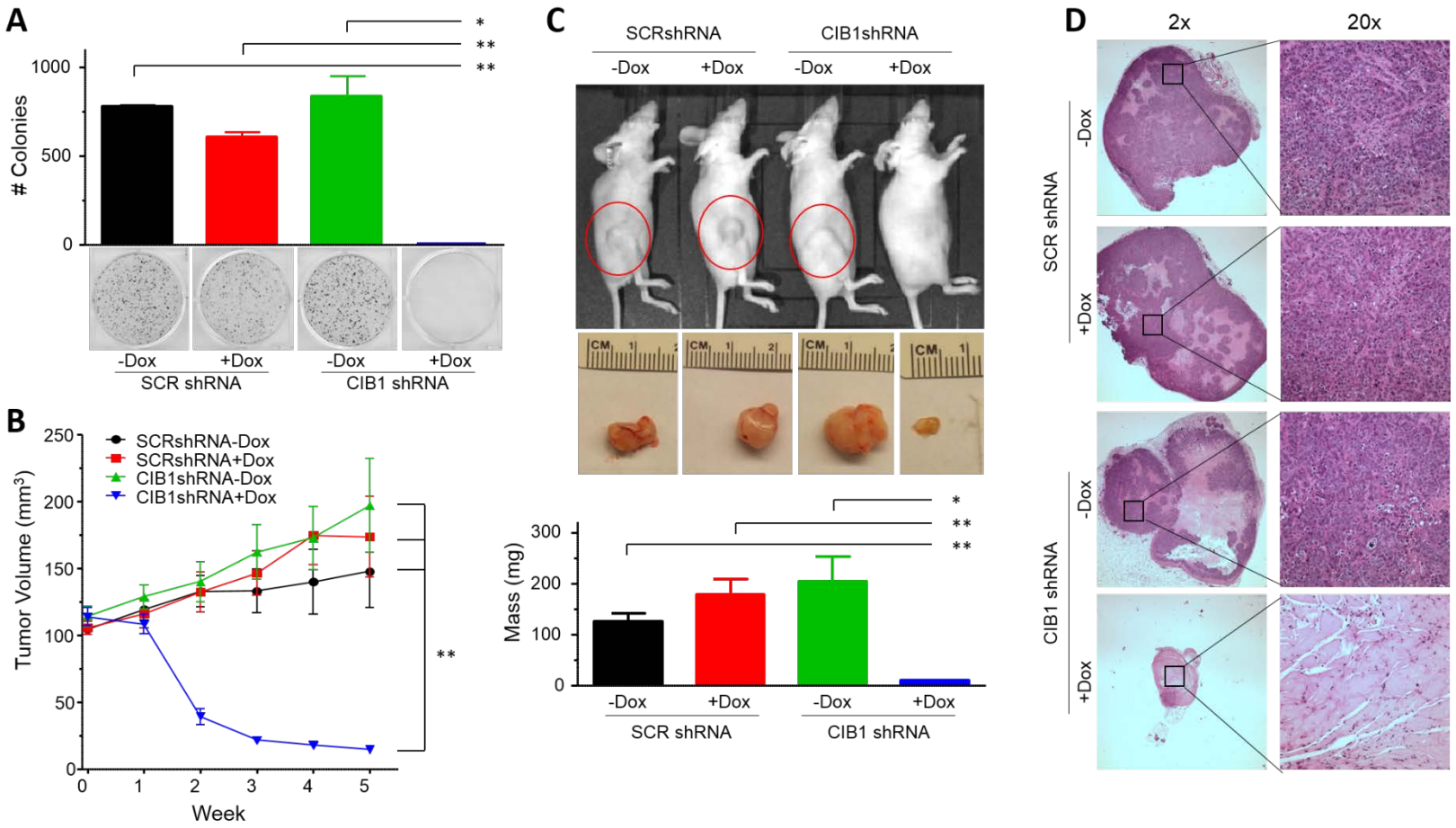
A
Colonies
1000
500
0
*
**
**
-Dox
+Dox
-Dox
+Dox
SCR shRNA
CIB1 shRNA
B
Tumor Volume (mm³)
250
200
150
100
50
0
SCRshRNA-Dox
SCRshRNA+Dox
CIB1shRNA-Dox
CIB1shRNA+Dox
**
0
1
2
3
4
5
Week
C
SCRshRNA
CIB1shRNA
-Dox
+Dox
-Dox
+Dox
Mass (mg)
300
200
100
0
*
**
**
-Dox
+Dox
-Dox
+Dox
SCR shRNA
CIB1 shRNA
D
2x
20x
SCR shRNA
-Dox
+Dox
CIB1 shRNA
-Dox
+Dox

Figure 2-5. CIB1 depletion shrinks TNBC tumors *in vivo*. MDA-468 cells were engineered to stably express doxycycline (Dox)-inducible CIB1 shRNA (MDA-468-CIB1shRNA) or scrambled shRNA (MDA-468-SCRshRNA). A) CIB1 depletion in MDA-468 cells results in complete loss of cell proliferation and colony formation in a 2D clonogenic assay. Data represent mean ± SEM, n = 3. ** P<0.005, * P<0.01. B) MDA-468 xenograft studies. Graph represents average tumor volume ± SEM. N=8 mice per treatment group. P-values were calculated by Student's T-test for the average final tumor volume ** P< 0.005. C) Representative images show tumors bulging from the flanks of control mice, but not CIB1shRNA+Dox mice (upper panel). After 5 weeks, mice were sacrificed and resected tumors were imaged (middle panel) and weighed (lower panel). Data represent average mass ± SEM (n = 8) ** P<0.005, * P<0.01. D) Representative images of H&E stained tumor sections show that CIB1-depleted tumors are less dense than control tumors. Pink (eosin) – non-cellular tissue. Blue (hematoxylin) – cell nuclei. Figure used with permission from (155).

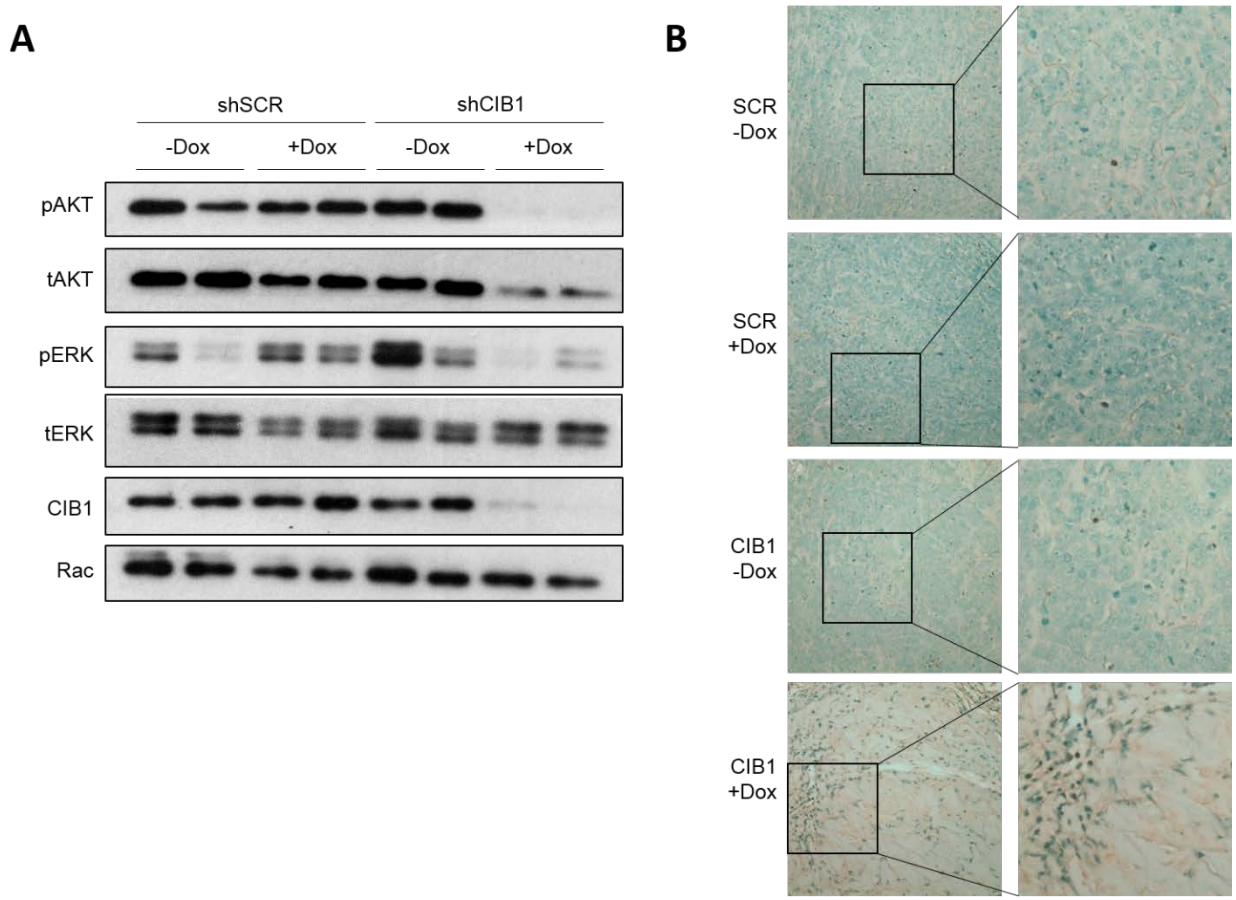

Figure 2-6. CIB1 depletion decreases pERK and pAKT and increases DNA damage *in vivo*. A) Relative levels of pAKT, AKT, pERK, ERK, CIB1, γH2AX, and Rac (loading control) in CIB1-depleted and control samples *in vivo*. MDA-468-CIB1shRNA+Dox exhibit complete depletion of CIB1, and decreased pERK and pAKT. B) CIB1-depleted tumors have more DNA damage than control tumors. Representative TUNEL-stained xenograft tumor sections show that more of cells from CIB1-depleted tumors are dead or dying (dark brown punctate dots) compared to control tumors. Figure used with permission from (155).

2.2.4 PAK1 activation partially rescues cells from CIB1 depletion

CIB1 binds and activates PAK1 (86), and we previously hypothesized that the role of CIB1 in promoting AKT and ERK activation was mediated by PAK1 (96). To test whether PAK1 activation could rescue cells from CIB1 depletion-induced cell death, we overexpressed constitutively active PAK1 (caPAK1) in MDA-468 cells, then knocked down CIB1 and measured cell death. We observed that expression of caPAK1 resulted in a partial rescue of cell death in response to CIB1 depletion (Figure 2-7). These data suggest that CIB1-PAK1 binding is not exclusively responsible for CIB1-dependent cell survival, and that additional factors may contribute to CIB1 signaling to promote survival and proliferation.

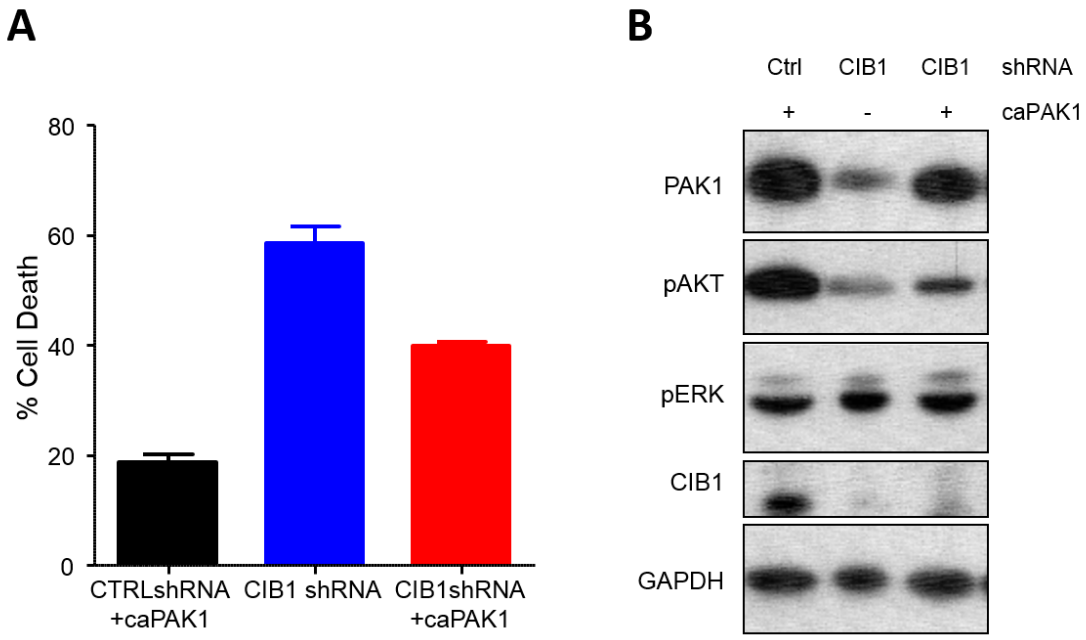

Figure 2-7. Expression of constitutively active PAK1 partially rescues CIB1 depletion-induced cell death. A) caPAK1 was overexpressed in MDA-468 cells, followed by treatment with either control or CIB1 shRNA. caPAK1 expression partially rescued cells from CIB1-depletion induced cell death. Graph represents average percent dead cells ± SEM (n = 2). B) Relative levels of PAK1, pAKT, AKT, pERK, ERK, CIB1, and GAPDH (loading control) in control or CIB1 shRNA treated cells ± caPAK1 overexpression. Figure used with permission from (155).

2.2.5 CIB1 depletion induces genetic programs that reduce proliferation and survival

Because CIB1 depletion induces cell death by a unique, non-apoptotic mechanism that is only partially understood (96), we measured global changes in gene expression by RNAseq analysis to gain additional mechanistic insight into the effects of CIB1 depletion. Total mRNA was isolated from *viable* control and CIB1-depleted MDA-468 cells <96 hours after shRNA induction, since extended CIB1 depletion induces nearly complete MDA-468 cell death (Figure 2-4A). We identified 812 genes that were significantly upregulated (Appendix A) or downregulated (Appendix B) upon CIB1 depletion. Because sensitivity to CIB1 depletion in the TNBC cell line panel was associated with cellular differentiation, as measured with the Differentiation Score (see Figure 2-2), we asked whether CIB1 depletion-induced changes in gene expression were associated with genes involved in cell differentiation. We compared the CIB1 depletion-induced differentially expressed genes (CIB1 KD gene signature) to 10,508 known gene signatures (from public databases such as GSEA and also from manual curation). Interestingly, several gene signatures that had strong Pearson correlation values with the CIB1 KD gene signature were prominent in genetic programs that mediate differentiation and cancer stem cell function (see Appendix C). For example, we observed an increase in 5 out of 7 genes from a mammary stem cell gene signature (165), and an increase in 11 out of 16 genes from an epithelial to mesenchymal transition (EMT) gene signature (166) (Figure 7B). We also observed a decrease in 5 out of 6 genes from a breast cancer proliferation gene signature (167). These results support previous observations that CIB1 depletion correlates with decreased cell proliferation, and indicate that CIB1 depletion activates genetic programs consistent with mammary stem cells and EMT. Interestingly, we observed nearly complete cell death in MDA-468 cells after extended CIB1 depletion (Figure 2-4A), suggesting that CIB1-depleted cells do not become stem cells, but rather acquire some stem-like characteristics as they are dying. As we described previously, CIB1 depletion in MDA-468 cells results in cell death by a unique non-apoptotic mechanism (96). It is possible that the observed

differential gene expression is a downstream cellular response to overcome the negative effects of CIB1 depletion, rather than a direct effect of loss of CIB1. Further experiments are required to follow up on this interesting observation.

Because CIB1 depletion induces MDA-468 cell death, we next examined the RNAseq data for differential expression of genes involved in cell survival and cell death. We identified 99 differentially expressed genes that were positively associated with increased cell death (several of these genes are listed in Figure 2-8C-D). For example, we observed a Log2 fold change of +4.1 for the gene DKK3 (Dickkopf-3). DKK3 is a secreted glycoprotein that potently inhibits Wnt signaling pathways (168), and has been characterized as a tumor suppressor. Interestingly, DKK3 expression is suppressed in breast cancer (169). Adenovirus-mediated delivery of the DKK3 gene to xenograft tumors resulted in tumor regression and induction of cell death in prostate, testicular, and breast cancer models (170-172). Taken together, these results suggest that CIB1 depletion-mediated upregulation of DKK3 may have therapeutic benefit in killing cancer cells and inducing tumor regression, and support the tumor regression data presented herein (See Figures 2-5 and 2-6).

CIB1 depletion also resulted in decreased expression of several known cancer drug targets, suggesting that inhibiting CIB1 could broadly inhibit multiple targets simultaneously (Figure 2-8D). For example, CIB1 depletion led to decreased expression of two isoforms of glutathione-s-transferase, an enzyme that protects cells from oxidative stress and is implicated in chemotherapy drug resistance, indicating that CIB1 interference may sensitize TNBC cells to chemotherapy or other stress-inducing targeted therapies (173). Several naturally occurring compounds are known to inhibit glutathione-s-transferases, including quinine, thonningianin A, quercetin, cucumin, and coniferyl ferulate (174). Furthermore, glutathione-s-transferase inhibition is an effective means to reverse multidrug resistance in pre-clinical studies and has been proposed as an adjuvant therapy or chemopreventive treatment (174-177). Tissue factor is

another example of a cancer drug target gene downregulated upon CIB1 depletion. Tissue factor is normally considered in the context of the coagulation cascade, but has recently been shown to promote cancer progression, including breast cancer (178,179). Treatment with tissue factor inhibitor ixolaris reduced tumor growth and metastasis in mouse tumor models (180,181). Therefore, CIB1 depletion-induced knockdown of tissue factor provides another beneficial effect of targeting CIB1 in TNBC. These examples (glutathione-s-transferase and tissue factor) of CIB1 depletion-induced downregulated genes suggest that inhibition or knockdown of CIB1 may simultaneously inhibit multiple cancer drug targets.

Taken together, these results demonstrate meaningful changes in gene expression induced by CIB1 depletion. Further experiments should explore the role of CIB1 in EMT and mammary stem cells to better understand how CIB1-dependent gene expression influences these genetic programs. Nonetheless, the striking number of genes involved in cell survival and cell death that are differentially expressed upon CIB1 depletion demonstrates an important role for CIB1 in maintenance of cell viability. We propose that examination of CIB1-dependent differentially expressed genes could lead to identification of additional novel drug targets or potential combination therapies.

A

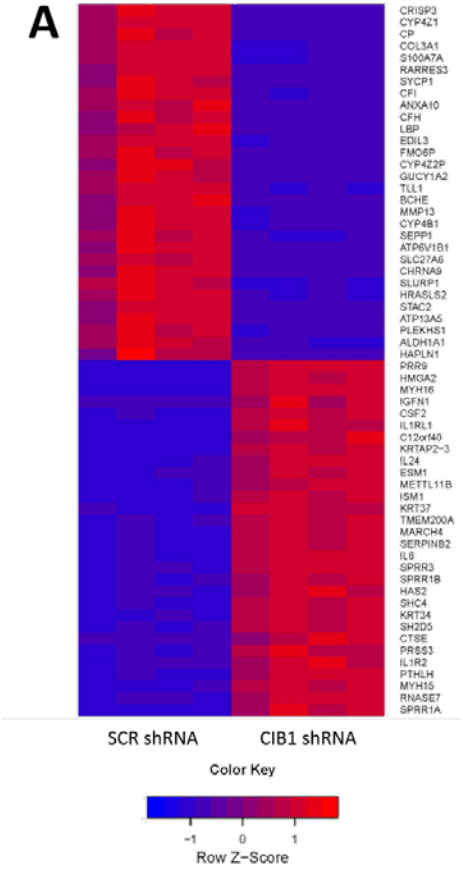

B

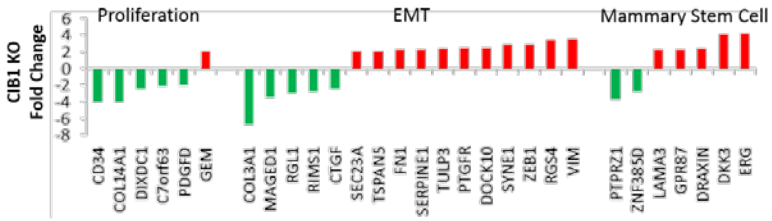

C

Gene Symbol	Gene Name	Log2 Fold Change
IL24	Interleukin-24	+5.6
DKK3	Dickkopf-3	+4.1
PDCD1 LG2	Programmed Cell Death 1 Ligand 2	+3.5
NLRP3	NOD-like receptor, pyrin domain-containing 3	+3.0
FYN	FYN	+2.5
IL18	Interleukin-18	+2.4
ABL2	ABL2	+2.2
DUSP6	Dual-specificity phosphatase 6	+2.1

D

Gene Symbol	Gene Name	Log2 Fold Change	Inhibitor
TF	Tissue Factor	-4.3	Ixolaris
CLU	Clusterin	-3.5	OGX-011
EDNRB	Endothelin receptor, type B	-3.5	BQ788
BDNF	Brain Derived Neurotrophic Factor	-3.5	
KIT	KIT	-2.5	PKC412
GSTP1	Glutathione S-transferase P1	-2.4	Quercetin
NRAS	NRAS	-2.4	
GSTA1	Glutathione S-transferase alpha 1	-2.1	Curcumin
CCR2	Chemokine CC motif Receptor 2	-2.1	
HDAC6	Histone Deacetylase 6	-1.8	Tubacin
JAK1	Janus Kinase 1	-1.6	Ruxolitinib

Figure 2-8. CIB1 depletion results in differential expression of 812 genes. A) Heat map of top 60 genes differentially expressed upon CIB1 depletion (red = upregulated; blue = downregulated). B) Overlap of 812 differentially expressed genes with three known breast cancer gene signatures (165-167). Five of six genes from a proliferation signature decreased, eleven of sixteen genes from an EMT signature increased, and five of seven genes from a mammary stem cell signature increased. C-D) Selected upregulated (C) and downregulated (D) genes predicted to increase cell death. Several gene products have known inhibitors that have been tested for efficacy in cancer. Figure used with permission from (155).

2.2.6 CIB1 mRNA expression does not correlate with TNBC prognosis

Recent reports have suggested that CIB1 expression may have prognostic implications in breast cancer (114). Since CIB1 protein levels did not appear to correlate with susceptibility to CIB1 depletion in the TNBC cell line panel examined in Fig. 1, we predicted that CIB1 mRNA expression might not be prognostic of survival in TNBC patients. We therefore tested the association of CIB1 and disease progression in four independent breast cancer gene expression datasets (157,182-184). Though some datasets trended towards an association of high CIB1 expression and faster disease recurrence, Kaplan-Meier survival analyses found no significant association ($p<0.05$) of patient relapse-free survival and CIB1 mRNA level within estrogen receptor negative tumors or triple negative tumors in any of the datasets tested (Figure 2-9). These results indicate that CIB1 expression levels alone are not a reliable indicator of prognosis in TNBC.

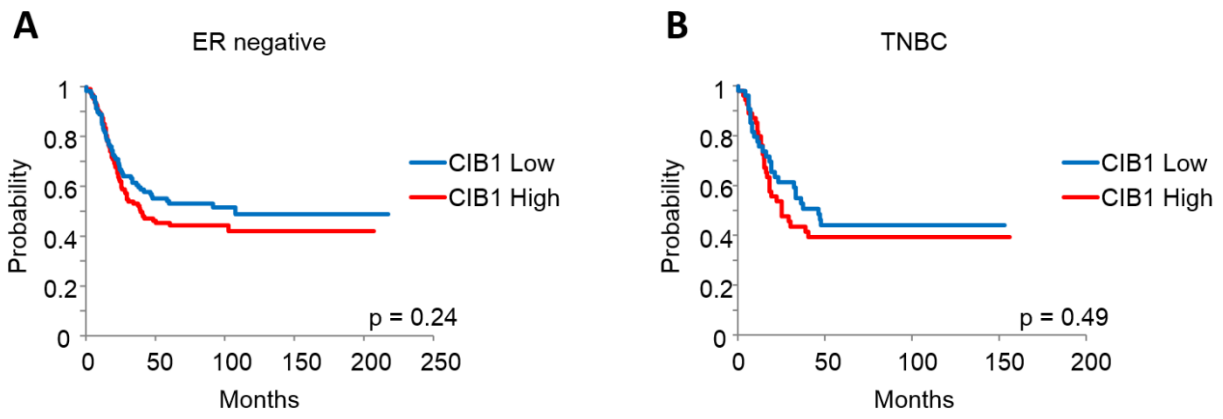

Figure 2-9. CIB1 expression is not prognostic for TNBC patient survival. A) CIB1 expression in a population of human ER-negative tumors does not correlate with probability of relapse-free survival by Kaplan-Meyer survival analysis (n=256). Human breast tumor gene expression microarray data was obtained from a dataset generated by Harrell *et al* (182). B) Same as in (A) but focusing on subset of TNBC within the ER-negative tumors (n=110). Figure used with permission from (155).

2.3 Discussion

TNBC is a breast cancer subtype with generally poor prognosis and no available targeted treatment options (14). Two oncogenic pathways, RAF-MEK-ERK and PI3K-AKT, are aberrantly active in the majority of TNBC (151). Because CIB1 promotes both of these signaling pathways (96), we hypothesized that CIB1 might be essential to TNBC cell survival. The data presented here provide evidence that CIB1 depletion impairs cell survival in a majority of TNBC cell lines and shrinks TNBC xenograft tumors, suggesting that CIB1 may have a broad role in TNBC survival and tumor growth. Furthermore, dependence on CIB1 expression is associated with active AKT and/or low PTEN expression. PTEN mutation or deletion is significantly associated with incidence of basal-like breast cancer in mice and humans (35,185). These data suggest that CIB1 inhibition may be an effective therapeutic option for TNBC patients with PTEN-deficient tumors.

CIB1 depletion impairs ERK and AKT activation in the majority of cell lines, but often does not completely eliminate phosphorylation of these two kinases (see Figure 2-4C). This raises the question of whether the effects of CIB1 depletion on cell survival and proliferation are due exclusively to the decrease in p-ERK and p-AKT, or whether additional mechanisms might be contributing to the observed phenotype. The interaction between CIB1 and the kinases SK1 and ASK1 (see Table 1-2) provides two potential alternative means by which CIB1 could promote cell proliferation and survival, and protect from cell death (78,84,85). CIB1 activates SK1, which promotes cell survival by generating sphingosine-1-phosphate, an important anti-apoptotic lipid messenger (186-188). In addition, CIB1 inhibits ASK1, thereby preventing ASK1-mediated induction of cell death in response to reactive oxygen species (ROS), ER stress, and other stimuli (189,190). The interaction of CIB1 with either of these kinases may contribute to the CIB1 depletion-induced cell death observed in the data presented herein (see Figure 2-1). Taken together, these reports suggest that CIB1 may promote cell survival either by promoting AKT and

ERK activity, or via its interaction with SK1 or ASK1. Alternatively, perhaps the observed effects of CIB1 depletion rely on simultaneous aberration of a combination of these pathways. Further work should be done to explore potential synergism between these cell signaling pathways in the induction of cell death in response to CIB1 depletion.

Because CIB1 is essential for TNBC survival and tumor growth, we asked whether CIB1 expression is prognostic of TNBC patient survival. Recently CIB1 expression was reported to be relatively higher in hepatocellular carcinoma tumor center compared to non-tumorous liver tissues from 100 patient samples (141), as well as in breast cancer tissue compared to matched non-cancerous breast tissue from nine patient samples (114). We found no association between CIB1 mRNA expression and patient relapse-free survival in both TNBC and ER-negative breast cancer. In contrast to previous reports, our study used gene expression data from thousands of breast cancer patients across four established datasets (157,182-184). While the data presented here suggest that CIB1 expression is not prognostic in TNBC, it is possible that CIB1 does have prognostic implications in other types of cancer. Our results indicate that CIB1 expression is not predictive of TNBC patient prognosis, and further suggest that CIB1 overexpression does not promote tumorigenesis per se.

CIB1 appears to have a critical role in promoting AKT activation and cell survival in cells reliant on the AKT oncogenic pathway. However, CIB1 itself has never been described as an oncogene. Although we find that CIB1 depletion is lethal to TNBC cells with high pAKT/low PTEN activity (Figure 2-10), CIB1 depletion is tolerated in non-cancerous cells, such as primary endothelial cells (133) and non-cancerous mammary epithelial cells (Figure 2-3), and in TNBC cells that do not rely on AKT signaling (Figure 2-1A). Furthermore, CIB1 knockout mice have no developmental defects (163), suggesting that CIB1 could be a potentially safe therapeutic target. The properties of CIB1 observed here are consistent with non-oncogene addiction, a phenomenon in which cancer cells require, or become ‘addicted’ to a non-mutated, non-

overexpressed gene/protein that is nonetheless essential to maintain oncogenic signaling pathways (58,59). For example, ATM-deficient tumor cells display non-oncogene addiction to the enzyme DNA-dependent protein kinase catalytic subunit (DNA-PKcs), and DNA-PKcs has been identified as a potential drug target in ATM-defective malignancies (191). Based on this example, our data suggest that PTEN-defective TNBC tumors may display non-oncogene addiction to CIB1, implicating CIB1 as a novel drug target in TNBC.

In summary, CIB1 inhibition induces TNBC cell death in cell culture and tumor regression in vivo. These results warrant further investigation of CIB1 in non-oncogene addiction and as a candidate for TNBC therapy.

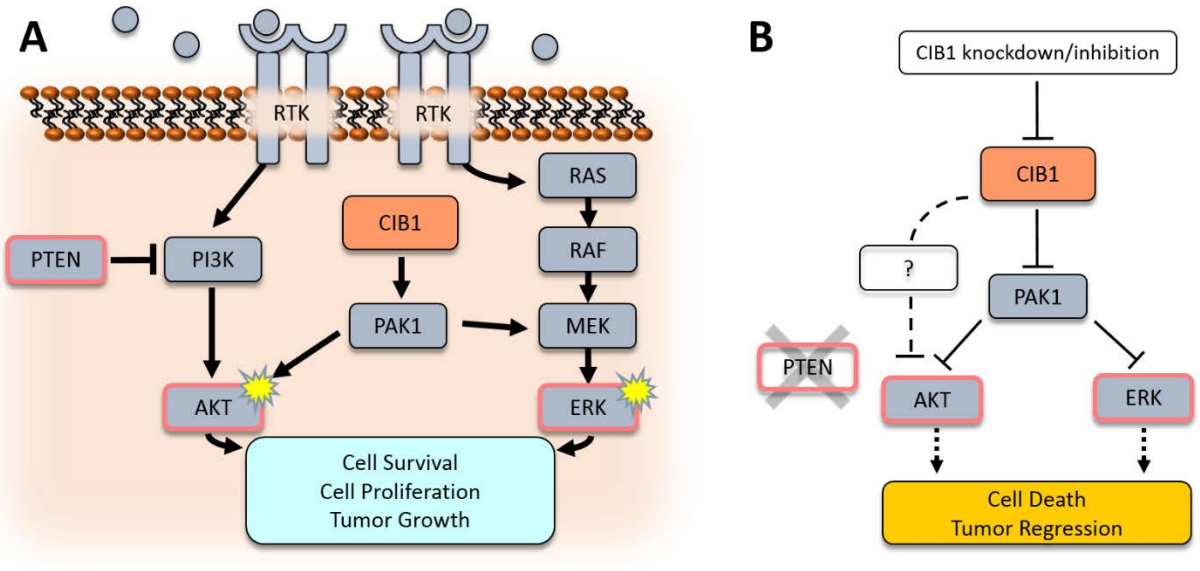

Figure 2-10. Proposed mechanism of CIB1 regulation of TNBC cell survival and potential role of CIB1 in non-oncogene addiction. A) CIB1 promotes TNBC cell survival, proliferation, and tumor growth via AKT and ERK signaling pathways. B) CIB1 depletion results in loss of AKT and ERK. This effect is mediated in part by PAK1, but also likely involves additional, undetermined factors (dotted line). CIB1 depletion is most effective in PTEN-deficient cells and/or cells with elevated AKT activation. Because PTEN also acts as an upstream regulator of PI3K/AKT signaling, inactivating mutations or deletions of PTEN commonly result in hyper-activation of this pathway. Thus, TNBC cells with low or absent PTEN show increased sensitivity to CIB1 depletion. Together with the observations that CIB1 depletion/loss has minimal effect on non-cancerous cells (133) or TNBC cells with wild-type PTEN, our findings suggest a role for CIB1 in the concept of non-oncogene addiction. Figure used with permission from (155).

2.4 Methods

Cell lines and cell culture – Cell lines and cell culture conditions are listed in Table 2-2.

Cell Line	Media
BT549	RPMI+10%FBS+10ug/mL Insulin
HCC1143	RPMI+10%FBS
HCC1937	RPMI+10%FBS
Hs578T	DMEM+10%FBS+10ug/mL Insulin
MDA-231	DMEM+10%FBS
MDA-436	DMEM+10%FBS+10ug/mL Insulin
MDA-453	DMEM+10%FBS
MDA-468	DMEM+10%FBS
SUM102	DMEM/F12+5%FBS+10ug/mL Insulin+1ug/mL Hydrocortisone
SUM149	DMEM/F12+5%FBS+10ug/mL Insulin+1ug/mL Hydrocortisone
SUM159	DMEM/F12+5%FBS+10ug/mL Insulin+1ug/mL Hydrocortisone
ZR-75-1	RPMI+10%FBS+10ug/mL Insulin
SKBR3	McCoy's5a+10%FBS
ME16C	MEBM (MEGM Bullet Kit: MEGM+BPE+hEGF+Hydrosortisone+Insulin

All cell lines were grown at 37°C in 5% CO_2 humidified air.

Table 2-2. Cell lines and cell culture conditions used in TNBC Panel. Table used with permission from (155).

Mice and Xenografts – MDA-468-CIB1shRNA and MDA-468-SCRshRNA ($5x10^6$ cells) in PBS were mixed 1:1 with Cultrex Basement Membrane Extract Type III (Trevigen, Gaithersburg, MD) and injected subcutaneously into the flanks of 6-week old female Nu/Nu mice (Charles River Laboratories, Wilmington, MA). Mice were enrolled at a tumor size of ~$100mm^3$ in the following treatment arms: 1% Sucrose (Sigma, St. Louis, MO), 1% sucrose + 2 mg/mL doxycycline (Sigma, St. Louis, MO); administered via drinking water 3x/week. Tumors were measured twice per week with calipers (tumor volume = length x width x width / 2). Mice were euthanized after 5 weeks of treatment and tumors were resected for further analysis.

RNAseq analysis – MDA-468_SCRshRNA and MDA-468_CIB1shRNA cells were treated with doxycycline for <96 hours. After removing dead cells, RNA was isolated from viable cells (RNeasy kit, Qiagen, Venlo, Netherlands), and cDNA generated (QuantiTect Reverse Transcription kit, Qiagen). cDNA was sequenced at the UNC High Throughput Sequencing Facility on an Illumina HiSeq 2000 (Illumina, San Diego, CA). Differential gene expression analysis was performed using DESeq2 (192) and differentially expressed genes were selected based on Log2 fold change ≥ ± 2 and Benjamini-Hochberg adjusted p-value < 0.05. Lists of differentially expressed genes are displayed in Appendices A (upregulated genes) and B (downregulated genes). Differentially expressed genes were analyzed using Ingenuity Pathway Analysis (Qiagen). The median-centered gene expression dataset and methods from Prat et al (156) were used for Significance Analysis of Microarrays on the CIB1 KD sensitive versus insensitive cell lines, and for the identification of cell line Differentiation Scores; both of these analyses were performed with R version 3.1. To identify other gene signatures with similar profiles in human breast tumors (182), 10,508 gene signatures were retrieved from the GSEA database and via manual curation, each signature score was identified for each tumor by taking the average value of all signature genes within the median-centered gene set, then Pearson Correlation Values were obtained in Excel contrasting the CIB1 KD signature with all signatures.

Colony formation assay – MDA-468-control and -CIB1shRNA cells were treated ± 1 µg/ml Dox for 48 hours prior to plating at a density of 2000 cells/well. Cells were allowed to grow 9 days in the absence or presence of Dox, with media changes every 4 days. Cells were stained with crystal violet (0.05% w/v in 4% formaldehyde) (Sigma, St. Louis, MO) and colonies counted using ImageJ software.

RNA interference – Cells were transduced with either control shRNA (ACCGCTCTTCACACAGATCCTCTTCAAGAGAGAGGATCTGTGTGAAGAGCTTTTTC), CIB1 shRNA 1

(ACCGTGCCCTTCGAGCAGATTCTTCAAGAGAGAATCTGCTCGAAGGGCACTTTTTC), or CIB1 shRNA 2, (CAGCCTTAGCTTTGAGGACTTCTCGAGAAGTCCTCAAAGCTAAGGCTG). For inducible RNAi experiments, MDA-468 cells were transduced with either inducible control shRNA (GCTACACTATCGAGCAATTTTGGATCCAAAATTGCTCGATAGTGTAGC) or inducible CIB1 shRNA (GGCTTAGTGCGTCTGAGATTTGGATCCAAATCTCAGACGCACTAAGCC) using the pLV-H1-TetO-Puro lentiviral plasmid (Biosettia, San Diego, CA). Lentiviral particles were prepared as described previously (96).

Cell proliferation and cell death assays – MDA-468-CIB1shRNA and MDA-468-SCRshRNA cells were plated at $3x10^5$ cells per 10cm dish, treated ± Doxycycline, and allowed to grow for 3, 5, or 7 days. Cells were harvested by trypsinization and counted using a hemacytometer. Cell viability was determined by trypan blue exclusion.

Flow cytometry – Cells were grown in the presence of Doxycycline for 5 days. MDA-468-CIB1shRNA and MDA-468-SCRshRNA cells were detached using 2 mM EDTA and $5x10^5$ cells were stained with FITC Annexin V (BD Biosciences), 7-AAD (eBioscience), or the combination of FITC Annexin V and 7-AAD according to the BD FITC Annexin V Apoptosis Detection Kit protocol. Data was collected from 10^4 cells using a FACS Canto flow cytometer (BD), then analyzed using FACS Diva software (BD).

Histology and microscopy – Fixed tumors were paraffin embedded, slides were cut and H&E staining completed by the Lineberger Comprehensive Cancer Center Animal Histopathology Core Lab. TUNEL assay was performed according to manufacturer's protocol (Promega). Microscopy was performed using an Olympus BX61 Wide Field Microscope at the UNC Microscopy Services Laboratory.

Kaplan-Meier survival analyses – Data from (157,182-184) were downloaded and processed as in (193). Kaplan-Meier survival analyses and Log-Rank p-values were performed with Winstat.

Tumors were ranked from lowest to highest based on CIB1 expression levels and divided into two equal groups based on CIB1 gene expression.

Constitutively active PAK1 expression – Constitutively active PAK1 (caPAK1) harboring activating mutations L107F and T423E was cloned into the pCDH-EF1-MCS-T2A-Puro vector (System Biosciences, Mountain View, CA). Lentiviral particles were produced as described previously (96). MDA-468 cells were transduced with caPAK1, then after 48 hours cells were transduced with either CIB1 shRNA or Control shRNA. Cells were harvested 96 hours after shRNA treatment and counted. Cell viability was determined by trypan blue exclusion.

Western blotting – Cell and tumor lysates were prepared using CHAPS lysis buffer (20 mM HEPES, 150 mM NaCl, 5% v/v glycerol, 10 mM CHAPS, 0.1 mM $CaCl_2$, 0.05 mM $MgCl_2$, 20 mM NaF, 10 mM β-Glycerophosphate, 0.1 mM Sodium Pervanadate, 1.25 mg/mL N-Ethylmalemide, and Protease Inhibitor Cocktail III (BioVision). Protein concentration of tumor lysates was determined using BCA Assay (Thermo Scientific), equal amounts of total protein were separated by SDS-PAGE, transferred to PVDF, and incubated with indicated primary antibodies overnight at 4^{o}C, and visualization was performed using ECL2 (Pierce). The following antibodies were used: CIB1 chicken polyclonal antibody was produced as described previously (86); antibodies against pAKT^{473} (9271), pERK (9101), total AKT (4691), and γH2Ax (9718) were obtained from Cell Signaling Technology (Danvers, MA); ERK polyclonal (sc-94), PTEN (sc-9145) and PAK1 (sc-882) antibodies were purchased from Santa Cruz Biotechnology (Dallas, TX); Rac monoclonal antibody was purchased from EMD Millipore (Billerica, MA).

Statistical analysis – P-values were calculated using Student's T-test.

CHAPTER 3: CIB1 BINDS α-INTEGRIN CYTOPLASMIC TAILS *IN VITRO* AND IN CELLS

3.1 Introduction

Integrins are transmembrane cell adhesion receptors that form a critical link between the cellular cytoskeleton and extracellular matrix, and also have important roles in cell adhesion, migration, and signal transduction (194). Normal integrin function is essential in development, immune response, hemostasis, and cancer (194-198). Therefore, integrin structure, function, and binding partners have been studied intensively toward increased understanding of relevant biological processes and diseases.

3.1.1 Integrin activation and signaling is regulated by cytoplasmic binding proteins.

Integrin-dependent signaling pathways are precisely regulated to maintain physiological behavior. Integrins are heterodimeric receptors composed of an α subunit and a β subunit, and have a large extracellular domain, a single transmembrane domain, and a short cytoplasmic tail. Transmission of signals through the cell membrane via integrins is regulated by the binding of cytoplasmic proteins to the integrin tails. For example, kindlin and talin are cytoplasmic proteins that bind to integrin β-subunit cytoplasmic tails and have important roles in integrin activation (199-201).

3.1.2 CIB1 may modulate integrin-dependent cell function and signaling.

The Parise lab discovered CIB1 as a binding partner of integrin αIIb, and initially published that CIB1 bound to αIIb, but not other integrin α-subunits (68). Integrin αIIb is expressed exclusively on platelets and megakaryocytes, but CIB1 expression is ubiquitous

(70,108,111,118). CIB1 binding to αIIb regulated integrin αIIb agonist-induced signaling and function (81). Additional studies revealed that CIB1 bound to αIIb in a highly conserved domain spanning the transmembrane and cytoplasmic domains of the integrin (69,70). Because CIB1 binds a conserved region of αIIb and is ubiquitously expressed, we hypothesized that CIB1 may bind additional integrins and have a broader role in integrin biology.

3.1.3 Exploring CIB1-integrin binding *in vitro* and in cells

The binding of CIB1 to α-integrin cytoplasmic tail peptides was tested by several in vitro binding assays. The Kd for CIB1 binding to 8 different integrin peptides was determined by isothermal titration calorimetry, with a maximum Kd of 23.5μM (αM) and a minimum Kd of 0.9μM (α2), and the interactions were further tested by competitive binding assays to measure the ability of various α-integrin peptides to compete with αIIb for CIB1 binding (124). These results demonstrated that CIB1 is capable of binding to multiple α-integrin subunits. I asked whether CIB1-integrin binding is physiologically relevant, and explored this question through biochemical and cell-based assays. Here I present evidence that CIB1 interacts with specific residues in the transmembrane domain of the integrin cytoplasmic tail, and that CIB1 can access these residues in the presence of a cell membrane. I present additional data to support the functional consequences of CIB1 binding to integrin in cells. Finally, I discuss the relevance of these findings to cell biology and to broadly understanding CIB1 function in human health and disease.

3.2 Results

3.2.1 CIB1 binds α-integrin tails via a conserved region spanning the transmembrane and cytoplasmic tail domains of the integrin

Previous evidence demonstrated that CIB1 binds to integrin αIIb at a region spanning the transmembrane and cytoplasmic tail domains (See Figure 3-1) (69). To determine α-integrin residues that were essential for CIB1 binding, I designed α-integrin cytoplasmic tail peptides

harboring alanine substitutions. A thirteen amino acid region of integrin αIIb was shown to contain critical residues for CIB1 binding (69). Based on the homology between αIIb and αV (124), I hypothesized that this region was essential for CIB1-αV binding as well. To test this hypothesis, I measured the binding affinity of CIB1 to αV peptides using isothermal titration calorimetry (Figure 3-1). I generated four mutants with two, four, and six alanine substitutions at the N-terminus of an αV cytoplasmic tail peptide. Binding of CIB1 to alanine-substituted αV peptides was compared to CIB1 binding to αV-WT. The binding affinity for CIB1 and αV WT was 2.8 μM. Alanine substitutions at positions 1011-1012, or at positions 1013-1014 did not significantly affect binding affinity. However, combining these mutations to generate an αV-4A mutant ($1011^{LVFV/AAAA}$) significantly reduced binding affinity. An αV-6A mutant peptide similarly lacked detectable binding to CIB1. Interestingly, neither of the αV2A mutants significantly affected CIB1-αV binding, but the αV-4A mutant completely lost CIB1 binding ability. These data suggest that hydrophobic residues in the putative transmembrane region of integrin αV are critical for CIB1 binding to the αV cytoplasmic tail.

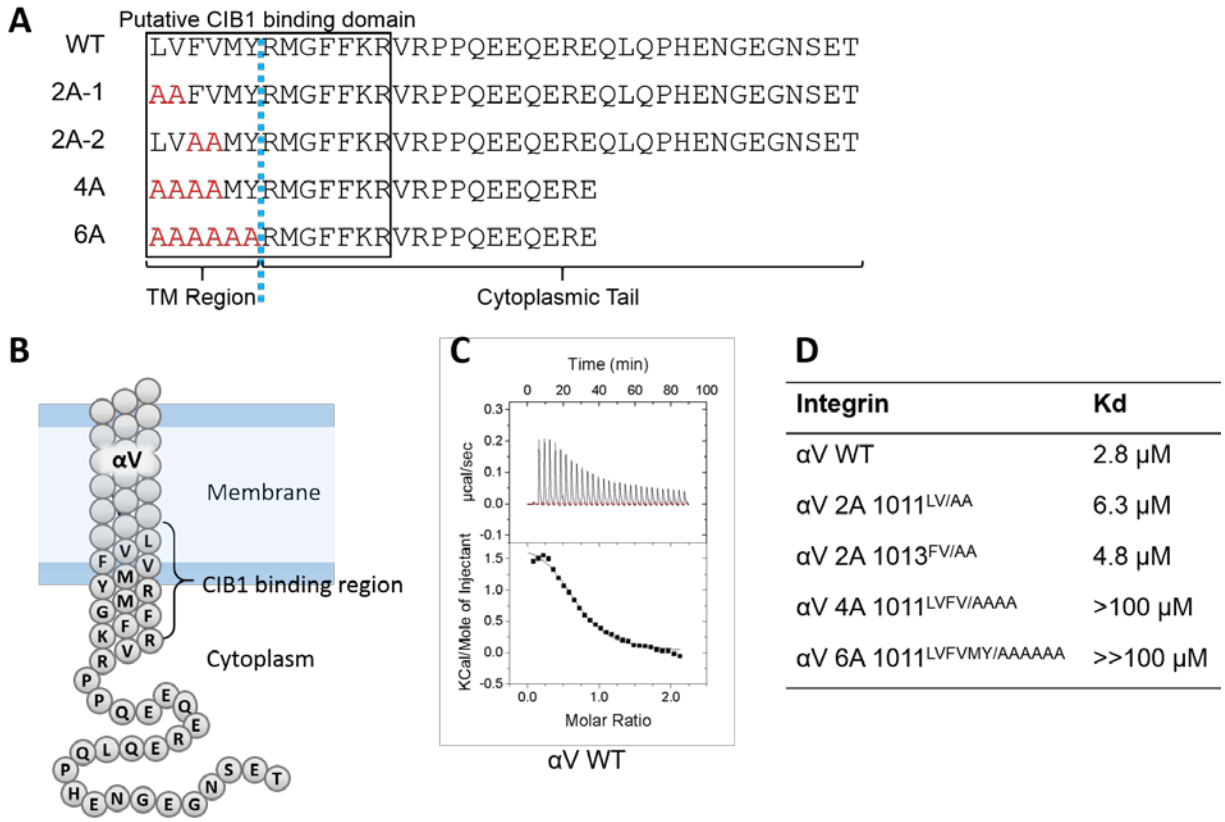

Integrin	Kd
αV WT	2.8 µM
αV 2A $1011^{LV/AA}$	6.3 µM
αV 2A $1013^{FV/AA}$	4.8 µM
αV 4A $1011^{LVFV/AAAA}$	>100 µM
αV 6A $1011^{LVFVMY/AAAAAA}$	>>100 µM

Figure 3-1. CIB1 binding to integrin αV cytoplasmic tail peptides is disrupted by alanine substitutions in the transmembrane region of the putative CIB1 binding domain. A) Amino acid sequences of αV peptides used in ITC experiments. The putative CIB1 binding domain (determined by Barry et al. 2002) is boxed. A dotted line separates residues in the transmembrane region from residues in the cytoplasmic region. B) Model of the integrin αV transmembrane and cytoplasmic tail domains. The transmembrane region and N-terminal portion of the cytoplasmic tail of the integrin form an α-helix. C) Isotherm (upper panel) and integrated peaks fit with one site binding model (lower panel) of αV WT binding to CIB1. D) Table of binding affinities for CIB1 binding to WT and alanine-substituted αV CTs. αV 4A and αV 6A have binding affinities outside of the detectable limit by ITC (100 µM). Some of the data presented in C-D was published in Freeman et al. and reprinted with permission from (124). Copyright 2013 ACS.

3.2.2 CIB1 can access integrin αV membrane proximal residues in the presence of a physiologically relevant lipid bilayer

Because CIB1 binds to αV at a region spanning the cytoplasmic and transmembrane domains, it is possible that the cell membrane physically impedes CIB1 from accessing its αV binding domain inside a cell. We hypothesized that CIB1 can access its binding site on the integrin, even when the integrin is embedded in a lipid bilayer membrane. To test this hypothesis we embedded integrin αV polypeptides into nanodiscs, soluble lipid bilayer discs, and tested CIB1 binding to integrin αV via pulldown assays (Figure 3-2).

Nanodiscs were assembled containing either αIIb WT, αIIb 2A, αIIb 4A, or αIIb 6A, or no integrin (empty nanodiscs). Nanodiscs were mixed with purified recombinant CIB1, then pulled out of solution using Ni2+ beads to bind the histidine-tagged MSP1 protein. Protein complexes were eluted off the beads and eluted proteins were detected by Western blot. I found that CIB1 binds to αIIb WT nanodiscs, but not empty nanodiscs (Figure 3-3B). I then compared the binding of CIB1 to αIIb mutant nanodiscs and found that CIB1 bound to αIIb 2A nanodiscs, but that binding was significantly reduced to αIIb 4A and αIIb 6A nanodiscs (Figure 3-3C). These results mirror the ITC binding data generated for CIB1 binding to α-integrin peptides. Because the mutated residues reside in the membrane-spanning region of the integrin, the results support the hypothesis that CIB1 can access its integrin binding site even when the integrin is embedded in a lipid bilayer.

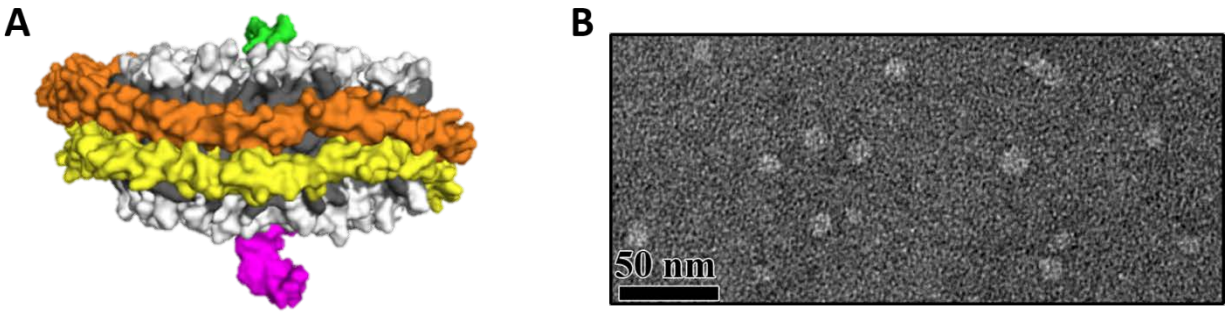

Figure 3-2. Nanodisc structure and synthesis. A) Nanodiscs are produced by mixing membrane scaffolding protein (MSP, yellow & orange), phosphatidylcholine/phosphatidylserine (white), and integrin C-terminus (green and purple). The integrin C-terminus is composed of the transmembrane and cytoplasmic tail regions of the integrin. Nanodisc self-assembly results in the integrin embedding itself into the lipid bilayer to protect the hydrophobic transmembrane domain. **Image generated by Thomas Freeman. B) Negative-stain electron microscopy of pre-assembled nanodiscs. Each white circle is an individual nanodisc with diameter ~10 nm.

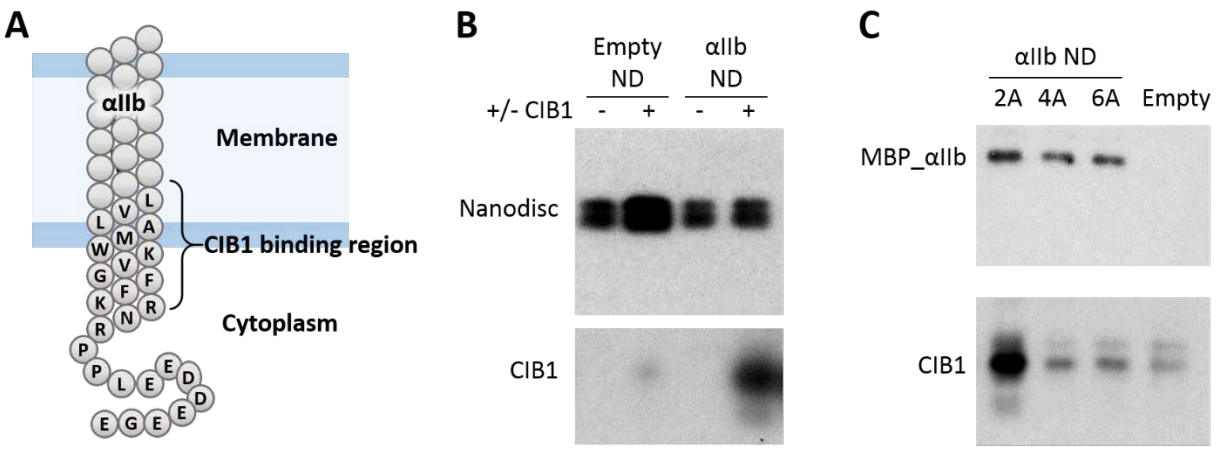

Figure 3-3. CIB1 binding to membrane-embedded α-integrin subunits is disrupted by mutations in the C-terminal portion of the integrin transmembrane domain. A) Model of the integrin αIIb transmembrane and cytoplasmic tail domains. B) CIB1 binds to αIIb WT nanodiscs, but not to empty nanodiscs. C) CIB1 binds to nanodiscs containing αIIb-2A, but not to αIIb-4A or αIIb-6A.

Although preliminary results from CIB1-nanodisc binding assays were encouraging, we encountered technical hurdles that impeded further experimentation and data collection. These technical challenges stem from the goal to reduce non-specific binding, a challenge inherent in binding assays. Several attempts were made to reduce non-specific binding of CIB1 to empty nanodiscs or free protein in these assays, to enable accurate measurement of CIB1 binding to membrane-embedded integrin. I will outline here several challenges, respective troubleshooting steps, and outcomes.

The first challenge addressed was to optimize the assay buffer for nanodisc pulldown experiments. The base buffer, TBS (20 mM Tris, 150 mM NaCl in dH2O), was supplemented with 30 mM imidazole, 5% glycerol, 10% glycerol, or a combination of imidazole plus glycerol, and CIB1 binding to empty nanodiscs was measured in each buffer to determine optimum conditions to reduce non-specific binding. Experiments performed in TBS supplemented with imidazole and 10% glycerol demonstrated the lowest signal of CIB1 binding to empty nanodiscs, but the addition of glycerol had only modest effects compared to the addition of imidazole alone. Therefore, TBS-I buffer (TBS plus 30mM imidazole) was used for all subsequent experiments.

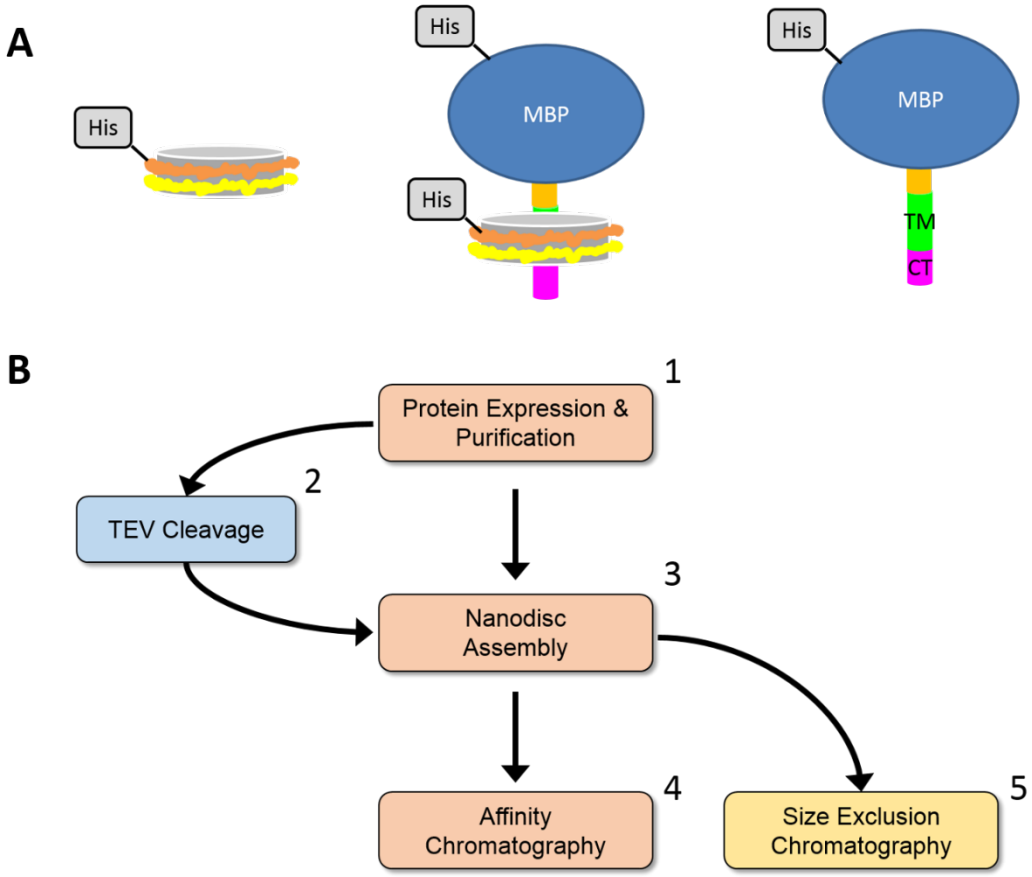

Figure 3-4. Nanodisc challenges and troubleshooting. A) Nanodisc preparations typically resulted in a mixed population of three species: Empty nanodiscs, MBP-integrin embedded nanodiscs, free MBP-integrin. As all three species carried a hexahistidine tag, the species are difficult to differentiate by affinity chromatography. TM = transmembrane domain; CT = cytoplasmic tail domain. B) Flow chart of experimental pathways to troubleshoot nanodisc challenges. *Path 1*: 1→3→4. Purified MSP1 and MBP-integrin are mixed with membrane lipids, nanodiscs are assembled and the products are purified by affinity chromatography. Path 1 results in the 3 species described in (A). *Path 2*: 1→2→3→4. Purified MBP-integrin is subjected to TEV cleavage to remove MBP, nanodiscs are assembled, and purified by affinity chromatography. Due to incomplete TEV cleavage, Path 2 results in all of the products in (A) plus cleaved integrin embedded in nanodiscs. *Path 3*: 1→3→5. Purified proteins were assembled into nanodiscs and purified by size-exclusion chromatography to remove empty nanodiscs and free MBP-integrin.

Testing for differential binding of CIB1 to WT or mutant integrin peptides embedded in nanodiscs introduced additional challenges and troubleshooting. The nanodiscs consisted of purified proteins MSP1 (membrane scaffold protein) and integrin peptides linked to MBP (maltose binding protein) organized with lipids into nanodisc complexes. Integrins were linked to MBP to facilitate expression and purification from E. coli. During nanodisc preparation, a mixed population of products was produced including integrin nanodiscs, empty nanodiscs, and free protein in solution (Figure 3-4). Because both MSP1 and MBP had a hexahistidine tag at the N-terminus of the protein, it was impossible to distinguish between the different populations during preparation, purification, and binding assays. This mixed population made experimental results difficult to interpret. To overcome these challenges, I attempted to cleave the MBP from purified MBP-integrin using TEV (Tobacco Etch Virus) protease followed by a negative selection using amylose resin to bind His-MBP. While this technique reduced the amount of MBP-integrin in solution, the cleavage reaction and purification did not reach 100% efficiency, as evidenced by the signal from integrin, MBP and MBP-integrin in the flow through, wash, and bead samples (Figure 3-5A).

Due to the persistent inability to completely cleave the His-MBP from the integrin peptide, I opted to pursue a different approach to obtain a pure population of integrin-embedded nanodiscs. Purified MBP-integrin, MSP1, and lipids were assembled into nanodiscs and then separated by size-exclusion chromatography. Two major peaks were observed. In each sample, the second peak corresponded to the predicted molecular weight of the nanodiscs in the sample (~150 kDa for empty nanodiscs, ~190 kDa for integrin-embedded nanodiscs) (Figure 3-5B). Fractions from these peaks were run on a gel and subjected to Western blotting to confirm that the fractions contained both MSP1 and MBP-integrin, suggesting that these fractions contained intact nanodiscs (data not shown). Unfortunately, the size exclusion chromatography was not sensitive enough to separate integrin-embedded nanodiscs from empty nanodiscs. In addition, when free MBP-integrin was run through the column, a single peak at ~350 kDa was observed

(data not shown), approximately 7x the predicted molecular weight of MBP-integrin, which differs from the molecular weight observed by gel (Figure 3-5). Therefore, size exclusion chromatography was was unable to effectively separate empty nanodiscs, MBP-integrin nanodiscs, and free MBP-integrin in solution. Despite multiple approaches, a homogenous population of integrin-embedded nanodiscs was never achieved and the results of binding assays were inconclusive.

Future nanodisc experiments should be designed to more thoroughly explore the CIB1-integrin interaction in the presence of a membrane. To avoid the technical challenges described herein, a better experimental design should be considered in which the proteins used in the assay carry different tags, thus enabling easier differentiation of species in binding assays. For example, using a biotinylated MSP would result in nanodiscs with a biotin tag, facilitating easy binding to streptavidin. To detect CIB1-integrin binding, simple in vitro pulldown assays (for example, using streptavidin beads to isolate biotinylated nanodiscs) could be designed to detect CIB1-integrin binding. These experiments could be followed by a more quantitative approach, such as surface plasmon resonance. For example, using Biacore terminology, the nanodiscs could be immobilized to a streptavidin chip as the “ligand”, then CIB1 could be flowed over the chip as the “analyte” to quantitatively measure CIB1 binding to membrane-embedded integrin, as in (202,203). Finally, generation of smaller nanodiscs (i.e. with fewer lipid molecules) has enabled the use of NMR to solve solution structures of proteins in complex with a membrane-bound binding partner (204,205). In this case, NMR could be utilized to create a 3-dimensional structure of CIB1 binding to the integrin in the presence of a cell membrane, to determine how CIB1 accesses its putative binding site, and allow functional inferences to CIB1 function in cell biology.

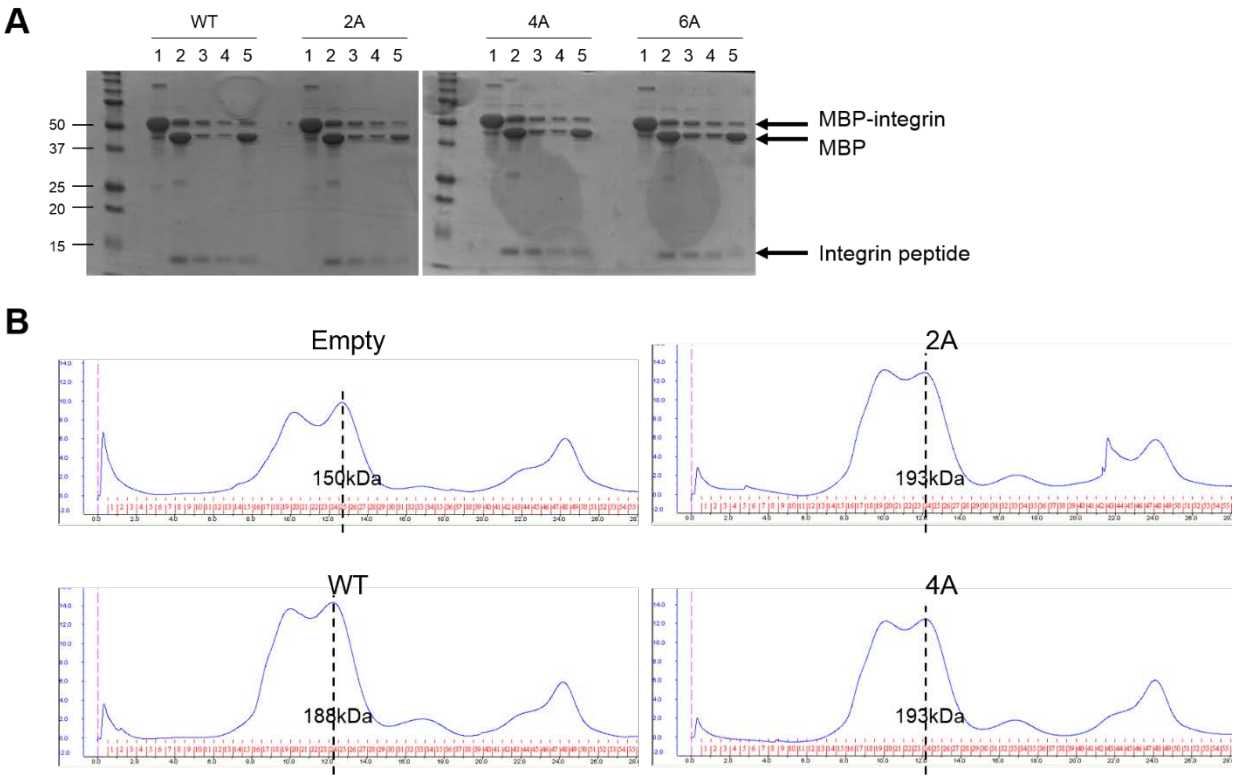

Figure 3-5. Cleavage and purification of MBP-αIIb and purification of nanodiscs. MBP-αIIb was subjected to cleavage by TEV protease and cleavage products were purified and run on a gel. Lanes: 1 – Pre-cleavage sample; 2 – Cleavage product; 3 – Flow-through; 4 – Wash; 5 – Beads. Cleavage reaction and amylose purification are inefficient at separating MBP-αIIb from cleaved αIIb. B) Size-exclusion chromatography of assembled nanodiscs. Chromatography successfully generated peaks at the appropriate predicted molecular weight of nanodiscs (Empty nanodiscs – 150 kDa; Integrin-embedded nanodiscs – 190 kDa).

3.2.3 Integrin mutants may affect CIB1-integrin function in cells

CIB1 regulates signaling through pathways that are also activated downstream of ligand binding to integrins (196). For example, our lab recently found that CIB1 is an upstream regulator of both ERK and AKT signaling pathways (96). However, it is unknown whether αv-dependent activation of these same pathways requires CIB1 or whether it is a parallel event, independent of CIB1. CIB1 is known to regulate activation of the related integrin αIIbβ3 (81), but the effect of CIB1 on αvβ3 activation or downstream signaling has never been studied.

In addition to its interaction with integrin αIIb (69,70,81), we demonstrated that CIB1 co-immunoprecipitates with integrins αV and α5 from whole cell lysates (Figure 3-6) (124). Since I found that introduction of amino acid substitutions in the CIB1 binding domain on the integrin disrupted CIB1-integrin binding in vitro, I asked whether these mutations to the full-length integrin had any effect on CIB1-integrin binding and function in cells. I hypothesized that cells expressing mutant integrin αV 4A would have impaired signaling and integrin-mediated adhesion, compared to cells expressing αV WT.

To explore the role of CIB1 binding to integrin αV in cells, I expressed full length integrin αV (WT or mutant) in the αV-null cell line M21L (206), and generated stable cell lines expressing either αV WT (M21L-αV WT), αV 2A (M21L-αV 2A), or αV 4A (M21L-αV 4A). To test whether αV mutations could disrupt CIB1-αV interaction in cells, I measured CIB1-αV binding via co-immunoprecipitation experiments. I immunoprecipitated CIB1 from whole cell lysates of M21L-αV WT, M21L-αV 2A, and M21L-αV 4A, and probed the immunoprecipitates for integrin αV by Western blot. As expected from in vitro binding experiments, I found that that less αV 4A co-immunoprecipitated with CIB1 than αV WT (Figure 3-7). Surprisingly, more αV 2A co-immunoprecipitated with CIB1 than αV WT, suggesting that the αV 2A mutant may enhance CIB1-αV binding in cells (Figure 3-7).

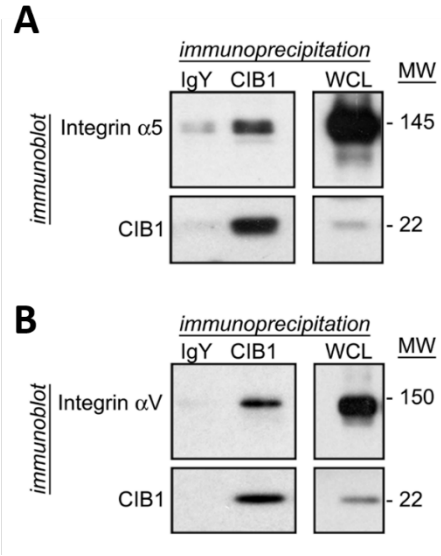

Figure 3-6. Integrins αV and α5 co-immunoprecipitate with CIB1. HEK293T cells were transfected with cDNA encoding integrin αV. Endogenous CIB1 was immunoprecipitated from integrin αV-transfected or integrin α5-transfected cell lysates. This figure is adapted from Freeman et al. and used with permission from (124). Copyright 2013 ACS.

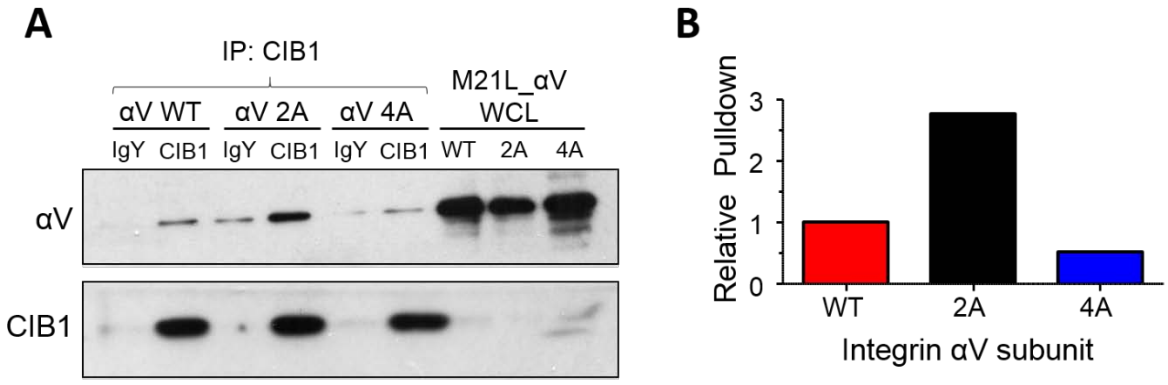

Figure 3-7. Integrin αV mutations alter CIB1-αV binding in cells. A) CIB1 was immunoprecipitated from M21L cells overexpressing αV WT, αV 2A, or αV 4A. Immunoprecipitates were probed by Western blotting for the presence of αV. Whole cell lysates were also run to compare relative levels of overexpressed αV. B) Densitometry of Western blot in (A). Approximately 2.5 times as much αV 2A immunoprecipitated with CIB1 as αV WT. Less than half as much αV 4A immunoprecipitated with CIB1 compared to αV WT.

3.2.4 CIB1 binding to integrin αV may affect cell signaling and proliferation

Integrin αVβ3 binds to the extracellular matrix component vitronectin. To test whether disruption of CIB1-αV binding affects cell adhesion, I plated M21L-αV WT and M21L-αV 4A cells on vitronectin and measured cell adhesion using a centrifugation-based adhesion assay. I found no difference in M21L cell adhesion to vitronectin after 30, 60, or 90 minutes between M21L-αV WT and M21L-αV 4A cells (Figure 3-8A).

In addition to cell adhesion, integrins transmit signals from the extracellular environment to the inside of the cell and thereby promote cellular processes including cell proliferation. To determine whether CIB1-αV binding affects cell proliferation, I plated equal numbers of M21L-αV WT/2A/4A and then measured total cell number after three days of growth. While the results show that there is not a statistically significant difference in cell proliferation between the cell types, the results trend towards a decrease in proliferation in cells expressing αV 2A, and trend toward an increase in proliferation in cells expressing αV 4A (Figure 3-8B).

To explore whether CIB1-αV binding affects cellular signaling, I examined ERK phosphorylation in M21L-αV WT/2A/4A cells plated on vitronectin. Cells were plated on vitronectin to focus the cell signaling response to integrin αV-mediated signaling. Cells were harvested at 30, 60, and 180 minutes after plating on vitronectin, then lysed and analyzed by Western blot, and signals quantified by densitometry. Although the relative ERK phosphorylation was not statistically significant between different cell types, cells expressing αV 4A trended towards increased ERK phosphorylation, whereas cells expressing αV 2A trended towards decreased ERK phosphorylation (Figure 3-8C).

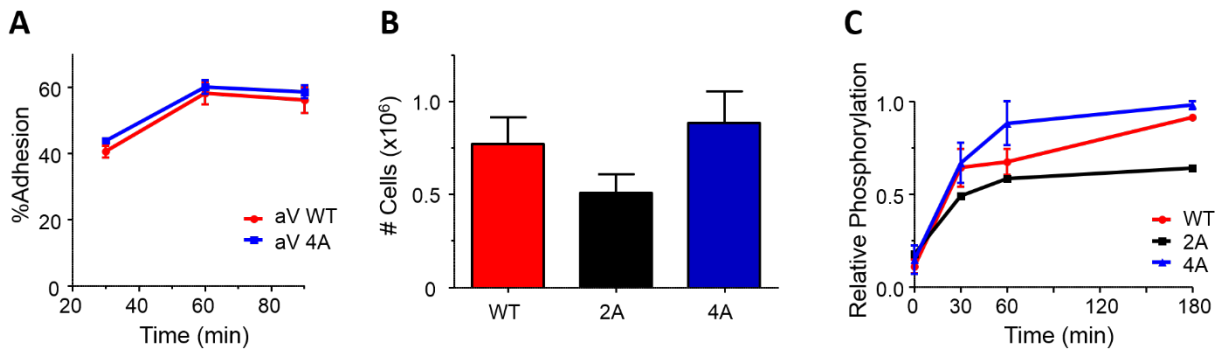

Figure 3-8. Integrin αV mutants may affect cell proliferation and cell signaling. A) Adhesion assay. M21L-αV WT and M21L-αV 4A cells were plated on vitronectin coated-plates and allowed to adhere for 30, 60, or 90 minutes. The relative percent of adherent cells was determined. No difference was observed between cells expressing αV WT and cells expressing αV 4A. B) Proliferation assay. M21L-αV WT/2A/4A cells were allowed to grow in cell culture and total cell number was assessed three days after plating. Though the difference in average cell number was not statistically significant between cell types, the data trend toward an effect of integrin mutants on cell proliferation. Data represent the average total cell number ± SEM. N = 5 (WT/4A); N = 3 (2A). C) Relative phosphorylation of ERK in M21L-αV WT/2A/4A cells plated on vitronectin. Cells were plated on vitronectin and then harvest 30, 60, or 180 minutes after plating. Cell lysates were analyzed by Western blot for relative levels of ERK phosphorylation and blots were quantified by densitometry. Although the difference between cell types was not statistically significant, cells expressing αV 4A trend toward increased pERK, whereas cells expressing αV 2A trend toward decreased pERK, relative to αV WT. N = 3.

3.2.5 CIB1 binds to different integrin α subunits via distinct residues in the CIB1 hydrophobic pocket

CIB1 interacts with α-integrin subunits via a hydrophobic binding pocket (71,72). The C-terminus of CIB1 forms an α-helix that, in the absence of a binding partner, lays in the hydrophobic pocket (75). The CIB1 structure based on a homology model of calcineurin B, an EF-hand containing protein relative of CIB1, demonstrates how the C-terminal helix may undergo a conformational shift to enable integrin binding to the CIB1 hydrophobic pocket (207). I utilized this structure to explore CIB1 binding to α-integrin peptides.

To determine whether CIB1 makes unique contacts with different α-integrin subunits, Freeman et al. performed all-atom replica exchange discrete molecular dynamics (DMD) simulations to model CIB1 binding to integrin αIIb and αV subunits (124). Using the lowest energy structures from the simulations, residues on CIB1 were identified that make contact with integrin αIIb and integrin αV. Nine residues in the CIB1 hydrophobic pocket contact αIIb and twelve residues contact αV. Notably, unique residues made contact with each integrin subunit, suggesting that CIB1 interacts with each integrin subunit via different residues in the hydrophobic pocket (Figure 3-9) (124).

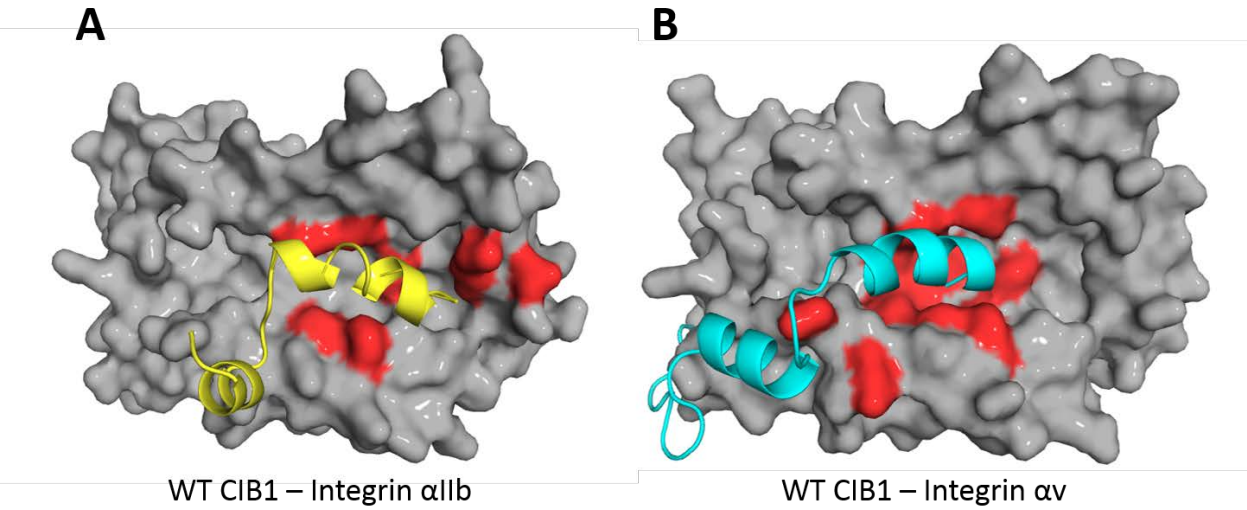

Figure 3-9. CIB1 makes unique contacts with different α-integrin subunits. Discrete molecular dynamics simulations of CIB1 binding to integrin αIIb (A, yellow) or αV (B, cyan). Figures represent lowest energy structures from molecular docking of integrin peptides to CIB1. CIB1 is shown in gray and residues making contact with the integrin peptide are colored red. Different residues make contact with each individual integrin peptide. This figure is adapted from work published by Freeman et al (124).

Since CIB1 makes unique contacts with different α-integrin subunits, I hypothesized that alanine substitutions to residues in the CIB1 hydrophobic pocket would affect the docking of integrin peptides to CIB1. To test this hypothesis, I generated alanine mutations in the CIB1 structure used for DMD simulations (PDB file 1DGU) at the residues that made contact with the integrins in the DMD simulations (see Figure 3-10B). I then performed docking simulations to determine whether the alanine substitutions affected integrin peptide docking to CIB1 (Table 3-1).

Several CIB1 mutants were further tested by Tina Leisner using in vitro pulldown assays with MBP-integrin cytoplasmic tail fusion proteins (124). Mutants 152LI/AA and 173F/A weakened CIB1 binding to αIIb, but had minimal effect on CIB1 binding to αV, whereas 114 IFDF/AADA greatly reduced CIB1 binding to αV with no detectable change in CIB1-αIIb binding (Figure 3-10A). Two of these mutants, 173F/A and 114 IFDF/AADA, had opposite results in in vitro binding assays as they did in the DMD simulations. Thus, although the predictions generated from the DMD simulations are interesting, more direct binding assays must be carried out to determine the effect of CIB1 mutations on CIB1-integrin binding. To better understand the cellular phenotypes of mutations to the CIB1 hydrophobic pocket, cell-based assays were attempted by expressing full length WT CIB1 and CIB1 mutants in CIB1 deficient cells; however these assays were unsuccessful due to decreased expression of CIB1 mutants relative to WT CIB1 (Figure 3-10C).

CIB1 mutation	Disrupt integrin αV binding?	Disrupt integrin α5 binding?
$114^{IFDF/AADA}$	No	Yes
$114^{IFDF/AADA}+173^{F/A}$	No	No
$115^{A/S}$	No	No
$131^{LVNCL/AANCA}$	Yes	No
$131^{LVNCL/AANCA}+173^{FQHI/AQHA}$	Yes	Yes
$135^{L/A}$	No	No
$135^{L/N}$	No	No
$173^{F/A}$	Yes	No
$173^{FQHI/AQHA}$	Yes	Yes
$177^{I/A}$	Yes	Yes

Table 3-1. Effect of CIB1 mutations on CIB1-integrin binding by DMD simulations. CIB1 mutants were docked with integrin αV and integrin α5 peptides and lowest energy state was compared to docking to WT CIB1, then displacement of peptides was assessed.

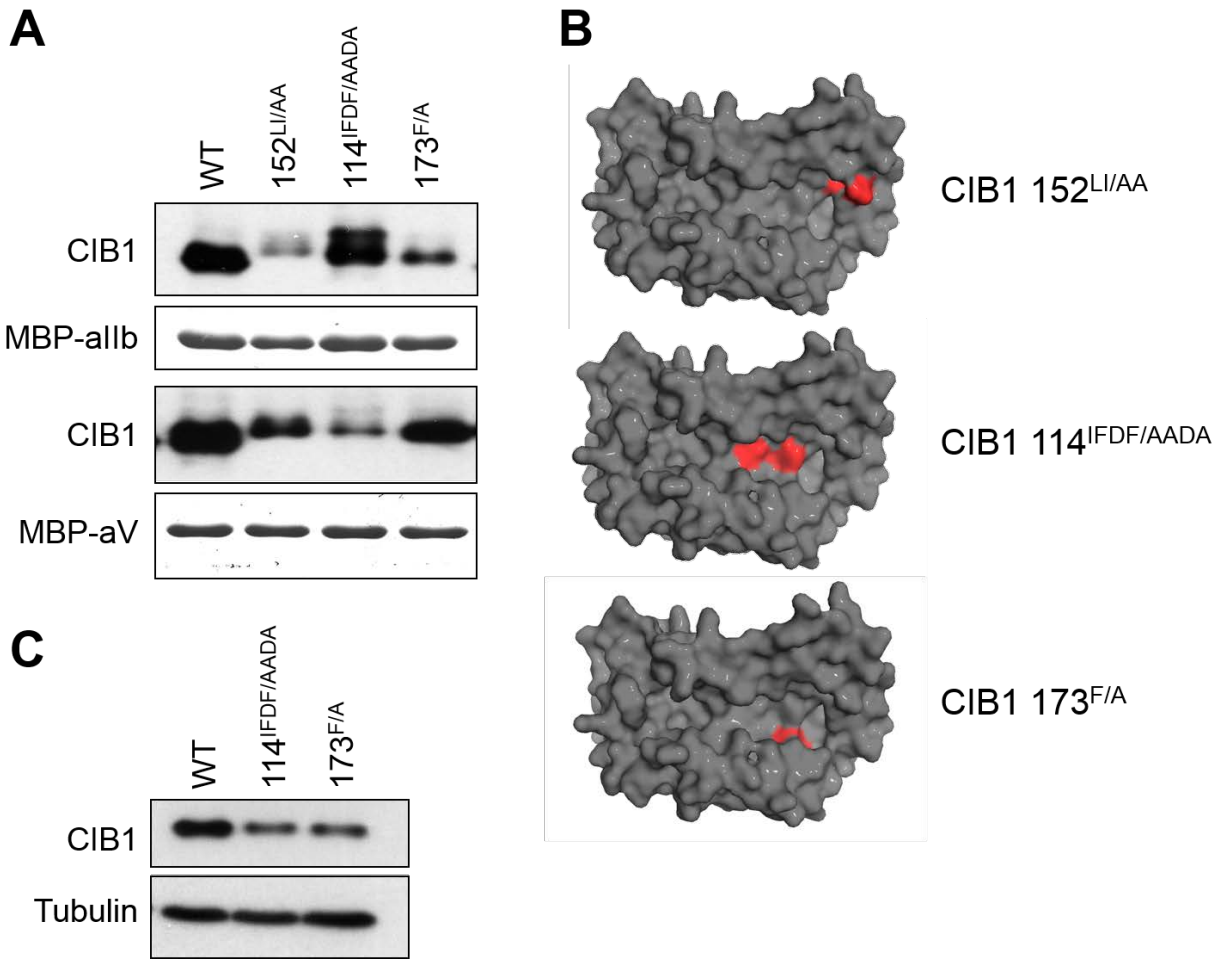
A
WT
152LI/AA
114IFDF/AADA
173F/A
ClB1
MBP-aIIb
ClB1
MBP-aV
B
ClB1 152LI/AA
ClB1 114IFDF/AADA
ClB1 173F/A
C
WT
114IFDF/AADA
173F/A
ClB1
Tubulin

Figure 3-10. Alanine substitutions in the CIB1 hydrophobic pocket disrupt CIB1 binding to α-integrin peptides. Purified CIB1 WT and three CIB1 mutants (152 LI/AA, 114 IFDF/AADA, 173 F/A) were mixed with MBP-αIIb or MBP-αV. MBP was pulled down and binding partners were analyzed by Ponceau-S staining (MBP-αIIb and MBP-αV) or Western blot (CIB1). A) CIB1 $152^{LI/AA}$ lacked binding to αIIb and slightly reduced binding to αV. CIB1 $114^{IFDF/AADA}$ lacked binding to αV, but maintained normal binding to αIIb. CIB1 $173^{F/A}$ had slightly reduced binding to αIIb, but no effect on αV. Panel A was adapted from a figure published by Freeman et al (124). B) Structural models of each CIB1 mutant with mutations highlighted in red. All three mutations are in the hydrophobic binding pocket at locations predicted to make contact with integrin peptides in DMD simulations. C) Western blot of lysates of cells expressing either WT or mutant CIB1. CIB1 114 IFDF/AADA and 173 F/A have lower expression than WT CIB1. Tubulin is included as a loading control.

3.3 Discussion

Integrin function is critical to cell biology, and there is a need to better understand the intracellular mechanisms by which integrins are regulated and through which integrins perform their various functions. Integrin αV is one integrin of particular interest due to its role in vascular biology and its upregulation on many cancer cells.

I explored the molecular interaction between CIB1 and the integrin αV subunit, and the functional effects of this interaction in cells. Until recently, CIB1 was considered to be a binding partner of one integrin, αIIb. Freeman et al. demonstrated that CIB1 binds to additional integrin subunits both in vitro and in cells. I explored the significance of specific amino acid residues in the putative CIB1-binding domain on the integrin. Specifically, residues αV-1011LVFVMY and αIIb-1014LVLAMW were examined by introducing amino acid substitutions/mutations to these residues and measuring the effect on CIB1-integrin binding by ITC and nanodisc pulldown experiments. These experiments revealed that α-integrin amino acid residues at the C-terminus of the transmembrane portion of the integrin are essential for CIB1 binding to αV and αIIb. This finding is significant because under normal conditions, these residues are embedded in the cell membrane near the interface of the membrane and cytoplasm. These findings may suggest that CIB1 embeds itself into the cell membrane in order to access its binding site on the integrin. Alternatively, the integrin may shift conformation in order to expose transmembrane residues and enable CIB1 to access its binding domain. Further experiments should be designed to better understand the structure of CIB1-integrin binding in a membrane environment. For example NMR may be used to determine the structure of the CIB1-integrin complex in nanodiscs, and potentially garner mechanistic insights into the role of CIB1 in integrin activation and signaling.

The role of CIB1 binding to integrin αIIb has been explored previously in platelets and megakaryocytes (platelet precursor cells) (81,83), but despite the ubiquitous expression of CIB1, the role of CIB1 binding to additional integrins has not been explored previously (124). I generated

integrin αV mutants and expressed wild-type and mutant αV subunits in the αV-deficient cell line M21L. The M21L-αV 4A cells had reduced CIB1-αV binding, as expected. Surprisingly, the M21L-αV 2A cells had more CIB1-αV binding compared to M21L-αV WT cells. These results may suggest that αV 2A binds to CIB1 with greater affinity than αV WT (although ITC and nanodisc pulldown in vitro assays do not confirm this finding). Regardless, this finding provided a unique opportunity to examine the differential effects of more/less CIB1-αV binding on cell proliferation and cell signaling. Although the results reported here did not reach statistical significance, the trends observed are worthy of discussion. M21L-αV 4A cells trended towards higher pERK signaling and proliferation. Conversely, M21L-αV 2A cells trended towards lower pERK signaling and reduced proliferation. One explanation of these results could be that CIB1-integrin binding per se reduces ERK activation and cell proliferation. However, an alternative explanation may be that when CIB1 is occupied by integrin αV 2A, it is less available to interact with other binding partners, such as PAK1, and promote ERK signaling and proliferation. Conversely, the αV 4A mutant reduced CIB1 binding, suggesting that more CIB1 is free in the cytoplasm to interact with PAK1 and other binding partners and promote ERK activation and cell proliferation. In this context, the results presented here predict that a CIB1 small molecule or peptide inhibitor may reduce cell signaling and cell proliferation. When considered with the data presented in Chapter 2, these data further confirm CIB1 as a target for cancer therapy.

3.4 Methods

Methods utilized here were performed as described previously (124), unless otherwise noted.

Protein purification and peptide synthesis – Human wild type CIB1 was cloned into pProEX HTc (Invitrogen), and further modified to include an upstream amino-terminal hexahistadine tag followed by a tobacco etch virus (TEV) cleavage site to facilitate removal of the hexahistadine tag. CIB1 mutants ^{114}IFDF/AADA, ^{152}LI/AA, and ^{173}F/A were made as previously described (208). MSP1 plasmid was obtained from Stephen Sligar. MBP-αIIb WT and mutant genes were generated by PCR-amplifying the C-terminus of αIIb and cloning into the pQE-MBP expression vector. MSP1, MBP-αIIb WT and mutants, and CIB1 WT and mutants were expressed and purified from *E. coli* BL21(DE3) as described previously with slight modifications as follows (209). After harvesting the cells, lysing by sonication, and centrifugation, clarified cell lysate was loaded onto an AKTA Purifier UPC 100 fitted with a 20 mL His-Prep FF 16/10 column (GE Healthcare). Fractions containing CIB1 were pooled and dialyzed in storage buffer (50 mM HEPES (pH 7.4), 150 mM NaCl, 10% (v/v) glycerol, and 100 µM $CaCl_2$). The 6xHis tag was removed by proteolysis using His-tagged TEV, which was added at approximately 1 mg/100 mg of CIB1 along with 1 mM DTT, and 0.5 mM EDTA. Cleavage was carried out overnight at room temperature. Mature CIB1 was isolated by subtractive Ni^{2+} affinity purification, where His-TEV was bound to the column, and CIB1 was collected in the flowthru. The DTT and EDTA was removed by dialysis in storage buffer. Protein concentration of mature CIB1 was measured by absorbance at 280 nm and ε = 2980 cm^{-1} M^{-1}.

Peptides were synthesized by either Bio-Synthesis, Inc. or via the High-Throughput Peptide Core and Arraying Facility at UNC-CH and purified by high performance liquid chromatography (HPLC). Peptide mass was confirmed by MALDI MS/MS on a 7400 Proteomics Analyzer (Applied Biosystems). Sequences used are listed in Figure 3-1A.

To generate cytoplasmic tails that could be precipitated with amylose resin beads, DNA encoding either residues 1014-1039 of human wild type αIIb, or residues 1011-1048 of human wild type αV was cloned into a pMAL vector (New England Biosystems) downstream of the malE gene. The fusion protein-encoding vectors were transformed into E. coli BL21Star(DE3), which were then grown at 37°C in 1 L of LB, and 1mM IPTG was added to induce over-expression of the MBP-α-integrin CT fusion proteins, which continued for 4 hours at 37°C. The cultures were harvested by centrifugation, resuspended in 50 mM HEPES (pH 7.4), 150 mM NaCl, lysed by sonication, and then clarified by centrifugation. The MBP fusion products were purified from the lysates amylose resin beads (New England Biolabs) according to the manufacturer's instructions. Samples were dialyzed against 50 mM HEPES (pH 7.4), 150 mM NaCl, 10% (v/v) glycerol overnight, tested for purity by SDS PAGE, and final protein concentration was measured using the BCA protein assay (Pierce).

Isothermal titration calorimetry (ITC) – ITC was performed to quantify the thermodynamics of binding between CIB1 and α-integrin tail peptides as previously described with minor modifications (132). Purified CIB1 was dialyzed extensively in 50 mM HEPES (pH 7.4), 150 mM NaCl, 0.1 mM CaCl2 (unless noted differently elsewhere), and diluted to a concentration of 100 μM. Peptides were freshly dissolved to concentrations ranging from 0.8 to 1 mM in the same buffer as CIB1. Isothermal titrations were performed using a MicroCal VP-ITC microcalorimeter. Injections of 10 μL of peptide were added at 300 s intervals at either 15 °C or 26 °C. The heats of dilution were estimated from injections made after saturation occurred. These values were subtracted from the data before one-site curve fitting was performed using Microcal, LLD Origin 7.

Co-immunoprecipitation – Co-IP was performed to determine whether CIB1 associates with αVβ3 or α5β1 integrin complexes in mammalian cells as previously described with some modifications (163). HEK293T cells were maintained in DMEM supplemented with 10% FBS and

1% non-essential amino acids at 37 °C and 5% CO_2. Plasmids encoding human integrin α5 or αV were transiently transfected in HEK293T cells using Fugene (Roche) according to manufacturer's instructions. Cells were harvested and lysed with CHAPS lysis buffer (25 mM HEPES [pH 7.4], 150 mM NaCl, 10 mM CHAPS, 30 mM NaF, 10 mM β-glycerophosphate, 0.2 mM Na_3VO_4, 1.25 mg/mL N-ethylmaleimide, 0.1 mM $CaCl_2$, 0.1 mM $MgCl_2$, 5% glycerol, and Protease Inhibitor Cocktail III (Calbiochem) diluted 1:100). Clarified lysates were incubated overnight with either chicken non-specific or anti-CIB1 IgY, and immune complexes were precipitated using goat anti-chicken IgY agarose beads (Aves Labs, Inc.). Beads were washed three times in lysis buffer and eluted with 1X non-reducing sample buffer. Samples were resolved by SDS-PAGE, transferred to PVDF membrane and probed with rabbit anti-integrin α5 polyclonal antibody (Millipore), mouse anti-integrin αV monoclonal antibody (BD Transduction) or chicken anti-human CIB1 IgY.

Co-precipitation – Purified recombinant MBP-αIIb or MBP-αV cytoplasmic tails were loaded onto amylose resin beads and washed 3x in assay buffer (25 mM HEPES, pH 7.4, 150 mM NaCl, 0.1 mM $CaCl_2$). MBP-tail beads were added to recombinant WT or mutant CIB1 proteins diluted in assay buffer (0.75 mg/ml) and incubated 1 h at 4°C. Beads were washed 3x with assay buffer and samples were analyzed by SDS-PAGE.

Nanodisc production and pulldown assays – Nanodiscs were generated using a protocol developed by the Stephen Sligar Lab (210-212). Phosphatidylcholine (PC) and phosphatidylserine (PS) lipids (Avanti Polar Lipids) were dried with nitrogen gas to evaporate chloroform. Dried lipids were resuspended in 200mM CHAPS (AppliChem) and stored at 4 °C. Nanodisc components were mixed at the following ratios in this order: MSP1 (25 nmol, 5x αIIb); lipid (1.625 µmol, 65x MSP1; 90:10 mixture of PC:PS); cholate (14 mM); diluted to final volume of 660 µL in TBS (20 mM TRIS, 150 mM NaCl); αIIb peptide (5 nmol). Nanodisc mixtures were then rotated with 400 mg Bio Beads SM-2 Adsorbent (Bio-Rad) at 4°C for 2 hours (Bio Beads

were pre-washed according to manufacturer's protocol prior to mixing with nanodisc components). Samples were then run over Ni^{2+}-NTA superflow (Qiagen) to positively select for nanodiscs via His-tagged MSP1, washed 3x with TBS + 30mM imidazole (Sigma), and eluted with TBS + 250mM imidazole. Nanodisc-containing samples (determined by absorbance at 580nm) were pooled and dialyzed against 25mM TRIS + 150 mM NaCl overnight with 2 exchanges using 10,000 molecular weight cutoff Slide-a-lyzer Dialysis Cassettes (Thermo Scientific), then stored at 4 °C.

Nanodisc pulldown assays were done by mixing 25 µL nanodiscs with 1 µL CIB1 (110 µg/mL) and diluting with 464 µL TBS-I (20 mM TRIS, 150 mM NaCl, 0.1 mM CaCl2, 30 mM imidazole), rotating at room temperature for 5 min, then adding pre-washed Ni2+-NTA (10 µL packed beads) and rotating at room temperature for 1 hour. Beads were then washed 2x with TBS-I and resuspended in 1x sample buffer (2x sample buffer diluted with 250 mM imidazole) and heated at 95 °C to elute proteins, then stored at -20 °C. Samples were analyzed by Western blot to qualitatively assess the amount of CIB1 protein that precipitated with the nanodisc/ Ni2+-NTA beads.

Electron microscopy – Transmission electron microscopy images of prepared nanodiscs were obtained at the UNC Microscopy Services Laboratory to confirm uniform size and shape of nanodiscs. We followed a protocol similar to previously published protocols (213). Briefly, samples were prepared by discharging carbon grids using a glow discharge system. A drop of sample was pipetted onto the grid and allowed to stand, then blotted with a piece of sterile filter paper. The grid was then inverted and placed on a droplet of 2% (wt/vol) uranyl acetate briefly, then blotted again with filer paper. The grids were then allowed to air dry and then imaged using a Zeiss TEM 910 Transmission Electron Microscope.

Size-exclusion chromatography – A Superdex 200 10/300 GL column was used (Sharon Campbell lab). Column was washed with 4 column volumes (column volume = 23.562 mL) of 1x

TBS (25mM TRIS, 150 mM NaCl, de-gassed). 0.5mL of each sample was loaded into 1mL loop using a 1 mL syringe and flowed through column at 0.5 mL/min and washed with 1.5 column volumes buffer between each sample. Fractions were collected each minute. The molecular weight of the peaks in the column were calculated using the following equation:

$$y = 22.88 + (-4.65)(\log_{10}MW)$$

where y = the elution volume (mL) and MW = the molecular weight in kDa. Appropriate fractions were further analyzed by Western blot to confirm the presence of nanodisc proteins (MSP1 and MBP-integrin).

Full-length integrin mutagenesis and expression – Full-length integrin αV was cloned into the pLVX_IRES_GFP (generously donated by Dr. Scott Magness, UNC) mammalian expression vector. Mutations were made using Quikchange site-directed mutagenesis kit (Agilent Technologies) to mutate residues 1011-1012 (LV/AA) and 1011-1014 (LVFV/AAAA) to alanine. Purified DNA plasmids were packaged into lentivirus by transfecting HEK293T cells and harvesting virus-containing media 2 days post-infection. Target cells (HEK293T and M21L) were transduced and GFP fluorescence was used to determine transduction efficiency. Relative integrin expression was determined by flow cytometry and Western blotting using integrin αV antibody (flow cytometry – Millipore; Western blot – BD Biosciences).

Adhesion assays – 96-well plates were coated with vitronectin (PeproTech) 1 hour at room temperature, then washed with PBS. Wells were then blocked with 10 mg/mL BSA (Celliance). M21L-αV WT or mutant cells were detached with PBS-2mM EDTA and counted. $1x10^5$ cells were plated per well and the wells were then filled with serum free media. Plates were covered and spun 3 min at 400 rpm to force cells to the bottom of the wells. Plates were then incubated 30 min at 37 °C, uncovered. The plate was then covered and sealed, inverted, and spun at 740 rpm for 5 min. The plastic cover was carefully removed and wells were washed 1x with 200 µL PBS, then fixed with 100 µL 2% formaldehyde for 20 min at room temperature, washed 1x with 200 µL dH_2O,

stained with 100 µL .1% crystal violet (Sigma) for 30 min at room temperature, and washed with 200 µL dH_2O. The plate was allowed to air dry, then crystal violet was solubilized by adding 100 µL 1% SDS per well and shaking the plate at 900 rpm for 10 min at room temperature. The plate was then read using a SpectraMax plate reader (Molecular Devices) at 590 nm.

Proliferation assays – M21L-αV WT/2A/4A cells were plated at a density of $1x10^5$ cells per plate and allowed to grow for 3 days, then harvested and counted using hemacytometer. Cell viability was determined by trypan blue exclusion (Sigma). Average total number of cells from either five (WT, 4A) or three (2A) independent experiments was plotted.

Cell signaling assays – 12-well plates were coated with 10 µg/mL vitronectin for 1 hour at 37 °C, then blocked with 10 mg/mL BSA. M21L-αV WT/2A/4A cells were detached using PBS-2mM EDTA and held in suspension for 1 hour at 37 °C with occasional mixing, then $5x10^5$ cells were plated per well. Plated cells were lysed after 30/60/180 minutes using CHAPS lysis buffer (10 mM CHAPS, 0.1 mM $CaCl_2$, 0.05 mM $MgCl_2$, 20 mM NaF, 10 mM βGP, 0.1 mM pervanadate, 1.25 mg/mL NEM, 20 mM HEPES, 150 mM NaCl, 5% glycerol). Cell lysates were separated by SDS-PAGE, transferred to PVDF, and probed with antibodies for pERK (Cell Signaling) and Rac (Millipore). Films were scanned and density of bands was assessed using ImageJ.

All-atom replica exchange discrete molecular dynamics (DMD) – Modeling of CIB1 binding to α5 and αV cytoplasmic tail peptides was performed to test for potential binding interactions with CIB1, and those models were compared to a simulation of αIIb binding to CIB1. The model of CIB1 used in the simulations was either a homology model of CIB1 based on the ligand-bound form of calcineurin B (PDB code: 1DGU) or the solution structure of αIIb-CT-bound CIB1 (PDB code: 2LM5) (207). The structure of αIIb was taken from (PDB code: 2KNC), and α5 and αV peptide structures were modeled after the αIIb structure using I-TASSER (214,215). The starting structure of each integrin peptide was placed approximately 40 Å away from CIB1 using the edit functions of PyMol (216). The DMD simulations were performed as described by Dagliyan, *et al.*

(217). In these simulations the backbone of CIB1 was fixed while all atoms of the peptides were free to move with some constraints added to preserve the secondary structure. The DMD engine approximates inter-atomic interactions by discrete square well potentials, and models proteins using the united atom representation. The Van der Waals forces, solvation interactions, and electrostatic interactions are modeled in a discretized manner as well. In replica exchange, a simulation is performed in replicate at different temperatures and the structures are exchanged between the replicates at regular intervals. This robust approach allows the engine to more easily overcome energy barriers. The length of each simulation was 10^6 time units, which is approximately 50 ns of real time. After the DMD simulations were complete, hierarchical clustering of the integrin binding conformations were performed using root-mean-square distances (RMSD) calculated over all heavy atoms in the peptide, and MedusaScore was used to evaluate the energy landscape of the clustered poses (218). The lowest energy complexes were taken from the largest clusters and further refined using MedusaDock to obtain the final structures (219). Images of the models were created using PyMol. Atom pair contacts made between CIB1 and the integrin CT peptides were identified in the docking models by finding all residues on CIB1 that were within 4 Å of any side chain atom on the integrin CT peptide using PyMol.

FUTURE DIRECTIONS

In this dissertation, I have presented experimental evidence and analysis for the role of CIB1 in cancer cell biology, and in the molecular interaction between CIB1 and integrin cell adhesion receptors. While the present body of work has contributed significantly to understanding the roles and functions of CIB1 at the molecular and cellular levels, several new questions have also been uncovered. Here I will discuss future directions that may be pursued to further explore the role of CIB1 in tumor growth, gene expression, and integrin binding.

A major finding of this work is that RNAi-mediated depletion of CIB1 from triple negative breast cancer tumors results in dramatic tumor shrinkage. This exciting result suggests that drug targeting of CIB1 may be a novel method to treat cancer. To test the hypothesis that CIB1 is a novel cancer drug target, two major questions need to be answered. First, does CIB1 depletion effectively shrink tumors in clinically-relevant tumor models? The two models that should be explored are patient derived xenografts (PDX) and/or genetically engineered mouse models (GEMM). While the xenograft experiments reported on here (see Chapter 2) provide a solid foundation for the in vivo relevance of targeting CIB1, PDX and GEMM TNBC models would provide more extensive, clinically-relevant data to address whether CIB1 is a target for cancer therapy. Second, what additional cancer subtypes are susceptible to CIB1 depletion? This work should be pursued at the cellular level by screening cancer cell lines from different tissue types and with varying molecular profiles. Cell lines found to be sensitive to CIB1 depletion should then be further explored using in vivo models of cancer. Identification of additional cancer subtypes susceptible to CIB1 depletion could broaden the scope of the present work, and also provide additional clues to the molecular markers that result in non-oncogene addiction to CIB1 (e.g. PTEN loss or elevated pAKT).

This work represents the first report of a role for CIB1 in the regulation of gene expression. Further work is necessary to better understand how CIB1 affects gene expression, particularly in

cancer cells. In particular, the following questions should be answered. First, which genes does CIB1 affect directly, and which genes does CIB1 affect indirectly? As reported here, more than 800 genes were differentially expressed following extended CIB1 depletion from MDA-MB-468 cells. To determine which genes are directly affected by CIB1 depletion, we have proposed a series of experiments with our collaborators from the Chuck Perou lab using microarrays to examine gene expression changes at varying time points following CIB1 depletion. Informatics approaches can then be used to identify groups or families of genes that are affected by CIB1 depletion. Additional questions can then be explored to determine the mechanism by which CIB1 regulates gene expression and whether CIB1-dependent gene expression changes are different in cancer cells versus normal cells.

Finally, this dissertation lays the groundwork for future experiments exploring CIB1-integrin binding and the functional consequences of this interaction. First, it is important to better understand the biochemical and biophysical properties of the interaction between CIB1 and α-integrin cytoplasmic tails. As described in section 3.2.2, future experiments should utilize nanodiscs to enable in vitro experiments to understand the binding affinity of CIB1 and integrin in the presence of a membrane. Furthermore, nanodiscs could enable solving the NMR structure of CIB1 in complex with the integrin cytoplasmic tail, which would provide a wealth of knowledge about how CIB1 interacts with membrane-embedded integrin. In addition to in vitro assays, additional experiments could be designed to more thoroughly explore the role of CIB1-integrin binding on cell biology, including integrin-dependent signaling. It would be particularly interesting to explore how this role changes depending on cell type, and varying based on the unique repertoire of integrins on a particular cell type.

The work described here has answered several significant questions regarding CIB1, but has also opened new and exciting avenues to pursue in cancer, genetics, biochemistry, and cell biology.

CONCLUSION

CIB1 is a multifunctional protein with emerging roles in cancer cell biology. Here I have presented experimental evidence for two important functions of CIB1: 1) The role of CIB1 in cell survival and tumor growth in triple negative breast cancer; 2) The interaction between CIB1 and α-integrin cytoplasmic tails and the role of this interaction on cell biology.

Due to the significant unmet need for novel targeted therapeutics in TNBC, I explored the role of CIB1 in TNBC cell survival and tumor growth. Here I have shown that CIB1 depletion is necessary for cell survival in multiple TNBC cell lines in vitro, and TNBC xenograft tumor growth in vivo. I further defined cell line characteristics that predict sensitivity to CIB1 depletion, including elevated AKT activation status and low PTEN expression. RNA sequence analysis was used to demonstrate that CIB1 activates gene programs associated with decreased TNBC survival and increased cell death. Importantly, CIB1 expression is not upregulated in breast cancer versus normal tissue, and does not correlate with prognosis in TNBC patients. Taken together, these data are consistent with the emerging theory of non-oncogene addiction, where a large subset of TNBCs depend on CIB1 for cell survival and tumor growth, independent of CIB1 expression levels.

To better understand the role of CIB1 as an integrin binding protein, I pursued an additional project to explore CIB1 binding to α-integrin cytoplasmic tails and the functional consequences of this interaction. Using biochemical and biophysical techniques including isothermal titration calorimetry, in vitro co-precipitation, and co-immunoprecipitation, I identified critical residues in the α-integrin transmembrane domain to be essential for CIB1-integrin binding. Using molecular modeling, I also characterized residues in the CIB1 hydrophobic pocket necessary for interaction with unique α-integrin subunits, which was further validated by in vitro co-precipitation assays. Finally, I tested the physiological role of CIB1-integrin binding in cells by expressing mutant

proteins in cells and measuring differences in integrin-dependent cell functions. I present evidence that CIB1 can interact with integrins in the presence of a cell membrane, and that CIB1-integrin binding may contribute to normal cell functions, including signaling and proliferation.

CIB1 is emerging as an essential element in TNBC as well as in integrin biology. The work presented herein demonstrates the diversity of CIB1 functions and the critical nature of this protein in cell biology.

APPENDIX A

Upregulated Genes

Gene Name	log2 Fold Change	padj
HMGA2	7.36	0.0E+00
MYH16	6.66	0.0E+00
IGFN1	6.54	8.3E-114
CSF2	6.50	1.8E-168
IL1RL1	6.08	0.0E+00
C12orf40	6.05	1.0E-46
KRTAP2-3	5.83	0.0E+00
IL24	5.56	6.2E-90
ESM1	5.43	5.9E-115
METTL11B	5.07	1.9E-31
ISM1	5.05	2.7E-153
KRT37	4.95	5.9E-39
TMEM200A	4.89	6.2E-36
MARCH4	4.78	9.9E-74
SERPINB2	4.77	0.0E+00
IL8	4.71	0.0E+00
SPRR3	4.69	0.0E+00
SPRR1B	4.67	3.0E-289
HAS2	4.66	2.4E-28
SHC4	4.66	4.1E-160
KRT34	4.64	0.0E+00
SH2D5	4.62	2.5E-96
CTSE	4.56	1.7E-32
PRSS3	4.54	5.8E-57
IL1R2	4.54	1.2E-158
PTHLH	4.51	2.3E-196
MYH15	4.47	2.0E-303
RNASE7	4.39	3.5E-39
SPRR1A	4.38	3.4E-41
LPPR5	4.34	2.8E-85
AGPAT9	4.33	0.0E+00
CORO2B	4.32	2.2E-92
IL1B	4.31	6.0E-19
NCAN	4.30	2.6E-50
ADAMTS6	4.18	4.8E-25
ERG	4.17	2.3E-47
TNFSF18	4.15	2.9E-33

NOX3	4.12	1.4E-17
DKK3	4.11	7.8E-30
SNCB	4.05	6.6E-53
FAM83C	4.04	8.6E-19
LOC100130476	4.00	1.4E-67
RAB3B	3.97	0.0E+00
IL13RA2	3.97	9.7E-127
CD274	3.90	0.0E+00
SH2D1B	3.89	1.4E-20
NTNG1	3.86	1.2E-39
SPOCD1	3.83	0.0E+00
WNT7A	3.82	2.0E-38
HEPHL1	3.82	0.0E+00
LGI2	3.79	1.7E-19
KHDC1L	3.78	2.9E-31
FAM25A	3.77	2.4E-127
SYT14	3.75	1.3E-100
IL6R	3.71	1.3E-71
ROBO4	3.71	2.2E-50
SMOC1	3.70	4.2E-174
INHBA	3.66	0.0E+00
ALOXE3	3.66	4.2E-146
FCRLA	3.66	8.0E-33
KRT6A	3.65	0.0E+00
KCNK13	3.65	5.2E-71
ALPK2	3.61	3.3E-115
LINC00707	3.58	0.0E+00
GJB4	3.57	1.6E-111
FOSL1	3.56	0.0E+00
ENTPD3	3.56	4.4E-41
PDCL2	3.53	6.0E-15
PDCD1LG2	3.52	2.5E-19
VIM	3.47	0.0E+00
ADRA1D	3.47	1.6E-169
SOCS2	3.46	0.0E+00
CYGB	3.46	5.5E-20
KPNA7	3.46	0.0E+00
AREG	3.46	9.9E-17
LOC728084	3.43	1.3E-16
FLJ35946	3.40	8.4E-72
NOG	3.40	1.5E-123
XIRP1	3.40	1.8E-38
DPF3	3.38	3.5E-27

RGS4	3.37	2.3E-12
MAOA	3.35	0.0E+00
ITGA2	3.34	0.0E+00
LY6K	3.30	0.0E+00
CES1P2	3.29	3.4E-20
SOCS2-AS1	3.28	6.9E-22
GCKR	3.27	5.4E-16
SP8	3.25	1.4E-153
LMCD1	3.25	1.2E-154
PCDH12	3.24	1.8E-33
CRCT1	3.22	4.5E-25
IL23A	3.22	1.0E-46
MUSK	3.22	3.9E-25
RGS20	3.22	3.5E-219
NPY2R	3.20	4.9E-10
PTPRH	3.19	3.3E-221
AXL	3.19	1.5E-120
LINC00312	3.17	5.1E-19
CXCL1	3.17	1.5E-297
TNFAIP3	3.14	0.0E+00
FST	3.14	7.8E-117
MMP1	3.13	3.3E-12
SYNGR3	3.12	6.3E-79
SYT13	3.10	3.7E-76
AKNAD1	3.09	6.9E-21
SBSN	3.09	2.2E-24
TRIM54	3.07	6.0E-29
CLMP	3.06	3.4E-93
VWA3B	3.06	6.1E-98
PPBP	3.05	2.1E-09
TH	3.03	6.9E-14
BACH2	3.03	7.5E-196
BMP6	3.02	2.1E-51
SBK2	3.00	1.7E-09
SPRR2A	2.99	6.6E-73
NLRP3	2.99	2.3E-24
KCTD5	2.98	5.3E-34
PKIB	2.96	8.0E-126
CHD5	2.94	6.7E-106
HPCAL4	2.93	4.6E-18
SLC22A18AS	2.92	1.8E-68
DRD2	2.91	7.1E-40
PDE1C	2.91	1.8E-140

CXCL6	2.91	2.7E-08
PRDM16	2.90	7.8E-12
TENM3	2.90	1.2E-10
ITGA5	2.89	0.0E+00
B3GAT2	2.88	2.0E-08
PHLDA1	2.88	0.0E+00
TPTEP1	2.88	4.5E-40
KRT86	2.88	1.4E-229
DMRT2	2.88	5.9E-13
ARNT2	2.87	3.9E-101
ZEB1	2.87	1.0E-26
SPINK7	2.86	4.8E-08
RPA4	2.86	4.9E-25
SYNE1	2.86	5.8E-157
TMEM255B	2.86	1.7E-32
COL15A1	2.84	2.8E-167
WFDC3	2.84	6.1E-40
RHEBL1	2.84	5.2E-125
ASB18	2.83	7.3E-08
PTPN22	2.81	2.0E-51
CDSN	2.78	3.5E-139
LOC256021	2.77	2.5E-22
PDE4B	2.76	0.0E+00
ART3	2.76	8.8E-52
ARID3B	2.75	0.0E+00
GJB3	2.74	0.0E+00
SFTA3	2.74	7.4E-08
TBX2	2.74	2.9E-17
ELOVL6	2.72	0.0E+00
SMIM3	2.70	0.0E+00
NCR3	2.70	3.1E-07
EMX1	2.70	7.2E-12
COL13A1	2.69	0.0E+00
CAMK1G	2.69	3.7E-14
LOC100287177	2.68	5.7E-12
IL1RN	2.67	0.0E+00
LOC152225	2.67	5.5E-89
LOC100288181	2.66	2.4E-45
FAM83A	2.64	1.3E-107
FOXF2	2.64	5.1E-21
LAMB3	2.63	0.0E+00
LOC401164	2.63	9.8E-08
GAL3ST3	2.62	3.6E-10

SYT6	2.61	9.1E-30
TRAF1	2.61	1.2E-54
COL17A1	2.61	2.7E-92
LOC646626	2.60	1.2E-21
CLDN6	2.60	2.3E-15
CWH43	2.60	4.3E-12
LOC100128993	2.59	1.0E-06
CDKN1A	2.59	0.0E+00
SPRY2	2.59	0.0E+00
ZNF365	2.59	3.4E-290
MAPK4	2.59	2.9E-30
PHYHIP	2.57	3.8E-13
C1QL2	2.56	1.2E-29
C6orf15	2.56	2.4E-48
PPM1K	2.56	8.3E-120
NLRP10	2.55	1.1E-08
CSNK1A1P1	2.55	1.1E-07
KRTAP2-1	2.55	1.6E-06
FAM3C	2.54	0.0E+00
C12orf39	2.53	6.4E-13
LINC00161	2.53	2.0E-06
C12orf75	2.53	0.0E+00
DNAJB5	2.52	0.0E+00
KIAA1755	2.52	2.6E-11
RPSAP52	2.52	1.0E-06
FYN	2.50	0.0E+00
KCNF1	2.50	1.7E-17
TTC9B	2.49	4.5E-12
TMEM132E	2.49	1.3E-08
KRT6B	2.49	0.0E+00
VSIG2	2.49	3.3E-07
XIRP2	2.48	3.2E-06
C6orf7	2.47	1.4E-10
DOCK10	2.47	2.1E-27
DCLK1	2.47	8.2E-11
GJB2	2.47	1.9E-165
KIF5A	2.45	4.5E-06
ELOVL4	2.45	0.0E+00
PBX4	2.45	2.8E-143
SLC5A1	2.44	0.0E+00
HMX3	2.44	7.5E-08
CRLF1	2.44	0.0E+00
WNT9A	2.43	9.5E-157

ISG20	2.43	1.1E-68
PRTN3	2.42	3.5E-08
KRTAP3-1	2.42	6.1E-118
ANKRD1	2.42	0.0E+00
AKAP12	2.41	3.0E-58
TAGLN3	2.41	2.0E-06
PTGFR	2.41	9.9E-18
IL18	2.41	0.0E+00
PRSS36	2.40	7.4E-34
GLIPR1	2.39	1.8E-131
ANKRD44	2.38	6.2E-62
AQPEP	2.37	1.2E-08
MGC32805	2.37	7.5E-13
CST7	2.36	6.8E-06
TM4SF4	2.35	3.5E-27
TULP3	2.35	0.0E+00
KCNMA1	2.35	9.6E-75
RNF182	2.35	3.3E-78
DRAXIN	2.34	7.5E-11
PLEK2	2.33	1.7E-293
GRM2	2.33	1.2E-19
BEST3	2.32	4.1E-15
DMRT3	2.32	4.2E-07
LINC00704	2.32	3.3E-233
GADD45A	2.31	0.0E+00
TGFA	2.31	0.0E+00
MUC16	2.31	2.2E-66
RAB39B	2.31	2.2E-22
LINC00659	2.31	1.7E-05
REN	2.31	8.2E-100
CALML3	2.30	3.7E-06
GPR87	2.30	5.4E-123
RORA	2.30	1.1E-40
PMAIP1	2.30	0.0E+00
HELT	2.30	1.3E-05
SERPINE1	2.29	0.0E+00
EREG	2.28	3.4E-44
GBX2	2.28	5.4E-20
ATG9B	2.28	1.1E-10
LOC286059	2.28	1.1E-07
TMEM59L	2.28	3.9E-16
GNG4	2.27	8.5E-80
GFPT2	2.27	3.4E-109

PDZD4	2.27	8.3E-51
LAMA3	2.26	0.0E+00
WFDC10B	2.26	2.5E-05
LDHAL6B	2.26	1.0E-07
VGF	2.26	2.1E-99
KRTAP4-12	2.25	1.8E-05
LINC00675	2.25	4.7E-27
SPRR2D	2.25	2.1E-07
FAM5B	2.24	1.5E-76
PRDM1	2.24	0.0E+00
TMEM151A	2.24	1.2E-16
FN1	2.23	0.0E+00
FAM155A	2.23	2.5E-05
FGF12	2.23	1.0E-07
FAM211A	2.22	2.2E-71
HLX	2.22	1.0E-27
BMP5	2.22	8.2E-16
ABL2	2.22	0.0E+00
ZBED2	2.21	4.9E-130
TMEM121	2.20	5.1E-21
CYP27B1	2.20	4.4E-26
RASGRP3	2.20	1.5E-136
ESAM	2.20	1.3E-139
CREG2	2.20	3.7E-09
SLITRK6	2.19	0.0E+00
LOC100127888	2.19	2.8E-16
LOC100506178	2.19	9.9E-09
RCVRN	2.19	3.5E-06
GPR183	2.19	2.2E-05
LINC00341	2.18	1.4E-19
HS3ST1	2.18	1.2E-127
DUSP14	2.18	0.0E+00
GAD1	2.18	4.8E-61
AHRR	2.18	2.0E-191
ANKRD18DP	2.18	2.4E-11
PLCXD2	2.18	8.4E-47
NFATC1	2.18	1.8E-40
YOD1	2.17	0.0E+00
ARNTL2	2.17	0.0E+00
SP9	2.17	3.7E-07
HOXB5	2.16	1.6E-10
KAT2B	2.16	8.5E-259
CTNNAL1	2.16	0.0E+00

C1QL1	2.16	4.1E-194
MRVI1-AS1	2.16	4.9E-06
KISS1	2.15	8.2E-12
CYP24A1	2.15	7.7E-07
GIPR	2.15	3.6E-23
NOS3	2.15	1.0E-07
LHX1	2.14	3.1E-66
FGFRL1	2.14	0.0E+00
IL10RA	2.14	2.2E-12
LRRN4	2.13	2.8E-06
DUSP6	2.13	0.0E+00
ACVR1C	2.13	2.2E-143
VSTM1	2.12	2.0E-05
TMEM55A	2.12	1.9E-35
GCNT3	2.12	1.2E-69
AHNAK2	2.11	0.0E+00
KIRREL2	2.11	1.8E-05
CRTAM	2.11	2.4E-11
LAMC2	2.11	0.0E+00
RNF38	2.11	0.0E+00
COL4A3	2.11	2.3E-109
SLC35D3	2.11	3.4E-05
SDCBP2	2.10	9.8E-47
ARID3A	2.10	7.1E-231
SGTB	2.09	0.0E+00
TSPAN5	2.09	0.0E+00
LOC256880	2.09	1.1E-13
HSD3B1	2.09	1.1E-05
SYT1	2.09	3.4E-20
HOXB9	2.09	2.0E-13
C9orf135	2.09	8.0E-07
C11orf91	2.08	1.0E-14
SERPINA6	2.08	8.8E-12
BTBD19	2.08	4.6E-22
TMEM156	2.08	0.0E+00
PGF	2.08	2.9E-11
SEC23A	2.08	0.0E+00
TINAG	2.07	4.1E-05
MPZ	2.07	8.8E-06
ECM1	2.07	1.3E-188
SERPINE2	2.06	2.8E-142
DKK1	2.06	0.0E+00
MMRN2	2.06	1.5E-181

MYO1E	2.06	0.0E+00
PANX2	2.05	1.1E-94
CCDC3	2.05	4.9E-50
LINGO1	2.05	9.8E-53
ANGPT4	2.05	1.4E-07
IL6	2.05	1.8E-60
GBP6	2.04	1.8E-12
STEAP1	2.04	1.9E-09
DUSP7	2.04	0.0E+00
CYP4F22	2.04	1.2E-04
TGFBR3L	2.04	2.3E-34
GPR1	2.04	3.4E-22
CDYL2	2.04	2.1E-05
ROCK1P1	2.03	1.3E-173
SNX29P2	2.03	1.1E-04
RNF223	2.03	0.0E+00
TMEM40	2.03	0.0E+00
HERPUD1	2.03	0.0E+00
UPP1	2.03	0.0E+00
DIRC3	2.02	1.5E-154
MRVI1	2.02	1.8E-29
TM4SF19	2.01	1.7E-04
SKAP1	2.01	1.5E-04
COL1A2	2.01	1.3E-04
A2ML1	2.01	2.4E-73
GEM	2.00	9.6E-32
CDK15	2.00	6.9E-06
PPP4R4	2.00	7.4E-07
AMMECR1	2.00	0.0E+00
ELK3	2.00	1.9E-293

APPENDIX B

Downregulated Genes		
Gene Name	log2 Fold Change	Padj
CRISP3	-8.32	0.0E+00
CYP4Z1	-7.00	3.4E-111
CP	-6.89	1.9E-205
COL3A1	-6.69	3.2E-148
S100A7A	-6.08	2.6E-219
RARRES3	-5.76	0.0E+00
SYCP1	-5.66	8.2E-48
CFI	-5.59	8.8E-264
ANXA10	-5.51	5.4E-44
CFH	-5.49	7.4E-59
LBP	-5.27	1.6E-32
EDIL3	-5.23	6.4E-92
FMO6P	-5.20	4.0E-36
CYP4Z2P	-5.18	3.6E-31
GUCY1A2	-5.16	1.2E-122
TLL1	-5.09	2.3E-38
BCHE	-5.08	1.4E-33
MMP13	-5.05	5.2E-84
CYP4B1	-5.04	0.0E+00
SEPP1	-5.03	5.9E-215
ATP6V1B1	-5.03	0.0E+00
SLC27A6	-5.01	1.0E-28
CHRNA9	-4.88	2.9E-34
SLURP1	-4.85	4.8E-30
HRASLS2	-4.84	1.7E-96
STAC2	-4.80	1.7E-82
ATP13A5	-4.72	6.2E-205
PLEKHS1	-4.60	1.1E-163
ALDH1A1	-4.60	1.0E-78
HAPLN1	-4.45	2.1E-26
TENM2	-4.43	3.9E-185
POF1B	-4.41	8.3E-29
ANO3	-4.41	4.4E-40
METTL7A	-4.36	9.5E-85
SLC34A2	-4.34	2.5E-104
TF	-4.32	1.5E-28
ELSPBP1	-4.30	3.6E-22
PIP	-4.25	3.3E-24

SYT12	-4.19	0.0E+00
FAM5C	-4.18	2.3E-18
CTNNA3	-4.16	3.2E-37
C1orf168	-4.14	3.2E-20
ADH1C	-4.13	4.5E-22
SLITRK5	-4.10	3.0E-24
ACY3	-4.09	3.6E-31
BPIFB1	-4.08	1.2E-56
NXF3	-4.06	3.7E-25
LRP2	-4.05	3.0E-22
PALM3	-4.02	3.7E-59
C11orf92	-4.01	8.3E-134
DEFB1	-4.00	5.4E-57
GABRP	-3.98	7.9E-24
CD34	-3.94	8.4E-53
AKR1C2	-3.94	0.0E+00
ALDH3B2	-3.93	0.0E+00
CLCA2	-3.93	0.0E+00
TACR1	-3.92	1.8E-31
LMO3	-3.91	1.7E-18
COL14A1	-3.91	1.5E-21
SCIN	-3.87	1.5E-64
RNF128	-3.86	7.6E-69
ABCC6P1	-3.86	4.2E-17
RERG	-3.85	0.0E+00
SPINK8	-3.84	1.4E-19
C8orf4	-3.84	5.0E-16
IL22RA2	-3.83	2.1E-264
TRIL	-3.81	2.6E-223
UGT1A6	-3.80	6.7E-33
MOGAT2	-3.77	6.9E-18
CXCL17	-3.72	2.1E-16
SPTLC3	-3.71	1.8E-171
CCL22	-3.69	0.0E+00
NKAIN2	-3.69	8.0E-19
SLC15A2	-3.66	6.1E-215
TXLNB	-3.65	1.5E-16
CFB	-3.62	0.0E+00
PTPRZ1	-3.62	6.1E-16
FAIM2	-3.61	1.3E-51
CXXC4	-3.60	2.3E-14
ACE2	-3.60	1.7E-125
SOSTDC1	-3.60	2.6E-26

MYL9	-3.59	3.6E-64
PLA2G4A	-3.55	1.5E-15
CLU	-3.54	0.0E+00
ZG16B	-3.52	2.0E-20
FOS	-3.51	1.5E-21
VCAM1	-3.50	2.2E-22
EDNRB	-3.50	6.7E-22
ALX1	-3.50	2.9E-12
BDNF	-3.50	1.4E-39
FAM198B	-3.50	3.3E-55
STK31	-3.49	4.4E-35
MSX2	-3.49	3.9E-12
MAGEA4	-3.48	8.8E-15
SLC51B	-3.47	5.4E-12
THSD7A	-3.46	7.4E-110
MAGED1	-3.45	1.5E-30
LGR6	-3.44	1.1E-31
COLEC12	-3.42	1.2E-11
ALDH3A1	-3.41	4.8E-132
LINC00478	-3.39	8.6E-20
LOC100128420	-3.39	2.3E-29
TBATA	-3.37	1.0E-13
CIB1	-3.36	0.0E+00
GPRC5B	-3.34	5.2E-95
SHROOM4	-3.31	2.8E-55
POU2AF1	-3.30	6.8E-28
TIMP3	-3.30	0.0E+00
MSMB	-3.29	4.0E-24
SPTSSB	-3.29	1.7E-99
EBF1	-3.27	1.7E-10
LINC00284	-3.24	4.8E-27
GRID2	-3.24	2.9E-11
LRRC31	-3.24	2.9E-13
LOC285629	-3.22	5.7E-51
BTN3A3	-3.22	1.8E-88
MUM1L1	-3.22	6.8E-24
KRT4	-3.21	0.0E+00
ALPP	-3.20	0.0E+00
HPGD	-3.19	5.4E-21
RASL11A	-3.18	2.0E-78
PDE11A	-3.18	5.7E-106
KRT38	-3.18	1.1E-14
TFAP2B	-3.17	6.5E-10

CAPN9	-3.17	1.3E-13
PGLYRP4	-3.17	9.7E-20
SYN3	-3.15	8.0E-10
MRAS	-3.15	0.0E+00
IGFL1	-3.14	2.9E-164
RXFP1	-3.14	8.8E-29
FATE1	-3.13	1.6E-10
GGT1	-3.12	2.9E-49
FSTL5	-3.11	3.3E-16
CPXM1	-3.10	1.1E-11
AKAP6	-3.09	0.0E+00
KXD1	-3.08	0.0E+00
CCDC83	-3.07	2.3E-18
MMP7	-3.07	7.4E-50
STMN2	-3.06	3.2E-09
MEGF10	-3.05	4.0E-136
PCDH18	-3.04	2.0E-18
CFTR	-3.04	2.0E-09
C11orf93	-3.04	1.1E-89
ALPPL2	-3.04	2.0E-32
IGFBP5	-3.03	0.0E+00
RASL10B	-3.02	6.8E-40
CYP4X1	-3.02	0.0E+00
PCDHA1	-3.00	7.0E-09
KLHDC3	-3.00	0.0E+00
ARHGAP42	-3.00	1.7E-27
GPD1	-2.99	6.1E-19
MUC15	-2.99	3.2E-302
AK7	-2.97	1.0E-12
TTC30A	-2.97	3.1E-120
SLC16A7	-2.96	1.3E-10
BBOX1	-2.95	6.3E-110
NRK	-2.94	2.5E-146
TLR3	-2.94	8.6E-88
RGL1	-2.94	9.1E-276
RUFY4	-2.93	3.9E-09
C1S	-2.92	2.5E-19
FMO3	-2.92	5.0E-09
ZNF275	-2.92	2.0E-08
CPED1	-2.91	8.1E-19
WDR52	-2.90	6.8E-91
CRISP2	-2.90	2.6E-08
SPATA17	-2.90	4.1E-14

NPY1R	-2.88	1.9E-35
ZSCAN4	-2.88	7.6E-29
ESPN	-2.86	7.6E-91
FOSB	-2.86	6.0E-173
CCDC85A	-2.86	4.5E-08
MYOT	-2.85	3.5E-27
TNNC1	-2.83	4.6E-83
LINC00277	-2.83	1.9E-08
SV2C	-2.82	7.1E-08
HTR2C	-2.82	2.1E-08
ERP27	-2.81	4.9E-229
RARRES1	-2.80	0.0E+00
ATP10B	-2.80	1.4E-46
LIPK	-2.79	2.0E-11
PTGER3	-2.79	3.3E-28
ZMAT4	-2.79	1.3E-08
CPAMD8	-2.79	7.4E-192
CD180	-2.78	4.9E-12
PIGR	-2.77	7.0E-23
LOC283335	-2.77	1.4E-42
FOXI1	-2.77	0.0E+00
ZNF385D	-2.77	8.0E-08
CATSPERB	-2.75	1.7E-16
CHST4	-2.75	3.7E-11
DNM3OS	-2.74	2.0E-10
OMA1	-2.74	1.2E-281
RIMS1	-2.73	4.4E-87
SIDT1	-2.73	1.7E-70
FGG	-2.72	1.5E-40
CPVL	-2.72	6.9E-149
MGP	-2.71	0.0E+00
PBX1	-2.71	0.0E+00
S100A7	-2.71	0.0E+00
CCL2	-2.70	4.2E-22
AKR1C1	-2.70	6.2E-56
TMCO5A	-2.68	1.2E-07
BCAT1	-2.68	1.7E-35
KCNB1	-2.67	1.3E-140
WDR64	-2.67	1.3E-73
KIF6	-2.66	7.1E-09
VWA5A	-2.66	4.0E-61
ZNF711	-2.66	1.9E-09
PCDHA11	-2.64	3.2E-14

TLR5	-2.64	1.4E-97
METAP1D	-2.64	6.9E-46
PCDH19	-2.63	1.1E-51
ZNF385B	-2.63	3.4E-08
C10orf107	-2.63	2.9E-07
TMEM150A	-2.62	6.7E-108
PLCH1	-2.62	2.6E-89
PRLR	-2.61	0.0E+00
SVOPL	-2.61	1.1E-09
CAB39L	-2.61	6.3E-82
LOC100129534	-2.60	2.7E-27
CLDN10	-2.60	1.8E-142
PPM1H	-2.60	1.7E-142
PIR	-2.60	8.5E-56
SEMA3G	-2.59	1.0E-33
ZNF804A	-2.59	3.9E-17
EPHX2	-2.58	8.0E-31
DNAJC30	-2.56	1.7E-70
ALMS1P	-2.55	1.0E-06
SBSPON	-2.54	1.7E-37
UNC5C	-2.54	1.7E-22
CNGA2	-2.54	9.7E-07
GULP1	-2.52	4.1E-16
A2M	-2.52	0.0E+00
SIAE	-2.52	2.1E-104
CCDC160	-2.51	3.7E-74
PDZK1IP1	-2.51	0.0E+00
KIT	-2.51	7.6E-11
IGF2BP1	-2.50	6.8E-10
TTC12	-2.49	6.3E-195
BST2	-2.48	8.1E-100
SLC7A2	-2.48	8.3E-09
CXCL10	-2.48	8.1E-07
PPFIBP2	-2.47	8.7E-159
CTGF	-2.46	8.8E-136
CRABP1	-2.46	6.4E-08
COL26A1	-2.46	1.3E-25
HSPB7	-2.45	6.2E-12
CRABP2	-2.44	0.0E+00
DUSP27	-2.43	1.0E-10
LOC100505695	-2.43	1.9E-07
CNTN5	-2.43	5.1E-06
DIXDC1	-2.43	6.4E-268

EDAR	-2.43	2.7E-12
AXIN2	-2.43	1.2E-177
DIRAS2	-2.43	1.4E-11
DIO2	-2.43	4.8E-91
SPG20	-2.43	3.0E-18
AKR1C3	-2.42	1.9E-12
CASP14	-2.42	0.0E+00
GSTP1	-2.42	1.6E-45
CAPN13	-2.41	0.0E+00
SERPINB4	-2.40	6.6E-46
CXorf57	-2.40	2.3E-14
DAPL1	-2.40	1.0E-37
FAM107A	-2.39	4.0E-06
ZNF648	-2.38	8.3E-06
DNAJC12	-2.38	4.0E-16
C2orf66	-2.37	4.4E-08
DZIP3	-2.36	1.4E-150
BDH2	-2.36	4.4E-109
MUCL1	-2.36	9.8E-06
TMC4	-2.36	1.4E-98
PTGIS	-2.36	5.1E-34
NRAS	-2.36	0.0E+00
SPRR2B	-2.36	5.8E-06
IFI44L	-2.35	3.4E-07
C3	-2.35	0.0E+00
C10orf71	-2.35	1.1E-05
OXGR1	-2.35	9.4E-10
LINC00158	-2.35	1.1E-05
TMEM133	-2.35	5.6E-07
PDE7B	-2.35	7.4E-13
CD14	-2.34	2.5E-11
USH2A	-2.34	9.4E-07
EGOT	-2.34	5.6E-12
VTCN1	-2.34	0.0E+00
SPA17	-2.34	2.8E-29
CDH2	-2.33	5.3E-16
C11orf65	-2.33	3.8E-10
LMO1	-2.33	3.4E-22
AADAC	-2.33	4.0E-06
RDH10	-2.32	0.0E+00
LIPA	-2.32	0.0E+00
FAM227B	-2.32	3.1E-12
MNF1	-2.31	0.0E+00

WDR78	-2.31	4.4E-45
THNSL1	-2.31	2.8E-65
MUC20	-2.30	7.0E-57
KLHL3	-2.30	2.5E-15
PLA2G16	-2.29	3.9E-185
SNAPC5	-2.29	3.8E-57
KCNK5	-2.29	0.0E+00
C14orf101	-2.28	2.2E-252
KIF26B	-2.28	3.6E-08
LOC401109	-2.27	9.2E-27
SYCE3	-2.27	6.6E-06
ERMAP	-2.27	1.9E-217
PCDH8	-2.27	5.4E-16
C20orf202	-2.27	2.3E-05
ADAMTS15	-2.27	2.2E-10
MAT1A	-2.27	2.3E-40
CDH13	-2.26	1.7E-05
EFCAB6	-2.26	3.1E-08
FAM86C2P	-2.26	8.3E-45
CASC1	-2.26	8.7E-08
LMAN2L	-2.26	1.4E-124
PI3	-2.26	2.2E-46
SELENBP1	-2.26	1.7E-114
GPR12	-2.26	1.4E-18
TP53TG1	-2.25	3.6E-20
LOC254559	-2.25	3.7E-65
STAB2	-2.25	7.7E-18
FOLR1	-2.24	4.4E-28
LDLRAD4	-2.24	3.5E-133
UPB1	-2.24	4.5E-19
ABCC11	-2.23	2.2E-08
CR2	-2.23	1.3E-18
BCMO1	-2.23	1.5E-17
REG1B	-2.23	3.3E-05
SCN2A	-2.22	7.4E-07
SEMA3E	-2.22	4.7E-239
FMO2	-2.22	8.0E-07
TMEM52B	-2.22	2.8E-43
SLC2A4	-2.22	2.9E-13
MYO16	-2.22	6.3E-11
SPEF2	-2.21	2.9E-53
LOC339874	-2.21	7.2E-06
ACN9	-2.21	1.1E-56

LOC100288842	-2.20	3.5E-10
LOC285419	-2.20	1.4E-05
COL8A1	-2.20	1.8E-06
CLCNKA	-2.20	8.8E-11
ARSD	-2.20	2.0E-304
XCR1	-2.20	3.8E-05
LDHD	-2.19	2.2E-09
FMO5	-2.19	1.7E-24
ST6GALNAC4	-2.19	1.6E-15
FSIP2	-2.19	5.4E-11
FMO9P	-2.19	1.7E-05
SAMD15	-2.18	2.4E-13
CCDC113	-2.18	6.5E-136
SOX5	-2.18	4.9E-05
TNS1	-2.18	0.0E+00
DENND2D	-2.18	9.2E-270
LOC643733	-2.18	1.1E-13
IFIT1	-2.18	2.5E-16
ID1	-2.18	9.4E-205
UMODL1	-2.17	8.3E-06
NPR1	-2.17	1.0E-07
NPY5R	-2.17	3.2E-05
RBBP8NL	-2.16	1.0E-64
ANTXR1	-2.16	0.0E+00
SAA2	-2.16	6.9E-55
GLYATL2	-2.16	0.0E+00
C6orf165	-2.16	1.0E-23
OLFM4	-2.16	0.0E+00
PNMT	-2.16	4.4E-05
LOC100506668	-2.15	5.5E-69
VGLL1	-2.15	0.0E+00
CASP1	-2.15	5.7E-45
KTN1-AS1	-2.14	6.2E-12
CTNNA2	-2.14	4.8E-05
OGDHL	-2.14	1.8E-12
SORBS2	-2.14	3.1E-15
ZBTB7C	-2.14	5.7E-152
WNT4	-2.14	3.0E-100
SDSL	-2.14	2.3E-52
GPM6A	-2.14	2.6E-05
FBXO15	-2.14	7.0E-05
TSC22D3	-2.14	6.1E-21
ZNF454	-2.13	8.7E-35

HS6ST3	-2.13	1.4E-50
CCDC89	-2.13	3.1E-05
SERPINA3	-2.13	0.0E+00
S100A7L2	-2.13	1.0E-05
KIAA1324	-2.13	1.5E-08
SCPEP1	-2.13	0.0E+00
PPP1R1B	-2.13	4.9E-23
USH1G	-2.12	1.4E-06
MYO3B	-2.12	9.3E-36
CCR2	-2.12	4.0E-06
SAMD11	-2.12	2.0E-21
LOC100505776	-2.12	5.6E-11
RPP25L	-2.12	1.7E-171
CLIC3	-2.12	2.4E-07
UPK2	-2.12	2.8E-15
GRAMD1C	-2.11	2.1E-83
LOC283194	-2.11	1.3E-12
LOC153684	-2.11	1.2E-07
AQR	-2.11	0.0E+00
GSTA4	-2.11	4.9E-31
DMGDH	-2.10	3.6E-10
PRODH	-2.10	4.0E-281
ABCC6P2	-2.09	5.0E-05
ACTL8	-2.09	4.7E-05
HFE	-2.09	1.8E-73
CETP	-2.08	1.0E-04
PALMD	-2.08	1.6E-146
C7orf63	-2.08	8.5E-11
POLR3GL	-2.08	3.0E-78
CCDC11	-2.08	3.7E-07
PKI55	-2.08	3.5E-40
CHRDL1	-2.07	7.6E-17
C9orf116	-2.06	1.3E-25
SNHG4	-2.06	5.5E-37
GUCY1A3	-2.06	0.0E+00
CCDC25	-2.06	0.0E+00
GSTA1	-2.06	9.0E-13
C12orf66	-2.06	3.8E-36
HCG26	-2.06	6.7E-10
C1orf192	-2.05	9.4E-33
LOC284344	-2.05	3.5E-13
CALCRL	-2.05	3.5E-05
C17orf97	-2.05	8.7E-62

TMPRSS12	-2.05	1.3E-04
RBM20	-2.04	3.3E-05
LOC100132078	-2.04	1.5E-04
BSND	-2.04	2.2E-08
RIC3	-2.04	1.8E-05
NCAM2	-2.03	1.4E-04
MTHFR	-2.03	4.1E-106
TMED6	-2.02	8.6E-08
UCP2	-2.02	0.0E+00
HIST1H2BD	-2.02	3.0E-70
DUSP19	-2.02	1.4E-30
HSD17B8	-2.02	7.0E-31
CAPN3	-2.02	7.9E-07
RCOR2	-2.01	5.5E-35
C11orf71	-2.01	2.3E-44
DOC2A	-2.01	2.9E-11
SEC16B	-2.01	3.3E-17
GJC3	-2.01	1.7E-10
PDGFD	-2.00	3.8E-16

APPENDIX C

Top 100 gene signatures based on Pearson Correlation with CIB1 KD gene signature.

Signature	Pearson Correlation
GSEA.NABA_MATRISOME_ASSOCIATED	0.838
GSEA.EXTRACELLULAR_SPACE	0.789
GSEA.KRAS.LUNG.BREAST_UP.V1_UP	0.780
GSEA.NABA_ECM_REGULATORS	0.778
GSEA.BMI1_DN_MEL18_DN.V1_UP	0.776
GSEA.EXTRACELLULAR_REGION_PART	0.774
GSEA.EXTRACELLULAR_REGION	0.769
GSEA.VART_KSHV_INFECTION_ANGIOGENIC_MARKERS_UP	0.765
GSEA.ZHOU_INFLAMMATORY_RESPONSE_FIMA_UP	0.751
GSEA.BMI1_DN.V1_UP	0.748
GSEA.MODULE_220	0.741
Luminobasal.IncreasedGenes.Haughian	0.738
GSEA.MEL18_DN.V1_UP	0.738
GSEA.ORGAN_DEVELOPMENT	0.735
GSEA.NABA_SECRETED_FACTORS	0.735
GSEA.MODULE_433	0.727
GSEA.TGANTCA_V$AP1_C	0.726
GSEA.LEF1_UP.V1_UP	0.726
GSEA.MULTICELLULAR_ORGANISMAL_DEVELOPMENT	0.725
GSEA.SYSTEM_DEVELOPMENT	0.724
GSEA.MODULE_324	0.723
GSEA.PLASARI_TGFB1_TARGETS_10HR_UP	0.721
GSEA.KRAS.600.LUNG.BREAST_UP.V1_UP	0.721
GSEA.HELLEBREKERS_SILENCED_DURING_TUMOR_ANGIOGENESIS	0.720
GSEA.ZHOU_INFLAMMATORY_RESPONSE_LIVE_UP	0.718
GSEA.PTEN_DN.V2_UP	0.716
GSEA.PRC2_EZH2_UP.V1_DN	0.712
GSEA.HALLMARK_KRAS_SIGNALING_UP	0.711
GSEA.MODULE_122	0.709
GSEA.ANATOMICAL_STRUCTURE_DEVELOPMENT	0.708
GSEA.KRAS.600_UP.V1_UP	0.706
GSEA.TGFB_UP.V1_UP	0.703
GSEA.WIEDERSCHAIN_TARGETS_OF_BMI1_AND_PCGF2	0.702
GSEA.MEISSNER_BRAIN_HCP_WITH_H3K4ME3_AND_H3K27ME3	0.701
GSEA.GSE17721_PAM3CSK4_VS_GADIQUIMOD_1H_BMDM_UP	0.699
GSEA.VART_KSHV_INFECTION_ANGIOGENIC_MARKERS_DN	0.698
GSEA.CELL_MIGRATION	0.698
GSEA.PETROVA_ENDOTHELIUM_LYMPHATIC_VS_BLOOD_DN	0.698
GSEA.MODULE_248	0.696
GSEA.LIM_MAMMARY_STEM_CELL_UP	0.691
GSEA.WANG_MLL_TARGETS	0.691
GSEA.HALLMARK_COAGULATION	0.690
GSEA.SERVITJA_ISLET_HNF1A_TARGETS_UP	0.689

GSEA.MODULE_33	0.689
GSEA.MODULE_444	0.688
GSEA.ISSAEVA_MLL2_TARGETS	0.687
GSEA.CORRE_MULTIPLE_MYELOMA_UP	0.685
GSEA.CHARAFE_BREAST_CANCER_LUMINAL_VS_MESENCHYMAL_DN	0.684
GSEA.KRAS.BREAST_UP.V1_UP	0.683
GSEA.MODULE_112	0.680
GSEA.GSE360_CTRL_VS_L_DONOVANI_DC_DN	0.680
GSEA.SATO_SILENCED_BY_METHYLATION_IN_PANCREATIC_CANCER_1	0.680
GSEA.GSE360_L_MAJOR_VS_T_GONDII_MAC_UP	0.679
GSEA.LINDVALL_IMMORTALIZED_BY_TERT_DN	0.679
GSEA.P53_DN.V2_UP	0.679
GSEA.DELYS_THYROID_CANCER_UP	0.677
GSEA.CROMER_TUMORIGENESIS_UP	0.675
GSEA.PID_FRA_PATHWAY	0.675
GSEA.ESC_V6.5_UP_EARLY.V1_DN	0.674
GSEA.HUANG_DASATINIB_RESISTANCE_UP	0.674
GSEA.LABBE_TARGETS_OF_TGFB1_AND_WNT3A_UP	0.673
GSEA.GSE360_L_MAJOR_VS_B_MALAYI_HIGH_DOSE_MAC_UP	0.672
GSEA.KRAS.LUNG_UP.V1_UP	0.672
GSEA.YAMASHITA_METHYLATED_IN_PROSTATE_CANCER	0.671
GSEA.PID_UPA_UPAR_PATHWAY	0.671
GSEA.MODULE_362	0.670
GSEA.MIYAGAWA_TARGETS_OF_EWSR1_ETS_FUSIONS_DN	0.670
GSEA.ORGAN_MORPHOGENESIS	0.670
GSEA.WANG_METHYLATED_IN_BREAST_CANCER	0.669
GSEA.JECHLINGER_EPITHELIAL_TO_MESENCHYMAL_TRANSITION_UP	0.669
GSEA.NIELSEN_MALIGNAT_FIBROUS_HISTIOCYTOMA_UP	0.668
GSEA.MODULE_64	0.667
GSEA.PTEN_DN.V1_DN	0.667
Troester.Wound.Signature	0.664
GSEA.PEDERSEN_TARGETS_OF_611CTF_ISOFORM_OF_ERBB2	0.663
GSEA.VALK_AML_CLUSTER_9	0.663
GSEA.PETROVA_PROX1_TARGETS_DN	0.660
GSEA.GNF2_MMP1	0.660
GSEA.GSE36392_TYPE_2_MYELOID_VS_MAC_IL25_TREATED_LUNG_UP	0.660
GSEA.MODULE_289	0.659
GSEA.MODULE_488	0.659
GSEA.CRX_DN.V1_DN	0.659
GSEA.MODULE_164	0.659
GSEA.RECEPTOR_BINDING	0.658
GSEA.WOO_LIVER_CANCER_RECURRENCE_UP	0.658
GSEA.RESPONSE_TO_EXTERNAL_STIMULUS	0.658
GSEA.MODULE_178	0.657
GSEA.LABBE_TGFB1_TARGETS_UP	0.656
GSEA.BILD_HRAS_ONCOGENIC_SIGNATURE	0.655
GSEA.PHONG_TNF_RESPONSE_VIA_P38_PARTIAL	0.654
GSEA.GSE17974_IL4_AND_ANTI_IL12_VS_UNTREATED_12H_ACT_CD4_T CELL_DN	0.654
GSEA.GSE22886_NAIVE_CD8_TCELL_VS_NEUTROPHIL_DN	0.654
GSEA.V$AP1_Q2	0.653

GSEA.CHIANG_LIVER_CANCER_SUBCLASS_CTNNB1_DN	0.653
METAPLASTIC.Up	0.652
GSEA.MODULE_12	0.652
GSEA.NAKAMURA_ADIPOGENESIS_EARLY_DN	0.652
GSEA.GSE6269_HEALTHY_VS_E_COLI_INF_PBMC_DN	0.652
GSEA.HUANG_FOXA2_TARGETS_DN	0.652
GSEA.LINDGREN_BLADDER_CANCER_CLUSTER_2B	0.651

REFERENCES

1. Society AC. Global Cancer Facts & Figures 2nd Edition. American Cancery Society. Atlanta2011.

2. Alberts B. Molecular biology of the cell. New York: Garland Science; 2002. xxxiv, 1548 p. p.

3. Prahallad A, Bernards R. Opportunities and challenges provided by crosstalk between signalling pathways in cancer. Oncogene 2015.

4. Pagliarini R, Shao W, Sellers WR. Oncogene addiction: pathways of therapeutic response, resistance, and road maps toward a cure. EMBO reports 2015;16(3):280-96.

5. Soussi T, Wiman KG. TP53: an oncogene in disguise. Cell death and differentiation 2015.

6. Workman P, Al-Lazikani B. Drugging cancer genomes. Nature reviews Drug discovery 2013;12(12):889-90.

7. Haber D, Harlow E. Tumour-suppressor genes: evolving definitions in the genomic age. Nature genetics 1997;16(4):320-2.

8. Weigelt B, Peterse JL, van 't Veer LJ. Breast cancer metastasis: markers and models. Nature reviews Cancer 2005;5(8):591-602.

9. Solomayer EF, Diel IJ, Meyberg GC, Gollan C, Bastert G. Metastatic breast cancer: clinical course, prognosis and therapy related to the first site of metastasis. Breast cancer research and treatment 2000;59(3):271-8.

10. Siegel R, Ma J, Zou Z, Jemal A. Cancer statistics, 2014. CA: a cancer journal for clinicians 2014;64(1):9-29.

11. Blows FM, Driver KE, Schmidt MK, Broeks A, van Leeuwen FE, Wesseling J, et al. Subtyping of breast cancer by immunohistochemistry to investigate a relationship between subtype and short and long term survival: a collaborative analysis of data for 10,159 cases from 12 studies. PLoS medicine 2010;7(5):e1000279.

12. Tryfonidis K, Senkus E, Cardoso MJ, Cardoso F. Management of locally advanced breast cancer-perspectives and future directions. Nature reviews Clinical oncology 2015;12(3):147-62.

13. Hirshfield KM, Ganesan S. Triple-negative breast cancer: molecular subtypes and targeted therapy. Current opinion in obstetrics & gynecology 2014;26(1):34-40.

14. Crown J, O'Shaughnessy J, Gullo G. Emerging targeted therapies in triple-negative breast cancer. Annals of oncology : official journal of the European Society for Medical Oncology / ESMO 2012;23 Suppl 6:vi56-65.

15. Hanahan D, Weinberg RA. Hallmarks of cancer: the next generation. Cell 2011;144(5):646-74.

16. Lawrence MS, Stojanov P, Mermel CH, Robinson JT, Garraway LA, Golub TR, et al. Discovery and saturation analysis of cancer genes across 21 tumour types. Nature 2014;505(7484):495-501.

17. De Luca A, Maiello MR, D'Alessio A, Pergameno M, Normanno N. The RAS/RAF/MEK/ERK and the PI3K/AKT signalling pathways: role in cancer pathogenesis and implications for therapeutic approaches. Expert opinion on therapeutic targets 2012;16 Suppl 2:S17-27.

18. Turke AB, Song Y, Costa C, Cook R, Arteaga CL, Asara JM, et al. MEK inhibition leads to PI3K/AKT activation by relieving a negative feedback on ERBB receptors. Cancer research 2012;72(13):3228-37.

19. Downward J. Targeting RAS signalling pathways in cancer therapy. Nature reviews Cancer 2003;3(1):11-22.

20. Cox AD, Der CJ. Ras history: The saga continues. Small GTPases 2010;1(1):2-27.

21. Takashima A, Faller DV. Targeting the RAS oncogene. Expert opinion on therapeutic targets 2013;17(5):507-31.

22. Pecot CV, Wu SY, Bellister S, Filant J, Rupaimoole R, Hisamatsu T, et al. Therapeutic silencing of KRAS using systemically delivered siRNAs. Molecular cancer therapeutics 2014;13(12):2876-85.

23. Sanchez-Munoz A, Gallego E, de Luque V, Perez-Rivas LG, Vicioso L, Ribelles N, et al. Lack of evidence for KRAS oncogenic mutations in triple-negative breast cancer. BMC cancer 2010;10:136.

24. Cerami E, Gao J, Dogrusoz U, Gross BE, Sumer SO, Aksoy BA, et al. The cBio cancer genomics portal: an open platform for exploring multidimensional cancer genomics data. Cancer discovery 2012;2(5):401-4.

25. Comprehensive molecular portraits of human breast tumours. Nature 2012;490(7418):61-70.

26. Tilch E, Seidens T, Cocciardi S, Reid LE, Byrne D, Simpson PT, et al. Mutations in EGFR, BRAF and RAS are rare in triple-negative and basal-like breast cancers from Caucasian women. Breast cancer research and treatment 2014;143(2):385-92.

27. Roberts PJ, Der CJ. Targeting the Raf-MEK-ERK mitogen-activated protein kinase cascade for the treatment of cancer. Oncogene 2007;26(22):3291-310.

28. Engelman JA. Targeting PI3K signalling in cancer: opportunities, challenges and limitations. Nature reviews Cancer 2009;9(8):550-62.

29. Song MS, Salmena L, Pandolfi PP. The functions and regulation of the PTEN tumour suppressor. Nature reviews Molecular cell biology 2012;13(5):283-96.

30. Hopkins BD, Hodakoski C, Barrows D, Mense SM, Parsons RE. PTEN function: the long and the short of it. Trends in biochemical sciences 2014;39(4):183-90.

31. Voskas D, Ling LS, Woodgett JR. Signals controlling un-differentiated states in embryonic stem and cancer cells: role of the phosphatidylinositol 3' kinase pathway. Journal of cellular physiology 2014;229(10):1312-22.

32. Worby CA, Dixon JE. Pten. Annual review of biochemistry 2014;83:641-69.

33. Milella M, Falcone I, Conciatori F, Cesta Incani U, Del Curatolo A, Inzerilli N, et al. PTEN: Multiple Functions in Human Malignant Tumors. Frontiers in oncology 2015;5:24.

34. Zhang HY, Liang F, Jia ZL, Song ST, Jiang ZF. mutation, methylation and expression in breast cancer patients. Oncology letters 2013;6(1):161-68.

35. Saal LH, Gruvberger-Saal SK, Persson C, Lovgren K, Jumppanen M, Staaf J, et al. Recurrent gross mutations of the PTEN tumor suppressor gene in breast cancers with deficient DSB repair. Nature genetics 2008;40(1):102-7.

36. Hollander MC, Blumenthal GM, Dennis PA. PTEN loss in the continuum of common cancers, rare syndromes and mouse models. Nature reviews Cancer 2011;11(4):289-301.

37. Normanno N, De Luca A, Bianco C, Strizzi L, Mancino M, Maiello MR, et al. Epidermal growth factor receptor (EGFR) signaling in cancer. Gene 2006;366(1):2-16.

38. Holderfield M, Nagel TE, Stuart DD. Mechanism and consequences of RAF kinase activation by small-molecule inhibitors. British journal of cancer 2014;111(4):640-5.

39. Zhao Y, Adjei AA. The clinical development of MEK inhibitors. Nature reviews Clinical oncology 2014;11(7):385-400.

40. Flaherty KT, Robert C, Hersey P, Nathan P, Garbe C, Milhem M, et al. Improved survival with MEK inhibition in BRAF-mutated melanoma. The New England journal of medicine 2012;367(2):107-14.

41. Akinleye A, Furqan M, Mukhi N, Ravella P, Liu D. MEK and the inhibitors: from bench to bedside. Journal of hematology & oncology 2013;6:27.

42. Brana I, Siu LL. Clinical development of phosphatidylinositol 3-kinase inhibitors for cancer treatment. BMC medicine 2012;10:161.

43. Furman RR, Sharman JP, Coutre SE, Cheson BD, Pagel JM, Hillmen P, et al. Idelalisib and rituximab in relapsed chronic lymphocytic leukemia. The New England journal of medicine 2014;370(11):997-1007.

44. Macias-Perez IM, Flinn IW. GS-1101: a delta-specific PI3K inhibitor in chronic lymphocytic leukemia. Current hematologic malignancy reports 2013;8(1):22-7.

45. Rodon J, Dienstmann R, Serra V, Tabernero J. Development of PI3K inhibitors: lessons learned from early clinical trials. Nature reviews Clinical oncology 2013;10(3):143-53.

46. Fruman DA, Rommel C. PI3K and cancer: lessons, challenges and opportunities. Nature reviews Drug discovery 2014;13(2):140-56.

47. Rhodes N, Heerding DA, Duckett DR, Eberwein DJ, Knick VB, Lansing TJ, et al. Characterization of an Akt kinase inhibitor with potent pharmacodynamic and antitumor activity. Cancer research 2008;68(7):2366-74.

48. Yap TA, Yan L, Patnaik A, Fearen I, Olmos D, Papadopoulos K, et al. First-in-man clinical trial of the oral pan-AKT inhibitor MK-2206 in patients with advanced solid tumors. Journal of clinical oncology : official journal of the American Society of Clinical Oncology 2011;29(35):4688-95.

49. Duncan JS, Whittle MC, Nakamura K, Abell AN, Midland AA, Zawistowski JS, et al. Dynamic Reprogramming of the Kinome in Response to Targeted MEK Inhibition in Triple-Negative Breast Cancer. Cell 2012;149(2):307-21.

50. Mendoza MC, Er EE, Blenis J. The Ras-ERK and PI3K-mTOR pathways: cross-talk and compensation. Trends in biochemical sciences 2011;36(6):320-8.

51. Shimizu T, Tolcher AW, Papadopoulos KP, Beeram M, Rasco DW, Smith LS, et al. The clinical effect of the dual-targeting strategy involving PI3K/AKT/mTOR and RAS/MEK/ERK pathways in patients with advanced cancer. Clinical cancer research : an official journal of the American Association for Cancer Research 2012;18(8):2316-25.

52. Bedard PL, Tabernero J, Janku F, Wainberg ZA, Paz-Ares L, Vansteenkiste J, et al. A Phase Ib Dose-Escalation Study of the Oral Pan-PI3K Inhibitor Buparlisib (BKM120) in Combination with the Oral MEK1/2 Inhibitor Trametinib (GSK1120212) in Patients with Selected Advanced Solid Tumors. Clinical cancer research : an official journal of the American Association for Cancer Research 2015;21(4):730-8.

53. Weinstein IB. Cancer. Addiction to oncogenes--the Achilles heal of cancer. Science 2002;297(5578):63-4.

54. Cobleigh MA, Vogel CL, Tripathy D, Robert NJ, Scholl S, Fehrenbacher L, et al. Multinational study of the efficacy and safety of humanized anti-HER2 monoclonal antibody in women who have HER2-overexpressing metastatic breast cancer that has progressed after chemotherapy for metastatic disease. Journal of clinical oncology : official journal of the American Society of Clinical Oncology 1999;17(9):2639-48.

55. Vogel C, Cobleigh MA, Tripathy D, Gutheil JC, Harris LN, Fehrenbacher L, et al. First-line, single-agent Herceptin(R) (trastuzumab) in metastatic breast cancer. a preliminary report. Eur J Cancer 2001;37 Suppl 1:25-29.

56. Vogel CL, Cobleigh MA, Tripathy D, Gutheil JC, Harris LN, Fehrenbacher L, et al. Efficacy and safety of trastuzumab as a single agent in first-line treatment of HER2-overexpressing metastatic breast cancer. Journal of clinical oncology : official journal of the American Society of Clinical Oncology 2002;20(3):719-26.

57. Bild AH, Yao G, Chang JT, Wang Q, Potti A, Chasse D, et al. Oncogenic pathway signatures in human cancers as a guide to targeted therapies. Nature 2006;439(7074):353-7.

58. Solimini NL, Luo J, Elledge SJ. Non-oncogene addiction and the stress phenotype of cancer cells. Cell 2007;130(6):986-8.

59. Luo J, Solimini NL, Elledge SJ. Principles of cancer therapy: oncogene and non-oncogene addiction. Cell 2009;136(5):823-37.

60. Dann RB, DeLoia JA, Timms KM, Zorn KK, Potter J, Flake DD, 2nd, et al. BRCA1/2 mutations and expression: response to platinum chemotherapy in patients with advanced stage epithelial ovarian cancer. Gynecologic oncology 2012;125(3):677-82.

61. Carey LA. Targeted chemotherapy? Platinum in BRCA1-dysfunctional breast cancer. Journal of clinical oncology : official journal of the American Society of Clinical Oncology 2010;28(3):361-3.

62. Bryant HE, Schultz N, Thomas HD, Parker KM, Flower D, Lopez E, et al. Specific killing of BRCA2-deficient tumours with inhibitors of poly(ADP-ribose) polymerase. Nature 2005;434(7035):913-7.

63. de Murcia JM, Niedergang C, Trucco C, Ricoul M, Dutrillaux B, Mark M, et al. Requirement of poly(ADP-ribose) polymerase in recovery from DNA damage in mice and in cells. Proceedings of the National Academy of Sciences of the United States of America 1997;94(14):7303-7.

64. D'Amours D, Desnoyers S, D'Silva I, Poirier GG. Poly(ADP-ribosyl)ation reactions in the regulation of nuclear functions. The Biochemical journal 1999;342 (Pt 2):249-68.

65. Wang ZQ, Stingl L, Morrison C, Jantsch M, Los M, Schulze-Osthoff K, et al. PARP is important for genomic stability but dispensable in apoptosis. Genes & development 1997;11(18):2347-58.

66. Tangutoori S, Baldwin P, Sridhar S. PARP inhibitors: A new era of targeted therapy. Maturitas 2015.

67. Lee JM, Ledermann JA, Kohn EC. PARP Inhibitors for BRCA1/2 mutation-associated and BRCA-like malignancies. Annals of oncology : official journal of the European Society for Medical Oncology / ESMO 2014;25(1):32-40.

68. Naik UP, Patel PM, Parise LV. Identification of a novel calcium-binding protein that interacts with the integrin alphaIIb cytoplasmic domain. The Journal of biological chemistry 1997;272(8):4651-4.

69. Barry WT, Boudignon-Proudhon C, Shock DD, McFadden A, Weiss JM, Sondek J, et al. Molecular basis of CIB binding to the integrin alpha IIb cytoplasmic domain. The Journal of biological chemistry 2002;277(32):28877-83.

70. Shock DD, Naik UP, Brittain JE, Alahari SK, Sondek J, Parise LV. Calcium-dependent properties of CIB binding to the integrin alphaIIb cytoplasmic domain and translocation to the platelet cytoskeleton. The Biochemical journal 1999;342 Pt 3:729-35.

71. Huang H, Ishida H, Yamniuk AP, Vogel HJ. Solution structures of Ca2+-CIB1 and Mg2+-CIB1 and their interactions with the platelet integrin alphaIIb cytoplasmic domain. The Journal of biological chemistry 2011;286(19):17181-92.

72. Yamniuk AP, Ishida H, Vogel HJ. The interaction between calcium- and integrin-binding protein 1 and the alphaIIb integrin cytoplasmic domain involves a novel C-terminal displacement mechanism. The Journal of biological chemistry 2006;281(36):26455-64.

73. Huang H, Bogstie JN, Vogel HJ. Biophysical and structural studies of the human calcium- and integrin-binding protein family: understanding their functional similarities and differences. Biochemistry and cell biology = Biochimie et biologie cellulaire 2012;90(5):646-56.

74. Yamniuk AP, Vogel HJ. Calcium- and magnesium-dependent interactions between calcium- and integrin-binding protein and the integrin alphaIIb cytoplasmic domain. Protein science : a publication of the Protein Society 2005;14(6):1429-37.

75. Gentry HR, Singer AU, Betts L, Yang C, Ferrara JD, Sondek J, et al. Structural and biochemical characterization of CIB1 delineates a new family of EF-hand-containing proteins. The Journal of biological chemistry 2005;280(9):8407-15.

76. Blamey CJ, Ceccarelli C, Naik UP, Bahnson BJ. The crystal structure of calcium- and integrin-binding protein 1: insights into redox regulated functions. Protein science : a publication of the Protein Society 2005;14(5):1214-21.

77. Grabarek Z. Insights into modulation of calcium signaling by magnesium in calmodulin, troponin C and related EF-hand proteins. Biochimica et biophysica acta 2011;1813(5):913-21.

78. Jarman KE, Moretti PA, Zebol JR, Pitson SM. Translocation of sphingosine kinase 1 to the plasma membrane is mediated by calcium- and integrin-binding protein 1. The Journal of biological chemistry 2010;285(1):483-92.

79. Hennigs JK, Burhenne N, Stahler F, Winnig M, Walter B, Meyerhof W, et al. Sweet taste receptor interacting protein CIB1 is a general inhibitor of InsP3-dependent Ca2+ release in vivo. Journal of neurochemistry 2008;106(5):2249-62.

80. Blazejczyk M, Wojda U, Sobczak A, Spilker C, Bernstein HG, Gundelfinger ED, et al. Ca2+-independent binding and cellular expression profiles question a significant role of calmyrin in transduction of Ca2+-signals to Alzheimer's disease-related presenilin 2 in forebrain. Biochimica et biophysica acta 2006;1762(1):66-72.

81. Yuan W, Leisner TM, McFadden AW, Wang Z, Larson MK, Clark S, et al. CIB1 is an endogenous inhibitor of agonist-induced integrin alphaIIbbeta3 activation. The Journal of cell biology 2006;172(2):169-75.

82. Bandyopadhyay C, Valiya-Veettil M, Dutta D, Chakraborty S, Chandran B. CIB1 synergizes with EphrinA2 to regulate Kaposi's sarcoma-associated herpesvirus macropinocytic entry in human microvascular dermal endothelial cells. PLoS pathogens 2014;10(2):e1003941.

83. Naik UP, Naik MU. Association of CIB with GPIIb/IIIa during outside-in signaling is required for platelet spreading on fibrinogen. Blood 2003;102(4):1355-62.

84. Yoon KW, Cho JH, Lee JK, Kang YH, Chae JS, Kim YM, et al. CIB1 functions as a Ca(2+)-sensitive modulator of stress-induced signaling by targeting ASK1. Proceedings of the National Academy of Sciences of the United States of America 2009;106(41):17389-94.

85. Son SM, Byun J, Roh SE, Kim SJ, Mook-Jung I. Reduced IRE1alpha mediates apoptotic cell death by disrupting calcium homeostasis via the InsP3 receptor. Cell death & disease 2014;5:e1188.

86. Leisner TM, Liu M, Jaffer ZM, Chernoff J, Parise LV. Essential role of CIB1 in regulating PAK1 activation and cell migration. The Journal of cell biology 2005;170(3):465-76.

87. Sun H, King AJ, Diaz HB, Marshall MS. Regulation of the protein kinase Raf-1 by oncogenic Ras through phosphatidylinositol 3-kinase, Cdc42/Rac and Pak. Current biology : CB 2000;10(5):281-4.

88. Li W, Chong H, Guan KL. Function of the Rho family GTPases in Ras-stimulated Raf activation. The Journal of biological chemistry 2001;276(37):34728-37.

89. Slack-Davis JK, Eblen ST, Zecevic M, Boerner SA, Tarcsafalvi A, Diaz HB, et al. PAK1 phosphorylation of MEK1 regulates fibronectin-stimulated MAPK activation. The Journal of cell biology 2003;162(2):281-91.

90. Chaudhary A, King WG, Mattaliano MD, Frost JA, Diaz B, Morrison DK, et al. Phosphatidylinositol 3-kinase regulates Raf1 through Pak phosphorylation of serine 338. Current biology : CB 2000;10(9):551-4.

91. Dummler B, Ohshiro K, Kumar R, Field J. Pak protein kinases and their role in cancer. Cancer metastasis reviews 2009;28(1-2):51-63.

92. Wang Z, Fu M, Wang L, Liu J, Li Y, Brakebusch C, et al. p21-activated kinase 1 (PAK1) can promote ERK activation in a kinase-independent manner. The Journal of biological chemistry 2013;288(27):20093-9.

93. Higuchi M, Onishi K, Kikuchi C, Gotoh Y. Scaffolding function of PAK in the PDK1-Akt pathway. Nature cell biology 2008;10(11):1356-64.

94. Ding Z, Liang J, Li J, Lu Y, Ariyaratna V, Lu Z, et al. Physical association of PDK1 with AKT1 is sufficient for pathway activation independent of membrane localization and phosphatidylinositol 3 kinase. PloS one 2010;5(3):e9910.

95. Huynh N, Liu KH, Baldwin GS, He H. P21-activated kinase 1 stimulates colon cancer cell growth and migration/invasion via ERK- and AKT-dependent pathways. Biochimica et biophysica acta 2010;1803(9):1106-13.

96. Leisner TM, Moran C, Holly SP, Parise LV. CIB1 prevents nuclear GAPDH accumulation and non-apoptotic tumor cell death via AKT and ERK signaling. Oncogene 2013;32(34):4017-27.

97. Zhao B. Regulation of cell survival by CIB1, a new modulator of phosphoinositide-dependent protein kinase-1 (PDK1) [Abstract]: University of North Carolina at Chapel Hill; 2007. 162 p.

98. Alessi DR, James SR, Downes CP, Holmes AB, Gaffney PR, Reese CB, et al. Characterization of a 3-phosphoinositide-dependent protein kinase which phosphorylates and activates protein kinase Balpha. Current biology : CB 1997;7(4):261-9.

99. Hemmings BA, Restuccia DF. PI3K-PKB/Akt pathway. Cold Spring Harbor perspectives in biology 2012;4(9):a011189.

100. Alessi DR. Discovery of PDK1, one of the missing links in insulin signal transduction. Colworth Medal Lecture. Biochemical Society transactions 2001;29(Pt 2):1-14.

101. Demorest ZL, MacDuff DA, Brown WL, Morham SG, Parise LV, Harris RS. The interaction between AID and CIB1 is nonessential for antibody gene diversification by gene conversion or class switch recombination. PloS one 2010;5(7):e11660.

102. Wu X, Lieber MR. Interaction between DNA-dependent protein kinase and a novel protein, KIP. Mutation research 1997;385(1):13-20.

103. Khadka P, Lee JH, Baek SH, Oh SY, Chung IK. DNA-PKcs-interacting protein KIP binding to TRF2 is required for the maintenance of functional telomeres. The Biochemical journal 2014;463(1):19-30.

104. Lee GE, Yu EY, Cho CH, Lee J, Muller MT, Chung IK. DNA-protein kinase catalytic subunit-interacting protein KIP binds telomerase by interacting with human telomerase reverse transcriptase. The Journal of biological chemistry 2004;279(33):34750-5.

105. Henderson MJ, Russell AJ, Hird S, Munoz M, Clancy JL, Lehrbach GM, et al. EDD, the human hyperplastic discs protein, has a role in progesterone receptor coactivation and potential involvement in DNA damage response. The Journal of biological chemistry 2002;277(29):26468-78.

106. Hollenbach AD, McPherson CJ, Lagutina I, Grosveld G. The EF-hand calcium-binding protein calmyrin inhibits the transcriptional and DNA-binding activity of Pax3. Biochimica et biophysica acta 2002;1574(3):321-8.

107. White C, Yang J, Monteiro MJ, Foskett JK. CIB1, a ubiquitously expressed Ca2+-binding protein ligand of the InsP3 receptor Ca2+ release channel. The Journal of biological chemistry 2006;281(30):20825-33.

108. Stabler SM, Ostrowski LL, Janicki SM, Monteiro MJ. A myristoylated calcium-binding protein that preferentially interacts with the Alzheimer's disease presenilin 2 protein. The Journal of cell biology 1999;145(6):1277-92.

109. Tahara E, Jr., Tahara H, Kanno M, Naka K, Takeda Y, Matsuzaki T, et al. G1P3, an interferon inducible gene 6-16, is expressed in gastric cancers and inhibits mitochondrial-mediated apoptosis in gastric cancer cell line TMK-1 cell. Cancer immunology, immunotherapy : CII 2005;54(8):729-40.

110. Heineke J, Auger-Messier M, Correll RN, Xu J, Benard MJ, Yuan W, et al. CIB1 is a regulator of pathological cardiac hypertrophy. Nat Med 2010;16(8):872-9.

111. Ito A, Uehara T, Nomura Y. Isolation of Ich-1S (caspase-2S)-binding protein that partially inhibits caspase activity. FEBS letters 2000;470(3):360-4.

112. Naik MU, Naik UP. Calcium-and integrin-binding protein regulates focal adhesion kinase activity during platelet spreading on immobilized fibrinogen. Blood 2003;102(10):3629-36.

113. Kauselmann G, Weiler M, Wulff P, Jessberger S, Konietzko U, Scafidi J, et al. The polo-like protein kinases Fnk and Snk associate with a Ca(2+)- and integrin-binding protein and are regulated dynamically with synaptic plasticity. The EMBO journal 1999;18(20):5528-39.

114. Naik MU, Pham NT, Beebe K, Dai W, Naik UP. Calcium-dependent inhibition of polo-like kinase 3 activity by CIB1 in breast cancer cells. International journal of cancer Journal international du cancer 2011;128(3):587-96.

115. Holtrich U, Wolf G, Yuan J, Bereiter-Hahn J, Karn T, Weiler M, et al. Adhesion induced expression of the serine/threonine kinase Fnk in human macrophages. Oncogene 2000;19(42):4832-9.

116. Hui L, Ji C, Hui B, Lv T, Ha X, Yang J, et al. The oncoprotein LMO3 interacts with calcium- and integrin-binding protein CIB. Brain research 2009;1265:24-9.

117. Tang N, Lin T, Yang J, Foskett JK, Ostap EM. CIB1 and CaBP1 bind to the myo1c regulatory domain. Journal of muscle research and cell motility 2007;28(6):285-91.

118. Whitehouse C, Chambers J, Howe K, Cobourne M, Sharpe P, Solomon E. NBR1 interacts with fasciculation and elongation protein zeta-1 (FEZ1) and calcium and integrin binding protein (CIB) and shows developmentally restricted expression in the neural tube. European journal of biochemistry / FEBS 2002;269(2):538-45.

119. Haataja L, Kaartinen V, Groffen J, Heisterkamp N. The small GTPase Rac3 interacts with the integrin-binding protein CIB and promotes integrin alpha(IIb)beta(3)-mediated adhesion and spreading. The Journal of biological chemistry 2002;277(10):8321-8.

120. Sobczak A, Debowska K, Blazejczyk M, Kreutz MR, Kuznicki J, Wojda U. Calmyrin1 binds to SCG10 protein (stathmin2) to modulate neurite outgrowth. Biochimica et biophysica acta 2011;1813(5):1025-37.

121. Ma S, Liu MA, Yuan YL, Erikson RL. The serum-inducible protein kinase Snk is a G1 phase polo-like kinase that is inhibited by the calcium- and integrin-binding protein CIB. Molecular cancer research : MCR 2003;1(5):376-84.

122. Naik MU, Naik UP. Contra-regulation of calcium- and integrin-binding protein 1-induced cell migration on fibronectin by PAK1 and MAP kinase signaling. Journal of cellular biochemistry 2011;112(11):3289-99.

123. Tsuboi S, Nonoyama S, Ochs HD. Wiskott-Aldrich syndrome protein is involved in alphaIIb beta3-mediated cell adhesion. EMBO reports 2006;7(5):506-11.

124. Freeman TC, Jr., Black JL, Bray HG, Dagliyan O, Wu YI, Tripathy A, et al. Identification of novel integrin binding partners for calcium and integrin binding protein 1 (CIB1): structural and thermodynamic basis of CIB1 promiscuity. Biochemistry 2013;52(40):7082-90.

125. Yoshida K, Park, A., Ozaki, S., Munakata, H. Interaction of calcium- and integrin-binding protein 1 with integrin alpha11 and its possible invovlement in pulmonary fibrosis. Advances in Biological Chemistry 2014;4:59-66.

126. Zhao F, Zhang S, Chen L, Wu Y, Qin J, Shao Y, et al. Calcium- and integrin-binding protein-1 and calcineurin are upregulated in the right atrial myocardium of patients with atrial fibrillation. Europace : European pacing, arrhythmias, and cardiac electrophysiology : journal of the working groups on cardiac pacing, arrhythmias, and cardiac cellular electrophysiology of the European Society of Cardiology 2012;14(12):1726-33.

127. Fang X, Chen C, Wang Q, Gu J, Chi C. The interaction of the calcium- and integrin-binding protein (CIBP) with the coagulation factor VIII. Thrombosis research 2001;102(2):177-85.

128. Naik MU, Naik UP. Calcium-and integrin-binding protein regulates focal adhesion kinase activity during platelet spreading on immobilized fibrinogen. Blood 2003;102(10):3629-36.

129. Vallar L, Melchior C, Plancon S, Drobecq H, Lippens G, Regnault V, et al. Divalent cations differentially regulate integrin alphaIIb cytoplasmic tail binding to beta3 and to calcium- and integrin-binding protein. The Journal of biological chemistry 1999;274(24):17257-66.

130. Naik MU, Nigam A, Manrai P, Millili P, Czymmek K, Sullivan M, et al. CIB1 deficiency results in impaired thrombosis: the potential role of CIB1 in outside-in signaling through integrin alpha IIb beta 3. Journal of thrombosis and haemostasis : JTH 2009;7(11):1906-14.

131. Denofrio JC, Yuan W, Temple BR, Gentry HR, Parise LV. Characterization of calcium- and integrin-binding protein 1 (CIB1) knockout platelets: potential compensation by CIB family members. Thrombosis and haemostasis 2008;100(5):847-56.

132. Shock DD, Naik UP, Brittain JE, Alahari SK, Sondek J, Parise LV. Calcium-dependent properties of CIB binding to the integrin alphaIIb cytoplasmic domain and translocation to the platelet cytoskeleton. BiochemJ 1999;342 Pt 3:729-35.

133. Zayed MA, Yuan W, Leisner TM, Chalothorn D, McFadden AW, Schaller MD, et al. CIB1 regulates endothelial cells and ischemia-induced pathological and adaptive angiogenesis. Circulation research 2007;101(11):1185-93.

134. Kostyak JC, Naik MU, Naik UP. Calcium- and integrin-binding protein 1 regulates megakaryocyte ploidy, adhesion, and migration. Blood 2012;119(3):838-46.

135. Leisner TM, Liu M, Jaffer ZM, Chernoff J, Parise LV. Essential role of CIB1 in regulating PAK1 activation and cell migration. JCell Biol 2005;170(3):465-76.

136. Yamniuk AP, Nguyen LT, Hoang TT, Vogel HJ. Metal ion binding properties and conformational states of calcium- and integrin-binding protein. Biochemistry 2004;43(9):2558-68.

137. Wright MH, Heal WP, Mann DJ, Tate EW. Protein myristoylation in health and disease. Journal of chemical biology 2010;3(1):19-35.

138. Ames JB, Ishima R, Tanaka T, Gordon JI, Stryer L, Ikura M. Molecular mechanics of calcium-myristoyl switches. Nature 1997;389(6647):198-202.

139. Li C, Pan W, Braunewell KH, Ames JB. Structural analysis of Mg2+ and Ca2+ binding, myristoylation, and dimerization of the neuronal calcium sensor and visinin-like protein 1 (VILIP-1). The Journal of biological chemistry 2011;286(8):6354-66.

140. Yuan W, Leisner TM, McFadden AW, Clark S, Hiller S, Maeda N, et al. CIB1 is essential for mouse spermatogenesis. MolCell Biol 2006;26(22):8507-14.

141. Junrong T, Huancheng Z, Feng H, Yi G, Xiaoqin Y, Zhengmao L, et al. Proteomic identification of CIB1 as a potential diagnostic factor in hepatocellular carcinoma. Journal of biosciences 2011;36(4):659-68.

142. Naik MU, Naik UP. Calcium- and integrin-binding protein 1 regulates microtubule organization and centrosome segregation through polo like kinase 3 during cell cycle progression. The international journal of biochemistry & cell biology 2011;43(1):120-9.

143. Worster DT, Schmelzle T, Solimini NL, Lightcap ES, Millard B, Mills GB, et al. Akt and ERK control the proliferative response of mammary epithelial cells to the growth factors IGF-1 and EGF through the cell cycle inhibitor p57Kip2. Science signaling 2012;5(214):ra19.

144. McCubrey JA, Steelman LS, Abrams SL, Lee JT, Chang F, Bertrand FE, et al. Roles of the RAF/MEK/ERK and PI3K/PTEN/AKT pathways in malignant transformation and drug resistance. Advances in enzyme regulation 2006;46:249-79.

145. Giltnane JM, Balko JM. Rationale for targeting the Ras/MAPK pathway in triple-negative breast cancer. Discovery medicine 2014;17(95):275-83.

146. Courtney KD, Corcoran RB, Engelman JA. The PI3K pathway as drug target in human cancer. Journal of clinical oncology : official journal of the American Society of Clinical Oncology 2010;28(6):1075-83.

147. Folkman J. Tumor angiogenesis: therapeutic implications. The New England journal of medicine 1971;285(21):1182-6.

148. Fornaro L, Caparello C, Vivaldi C, Rotella V, Musettini G, Falcone A, et al. Bevacizumab in the pre-operative treatment of locally advanced rectal cancer: a systematic review. World journal of gastroenterology : WJG 2014;20(20):6081-91.

149. Kumler I, Christiansen OG, Nielsen DL. A systematic review of bevacizumab efficacy in breast cancer. Cancer treatment reviews 2014;40(8):960-73.

150. Zayed MA, Yuan W, Chalothorn D, Faber JE, Parise LV. Tumor growth and angiogenesis is impaired in CIB1 knockout mice. Journal of angiogenesis research 2010;2:17.

151. Mirzoeva OK, Das D, Heiser LM, Bhattacharya S, Siwak D, Gendelman R, et al. Basal subtype and MAPK/ERK kinase (MEK)-phosphoinositide 3-kinase feedback signaling determine susceptibility of breast cancer cells to MEK inhibition. Cancer research 2009;69(2):565-72.

152. Hoeflich KP, O'Brien C, Boyd Z, Cavet G, Guerrero S, Jung K, et al. In vivo antitumor activity of MEK and phosphatidylinositol 3-kinase inhibitors in basal-like breast cancer models. Clinical cancer research : an official journal of the American Association for Cancer Research 2009;15(14):4649-64.

153. Britten CD. PI3K and MEK inhibitor combinations: examining the evidence in selected tumor types. Cancer chemotherapy and pharmacology 2013;71(6):1395-409.

154. Gordon V, Banerji S. Molecular pathways: PI3K pathway targets in triple-negative breast cancers. Clinical cancer research : an official journal of the American Association for Cancer Research 2013;19(14):3738-44.

155. Black JL, Harrell JC, Leisner TM, Fellmeth MJ, George SD, Reinhold D, et al. CIB1 depletion impairs cell survival and tumor growth in triple-negative breast cancer. Breast cancer research and treatment 2015;152(2):337-46.

156. Prat A, Karginova O, Parker JS, Fan C, He X, Bixby L, et al. Characterization of cell lines derived from breast cancers and normal mammary tissues for the study of the intrinsic molecular subtypes. Breast cancer research and treatment 2013;142(2):237-55.

157. Prat A, Parker JS, Karginova O, Fan C, Livasy C, Herschkowitz JI, et al. Phenotypic and molecular characterization of the claudin-low intrinsic subtype of breast cancer. Breast cancer research : BCR 2010;12(5):R68.

158. Barnabas N, Cohen D. Phenotypic and Molecular Characterization of MCF10DCIS and SUM Breast Cancer Cell Lines. International journal of breast cancer 2013;2013:872743.

159. Weigelt B, Warne PH, Downward J. PIK3CA mutation, but not PTEN loss of function, determines the sensitivity of breast cancer cells to mTOR inhibitory drugs. Oncogene 2011;30(29):3222-33.

160. Chao HH, He X, Parker JS, Zhao W, Perou CM. Micro-scale genomic DNA copy number aberrations as another means of mutagenesis in breast cancer. PloS one 2012;7(12):e51719.

161. Szabolcs M, Keniry M, Simpson L, Reid LJ, Koujak S, Schiff SC, et al. Irs2 inactivation suppresses tumor progression in Pten+/- mice. The American journal of pathology 2009;174(1):276-86.

162. Barretina J, Caponigro G, Stransky N, Venkatesan K, Margolin AA, Kim S, et al. The Cancer Cell Line Encyclopedia enables predictive modelling of anticancer drug sensitivity. Nature 2012;483(7391):603-7.

163. Yuan W, Leisner TM, McFadden AW, Clark S, Hiller S, Maeda N, et al. CIB1 is essential for mouse spermatogenesis. Molecular and cellular biology 2006;26(22):8507-14.

164. Brown JM, Attardi LD. The role of apoptosis in cancer development and treatment response. Nature reviews Cancer 2005;5(3):231-7.

165. Pfefferle AD, Spike BT, Wahl GM, Perou CM. Luminal progenitor and fetal mammary stem cell expression features predict breast tumor response to neoadjuvant chemotherapy. Breast cancer research and treatment 2015.

166. Taube JH, Herschkowitz JI, Komurov K, Zhou AY, Gupta S, Yang J, et al. Core epithelial-to-mesenchymal transition interactome gene-expression signature is associated with claudin-low and metaplastic breast cancer subtypes. Proceedings of the National Academy of Sciences of the United States of America 2010;107(35):15449-54.

167. Wirapati P, Sotiriou C, Kunkel S, Farmer P, Pradervand S, Haibe-Kains B, et al. Meta-analysis of gene expression profiles in breast cancer: toward a unified understanding of breast cancer subtyping and prognosis signatures. Breast cancer research : BCR 2008;10(4):R65.

168. Veeck J, Dahl E. Targeting the Wnt pathway in cancer: the emerging role of Dickkopf-3. Biochimica et biophysica acta 2012;1825(1):18-28.

169. Veeck J, Bektas N, Hartmann A, Kristiansen G, Heindrichs U, Knuchel R, et al. Wnt signalling in human breast cancer: expression of the putative Wnt inhibitor Dickkopf-3 (DKK3) is frequently suppressed by promoter hypermethylation in mammary tumours. Breast cancer research : BCR 2008;10(5):R82.

170. Edamura K, Nasu Y, Takaishi M, Kobayashi T, Abarzua F, Sakaguchi M, et al. Adenovirus-mediated REIC/Dkk-3 gene transfer inhibits tumor growth and metastasis in an orthotopic prostate cancer model. Cancer gene therapy 2007;14(9):765-72.

171. Tanimoto R, Abarzua F, Sakaguchi M, Takaishi M, Nasu Y, Kumon H, et al. REIC/Dkk-3 as a potential gene therapeutic agent against human testicular cancer. International journal of molecular medicine 2007;19(3):363-8.

172. Kawasaki K, Watanabe M, Sakaguchi M, Ogasawara Y, Ochiai K, Nasu Y, et al. REIC/Dkk-3 overexpression downregulates P-glycoprotein in multidrug-resistant MCF7/ADR cells and induces apoptosis in breast cancer. Cancer gene therapy 2009;16(1):65-72.

173. McIlwain CC, Townsend DM, Tew KD. Glutathione S-transferase polymorphisms: cancer incidence and therapy. Oncogene 2006;25(11):1639-48.

174. Chen C, Wu C, Lu X, Yan Z, Gao J, Zhao H, et al. Coniferyl Ferulate, a Strong Inhibitor of Glutathione S-Transferase Isolated from Radix Angelicae sinensis, Reverses

Multidrug Resistance and Downregulates P-Glycoprotein. Evidence-based complementary and alternative medicine : eCAM 2013;2013:639083.

175. Sharmila G, Bhat FA, Arunkumar R, Elumalai P, Raja Singh P, Senthilkumar K, et al. Chemopreventive effect of quercetin, a natural dietary flavonoid on prostate cancer in in vivo model. Clin Nutr 2014;33(4):718-26.

176. Sharmila G, Athirai T, Kiruthiga B, Senthilkumar K, Elumalai P, Arunkumar R, et al. Chemopreventive effect of quercetin in MNU and testosterone induced prostate cancer of Sprague-Dawley rats. Nutrition and cancer 2014;66(1):38-46.

177. van Zanden JJ, Ben Hamman O, van Iersel ML, Boeren S, Cnubben NH, Lo Bello M, et al. Inhibition of human glutathione S-transferase P1-1 by the flavonoid quercetin. Chemico-biological interactions 2003;145(2):139-48.

178. Koizume S, Miyagi Y. Breast cancer phenotypes regulated by tissue factor-factor VII pathway: Possible therapeutic targets. World journal of clinical oncology 2014;5(5):908-20.

179. Unlu B, Versteeg HH. Effects of tumor-expressed coagulation factors on cancer progression and venous thrombosis: is there a key factor? Thrombosis research 2014;133 Suppl 2:S76-84.

180. Carneiro-Lobo TC, Konig S, Machado DE, Nasciutti LE, Forni MF, Francischetti IM, et al. Ixolaris, a tissue factor inhibitor, blocks primary tumor growth and angiogenesis in a glioblastoma model. Journal of thrombosis and haemostasis : JTH 2009;7(11):1855-64.

181. de Oliveira Ada S, Lima LG, Mariano-Oliveira A, Machado DE, Nasciutti LE, Andersen JF, et al. Inhibition of tissue factor by ixolaris reduces primary tumor growth and experimental metastasis in a murine model of melanoma. Thrombosis research 2012;130(3):e163-70.

182. Harrell JC, Prat A, Parker JS, Fan C, He X, Carey L, et al. Genomic analysis identifies unique signatures predictive of brain, lung, and liver relapse. Breast cancer research and treatment 2012;132(2):523-35.

183. Curtis C, Shah SP, Chin SF, Turashvili G, Rueda OM, Dunning MJ, et al. The genomic and transcriptomic architecture of 2,000 breast tumours reveals novel subgroups. Nature 2012;486(7403):346-52.

184. Hatzis C, Pusztai L, Valero V, Booser DJ, Esserman L, Lluch A, et al. A genomic predictor of response and survival following taxane-anthracycline chemotherapy for invasive breast cancer. Jama 2011;305(18):1873-81.

185. Podsypanina K, Ellenson LH, Nemes A, Gu J, Tamura M, Yamada KM, et al. Mutation of Pten/Mmac1 in mice causes neoplasia in multiple organ systems. Proceedings of the National Academy of Sciences of the United States of America 1999;96(4):1563-8.

186. Melendez AJ, Carlos-Dias E, Gosink M, Allen JM, Takacs L. Human sphingosine kinase: molecular cloning, functional characterization and tissue distribution. Gene 2000;251(1):19-26.

187. Zhang Y, Wang Y, Wan Z, Liu S, Cao Y, Zeng Z. Sphingosine kinase 1 and cancer: a systematic review and meta-analysis. PloS one 2014;9(2):e90362.

188. Alshaker H, Sauer L, Monteil D, Ottaviani S, Srivats S, Bohler T, et al. Therapeutic potential of targeting SK1 in human cancers. Advances in cancer research 2013;117:143-200.

189. Kawarazaki Y, Ichijo H, Naguro I. Apoptosis signal-regulating kinase 1 as a therapeutic target. Expert opinion on therapeutic targets 2014;18(6):651-64.

190. Hattori K, Naguro I, Runchel C, Ichijo H. The roles of ASK family proteins in stress responses and diseases. Cell communication and signaling : CCS 2009;7:9.

191. Riabinska A, Daheim M, Herter-Sprie GS, Winkler J, Fritz C, Hallek M, et al. Therapeutic targeting of a robust non-oncogene addiction to PRKDC in ATM-defective tumors. Science translational medicine 2013;5(189):189ra78.

192. Love MI, Huber W, Anders S. Moderated estimation of fold change and dispersion for RNA-seq data with DESeq2. Genome biology 2014;15(12):550.

193. Harrell JC, Pfefferle AD, Zalles N, Prat A, Fan C, Khramtsov A, et al. Endothelial-like properties of claudin-low breast cancer cells promote tumor vascular permeability and metastasis. Clinical & experimental metastasis 2014;31(1):33-45.

194. Hynes RO. Integrins: bidirectional, allosteric signaling machines. Cell 2002;110(6):673-87.

195. Felding-Habermann B. Integrin adhesion receptors in tumor metastasis. Clinical & experimental metastasis 2003;20(3):203-13.

196. Guo W, Giancotti FG. Integrin signalling during tumour progression. Nature reviews Molecular cell biology 2004;5(10):816-26.

197. Kato A. The biologic and clinical spectrum of Glanzmann's thrombasthenia: implications of integrin alpha IIb beta 3 for its pathogenesis. Critical reviews in oncology/hematology 1997;26(1):1-23.

198. Yonekawa K, Harlan JM. Targeting leukocyte integrins in human diseases. Journal of leukocyte biology 2005;77(2):129-40.

199. Ye F, Kim C, Ginsberg MH. Molecular mechanism of inside-out integrin regulation. Journal of thrombosis and haemostasis : JTH 2011;9 Suppl 1:20-5.

200. Shattil SJ, Kim C, Ginsberg MH. The final steps of integrin activation: the end game. Nature reviews Molecular cell biology 2010;11(4):288-300.

201. Montanez E, Ussar S, Schifferer M, Bosl M, Zent R, Moser M, et al. Kindlin-2 controls bidirectional signaling of integrins. Genes & development 2008;22(10):1325-30.

202. Gluck JM, Koenig BW, Willbold D. Nanodiscs allow the use of integral membrane proteins as analytes in surface plasmon resonance studies. Analytical biochemistry 2011;408(1):46-52.

203. Bayburt TH, Sligar SG. Membrane protein assembly into Nanodiscs. FEBS letters 2010;584(9):1721-7.

204. Hagn F, Etzkorn M, Raschle T, Wagner G. Optimized phospholipid bilayer nanodiscs facilitate high-resolution structure determination of membrane proteins. Journal of the American Chemical Society 2013;135(5):1919-25.

205. Park SH, Berkamp S, Cook GA, Chan MK, Viadiu H, Opella SJ. Nanodiscs versus macrodiscs for NMR of membrane proteins. Biochemistry 2011;50(42):8983-5.

206. Cheresh DA, Spiro RC. Biosynthetic and functional properties of an Arg-Gly-Asp-directed receptor involved in human melanoma cell attachment to vitronectin, fibrinogen, and von Willebrand factor. The Journal of biological chemistry 1987;262(36):17703-11.

207. Hwang PM, Vogel HJ. Structures of the platelet calcium- and integrin-binding protein and the alphaIIb-integrin cytoplasmic domain suggest a mechanism for calcium-regulated recognition; homology modelling and NMR studies. Journal of molecular recognition : JMR 2000;13(2):83-92.

208. Barry WT, Boudignon-Proudhon C, Shock DD, McFadden A, Weiss JM, Sondek J, et al. Molecular basis of CIB binding to the integrin alpha IIb cytoplasmic domain. JBiolChem 2002;277(32):28877-83.

209. Gentry HR, Singer AU, Betts L, Yang C, Ferrara JD, Sondek J, et al. Structural and biochemical characterization of CIB1 delineates a new family of EF-hand-containing proteins. JBiolChem 2005;280(9):8407-15.

210. Denisov IG, Grinkova YV, Lazarides AA, Sligar SG. Directed self-assembly of monodisperse phospholipid bilayer Nanodiscs with controlled size. Journal of the American Chemical Society 2004;126(11):3477-87.

211. Civjan NR, Bayburt TH, Schuler MA, Sligar SG. Direct solubilization of heterologously expressed membrane proteins by incorporation into nanoscale lipid bilayers. BioTechniques 2003;35(3):556-60, 62-3.

212. Bayburt TH, Sligar SG. Self-assembly of single integral membrane proteins into soluble nanoscale phospholipid bilayers. Protein science : a publication of the Protein Society 2003;12(11):2476-81.

213. Shi L, Howan K, Shen QT, Wang YJ, Rothman JE, Pincet F. Preparation and characterization of SNARE-containing nanodiscs and direct study of cargo release through fusion pores. Nature protocols 2013;8(5):935-48.

214. Roy A, Kucukural A, Zhang Y. I-TASSER: a unified platform for automated protein structure and function prediction. Nature protocols 2010;5(4):725-38.

215. Yang J, Ma YQ, Page RC, Misra S, Plow EF, Qin J. Structure of an integrin alphaIIb beta3 transmembrane-cytoplasmic heterocomplex provides insight into integrin activation. Proceedings of the National Academy of Sciences of the United States of America 2009;106(42):17729-34.

216. Schrodinger, LLC. The PyMOL Molecular Graphics System, Version 1.4.1. 2010.

217. Dagliyan O, Proctor EA, D'Auria KM, Ding F, Dokholyan NV. Structural and dynamic determinants of protein-peptide recognition. Structure 2011;19(12):1837-45.

218. Yin S, Biedermannova L, Vondrasek J, Dokholyan NV. MedusaScore: an accurate force field-based scoring function for virtual drug screening. Journal of chemical information and modeling 2008;48(8):1656-62.

219. Ding F, Yin S, Dokholyan NV. Rapid flexible docking using a stochastic rotamer library of ligands. Journal of chemical information and modeling 2010;50(9):1623-32.